UNIVERSITY OF CALIFORNIA, SAN DIEGO

INJECTABLE EXTRACELLULAR MATRIX HYDROGELS FOR CARDIAC REPAIR

A dissertation submitted in partial satisfaction of the requirements for

the degree Doctor of Philosophy

in

Bioengineering

by

Sonya Baigam Seif-Naraghi

Committee in charge:

Professor Karen L. Christman, Chair
Professor Kirk Knowlton
Professor Michael Madani
Professor Andrew McCulloch
Professor Shyni Varghese
Professor Liangfang Zhang

2012

The Dissertation of Sonya Baigam Seif-Naraghi is approved, and it is acceptable in quality and form for publication on microfilm and electronically:

Chair

University of California, San Diego

2012

DEDICATION

For my sister, who is more inspiring than she thinks.

TABLE OF CONTENTS

LIST OF FIGURES

LIST OF TABLES

ACKNOWLEDGEMENTS

I would like to acknowledge the many parties that made this work possible. In addition to scientific and laboratory support, I have benefitted in a personal manner from my labmates and am very grateful for their support over the past four years. Dr. Jennifer Singelyn requires a special thank you, as she taught me a great deal about succeeding as a graduate student. Dr. Aboli Rane, Dr. Jessica DeQuach and soon-to-be Dr. Adam Young have all significantly contributed to my development as a scientist and a person.

My family deserves a big thank you for everything they have done and continue to do for me. I love you all. A tremendous thank you to my husband, Avery, for helping, prodding, supporting, and keeping me sane through this process. For the work in Chapter 2, I would like to thank Dr. Majid Ghassemian for assistance with mass spectroscopy data, Todd Johnson, Samantha Evans, and Anthony Monteforte for their help in tissue preparation, and Ryan Anderson for assistance with the ESEM. I would also like to acknowledge Dr. Michael Madani and Dr. Kirk Knowlton for their help in procuring human tissue samples, Carolina Rogers for her guidance, cooperation, and ever positive attitude when harvesting of porcine specimens, Cynthia Cam for assistance with biochemical assays, and Dana Rutherford for assistance with immunohistochemistry. For the work in Chapter 3, the authors would like to thank Todd Johnson, Samantha Evans, and Anthony Monteforte for their help in tissue preparation and sectioning as well as Greg Grover, Andrea Potocny and the Sailor Lab for assistance with FTIR.

This research was supported in part by the National Institutes of Health Director's New Innovator Award Program, part of the NIH Roadmap for Medical Research, through

grant number 1-DP2-OD004309-01. Other funding sources include the following: the CTRI under the University of California, San Diego, NIH CTSA grant #5UL1TR000100I would like to thank the National Science Foundation for the Graduate Research Fellowship, the Jacobs School of Engineering for the Jacobs Engineering Fellowship, and the HHMI for the Med-into-Grad Fellowship that I held as a graduate student.

Chapter 1, in part, is a reprint of the material as it is published as: Sonya B. Seif-Naraghi and Karen L. Christman. Tissue Engineering and the Role of Biomaterial Scaffolds: The Evolution of Cardiac Tissue Engineering. In (Eds. Regina Coeli dos Santos and Antonio Carvalho), Resident Stem Cells and Regenerative Therapy. Academic Press, Elsevier, Inc. 2012.

Chapter 2, in part, is published as the following two manuscripts: Sonya B. Seif-Naraghi, Michael Salvatore, Pam Schup-Magoffin, Diane Hu, Karen L. Christman. Design and characterization of an injectable pericardial matrix gel: a potentially autologous scaffold for cardiac tissue engineering. Tissue Engineering: Part A. 2010. 16(6): p. 2017-27 and Sonya B. Seif-Naraghi, Dinah Horn, Pam Schup-Magoffin, Michael M. Madani, Karen L. Christman. Patient-to-patient variability in autologous pericardial matrix scaffolds for cardiac repair. Journal of Translational Cardiovascular Research. 2011.

Chapter 3, in part, is a reprint of the material as it is published in: Sonya B. Seif-Naraghi, Dinah Horn, Pam Schup-Magoffin, Karen L. Christman. Extracellular matrix derived hydrogel enhances retention and delivery of a heparin-binding growth factor in ischemic myocardium. Acta Biomaterialia. 2012

Chapter 4, in part, is in preparation for submission for publication as: Sonya B. Seif-Naraghi, Aboli Rane, Vaibhav Bajaj, Shirley Zhang, Oi Ling Kwan, Pam Schup-Magoffin, Rebecca Braden, Anthony DeMaria, Karen L. Christman. Extracellular matrix hydrogel as growth factor delivery system for prolonged release of novel HGF dimer in a small animal model of myocardial infarction.

Chapter 5, in part, is in submission as: Sonya B. Seif-Naraghi*, Jennifer M. Singelyn*, Michael A. Salvatore, Kent Osborn, Jean Wang, Jessica A. DeQuach, Unatti Sampat, Oi Ling Kwan, Monet Strachan, Jonathon Wong, Pam Schup-Magoffin, Rebecca Braden, Kendra Bartels, Adam Kinsey, Mark Preul, Nabil Dib, Anthony DeMaria, Karen L. Christman. Safety and efficacy of an injectable extracellular matrix hydrogel for treating myocardial infarction in pre-clinical animal studies. *co-authors contributed equally.

The dissertation author was the primary author on all manuscripts.

VITA

2008 Bachelor's of Science in Engineering, Arizona State University

2008-2012 Graduate Student Researcher, University of California, San Diego

2012 Doctor of Philosophy, University of California, San Diego

Publications

Sonya B. Seif-Naraghi, Aboli Rane, Vaibhav Bajaj, Shirley Zhang, Oi Ling Kwan, Pam Schup-Magoffin, Rebecca Braden, Anthony DeMaria, Karen L. Christman. Extracellular matrix hydrogel as growth factor delivery system for prolonged release of novel HGF dimer in a small animal model of myocardial infarction. (in preparation).

Sonya B. Seif-Naraghi*, Jennifer M. Singelyn*, Michael A. Salvatore, Kent Osborn, Jean Wang, Jessica A. DeQuach, Unatti Sampat, Oi Ling Kwan, Monet Strachan, Jonathon Wong, Kendra Bartels, Adam Kinsey, Mark Preul, Nabil Dib, Anthony DeMaria, Karen L. Christman. Safety and efficacy of an injectable extracellular matrix hydrogel for treating myocardial infarction in pre-clinical animal studies. (in revision). *co-authors contributed equally.

Sonya B. Seif-Naraghi and Karen L. Christman. Tissue Engineering and the Role of Biomaterial Scaffolds: The Evolution of Cardiac Tissue Engineering. In (Eds. Regina Coeli dos Santos and Antonio Carvalho), Resident Stem Cells and Regenerative Therapy. Academic Press, Elsevier, Inc. In press.

Sonya B. Seif-Naraghi, Dinah Horn, Pam Schup-Magoffin, Karen L. Christman. Extracellular matrix-derived hydrogel enhances retention and delivery of a heparin-binding growth factor in ischemic myocardium. Acta Biomaterialia. 2012.

Sonya B. Seif-Naraghi, Dinah Horn, Pam Schup-Magoffin, Michael M. Madani, Karen L. Christman. Patient-to-patient variability in autologous pericardial matrix scaffolds for cardiac repair. Journal of Translational Cardiovascular Research. 2011.

Sonya B. Seif-Naraghi, Jennifer M. Singelyn, Jessica A. DeQuach, Pam J. Schup-Magoffin, Karen L. Christman. Fabrication of Biologically Derived Injectable Materials for Myocardial Tissue Engineering. Journal of Visualized Experiments. 2010.

David A. Delaine, Sonya B. Seif-Naraghi, Shahed Al-Haque, Nicolo Wojewoda, Yvonne Meninato, Jennifer DeBoer. Student involvement as a vehicle for empowerment: a case study of the student platform for engineering education development. European Journal of Engineering Education. 2010. 35(4): p. 367-78.

Sonya B. Seif-Naraghi, Michael Salvatore, Pam Schup-Magoffin, Diane Hu, Karen L. Christman. Design and characterization of an injectable pericardial matrix gel: a potentially autologous scaffold for cardiac tissue engineering. Tissue Engineering: Part A. 2010. 16(6): p. 2017-27.

Jennifer M. Singelyn*, Jessica A. DeQuach*, Sonya B. Seif-Naraghi, Robert B. Littlefield, Pamela J. Schup-magoffin, Karen L. Christman. Naturally derived myocardial matrix as an injectable scaffold for cardiac tissue engineering. Biomaterials. 2009. 30(29): p. 5409-16. *co-authors contributed equally.

Fields of study

Major Field: Bioengineering (Cardiac Tissue Engineering)

Professor Karen L. Christman

ABSTRACT OF THE DISSERTATION

INJECTABLE EXTRACELLULAR MATRIX HYDROGELS FOR CARDIAC REPAIR

by

Sonya Baigam Seif-Naraghi

Doctor of Philosophy in Bioengineering

University of California, San Diego, 2012

Professor Karen L. Christman, Chair

Cardiovascular disease is the leading cause of death in the United States and the rest of the western world. Interrupting the progression of negative remodeling after a myocardial infarction (MI) could mitigate the damage caused by a heart attack and preventing the onset of heart failure. Extracellular matrix (ECM) hydrogels have emerged as potential scaffolds for cardiac repair; however, all ECM hydrogels previously explored have been derived from xenogeneic sources, raising concerns regarding immunogenicity, disease transfer, and increased regulation by the FDA. In this

dissertation work, a potentially autologous pericardial matrix hydrogel is developed, characterized, and tested. The presence of sulfated sugars in the material led to the hypothesis that heparin-binding growth factors could be sequestered for prolonged delivery and increased effect *in vivo*. The positive results of this work prompted the exploration of delivering a novel growth factor candidate with the pericardial matrix to evaluate the potential effect on cardiac function post-MI, demonstrating the potential value of this growth factor delivery system *in vivo*. Though concerns regarding using a xenogeniec material provided the basis for first investigating an autologous option, understanding the effect on the host response is important, prompting evaluation of the inflammatory response to rat myocardial matrix compared to porcine myocardial matrix. Using a non-decellularized myocardial matrix and saline as controls, we sought to understand the inflammatory response to allogeneic and xenogeneic materials in healthy animals. The only signs of chronic inflammation were seen in the non-decellularized positive controls; little difference was noted between the porcine and rat ECM hydrogels, supporting the conclusion that there may be no added value to allogeneic over xenogeneic materials. Exposure to myocardial matrix had no effect on clotting times or platelet activation in human blood and platelet-rich-plasma samples. Direct injection of the ECM hydrogel into the lumen of the left ventricle did not cause notable ischemia, edema, or hemorrhage in peripheral organs. This work establishes the safety and biocompatibility of the myocardial matrix and, taken with recent results from pre-clinical large animal studies, provides a foundation for moving forward with clinical trials.

CHAPTER ONE: Introduction

1.1 Introduction to Tissue Engineering

1.1.1 History

Tissue engineering is a growing field with multidisciplinary players in engineering, biology, and medicine. The general goal of tissue engineering is to restore, maintain, or enhance tissue and/or organ function. The first use of the term "tissue engineering" to describe the research efforts toward this goal can be traced to Professor Y.C. Fung, of the University of California, San Diego. In 1985, Professor Fung submitted a proposal to the National Science Foundation requesting funding for a research center entitled "Center for the Engineering of Living Tissues". The proposal was rejected, but two years later at a proposal review panel meeting there was a discussion focused on solidifying the concept of this quickly growing field, and Professor Fung volunteered the phrase again [1]. The field was further established within the scientific community when Drs. Langer and Vacanti published the first review of tissue engineering in Science in 1993 [2]. This collaboration is also well known for their seminal publication in which an ear-shaped polymeric template was seeded with chondrocytes and subcutaneously implanted in a small animal [3]. While this was a very early example of tissue engineering, which achieved no functional outcome, it launched the field into popular view.

Though the field was not formally defined until 1987, there were prior examples of what would now be considered tissue engineering. Primitive vascular and skin grafts emerged in the early 20^{th} century, and as cell culture techniques improved these technologies advanced. Preliminary work with cells and materials aimed at mimicking

the function of the kidney, the pancreas/islet cells, and the liver starting emerging in the wake of World War II. Research on growing bone and cartilage developed shortly thereafter, facilitated by the discovery of factors involved in bone induction. Studies representing the pre-1987 body of tissue engineering work were reviewed extensively in a report on the Emergence of Tissue Engineering as a Research Field, produced by the NSF in 2003 [1].

In the years following the Langer/Vacanti review, articles citing tissue engineering increased exponentially. Combinations of cells, biomaterials, and exogenous factors aimed at repairing or reproducing every tissue and organ system have emerged. Investigated biomaterials span the natural and synthetic spectra; cell types vary from mature adult cells to embryonic stem cells (ESCs) and induced pluripotent stem cells; exogenous factors range from angiogenic growth factors such as vascular endothelial growth factor [4] and basic fibroblast growth factor (bFGF), bone inductive factors such as bone morphogenic protein 2 (BMP-2), and steroids and hormones that can be used to manipulate certain cell types. The classical tissue engineering paradigm involves cell-seeded constructs, which are cultured *in vitro,* prior to implantation. More recently *in situ* engineered and acellular scaffold approaches have been explored. A secondary application for the developing therapeutic systems was identified in the area of model systems for *in vitro* testing – toxicity, pathogenicity, and drug metabolism and uptake. While these applications arguably utilize tissue engineering principles, this chapter will focus on therapeutic systems, specifically tissue engineering approaches to cardiac repair

post-myocardial infarction. Several other excellent resources exist that extensively detail the history and progress of tissue engineering [5, 6].

1.1.2 Scope

Given the interdisciplinary nature of tissue engineering, success in the relevant areas of medicine, biology, and engineering all provide impetus for advancing the field. This is seen clearly with the advancement of techniques for the culture and differentiation of stem cells as well as the introduction of induced pluripotent stem cells. Additionally, as the technology used to develop bioreactors improves, so will the ability of tissue engineers to manipulate their constructs. Finally, each new insight into the mechanisms of disease provides an opportunity for a tissue engineer to incorporate that understanding into the design of relevant therapies. Thus, as these areas advance, their success has an immediate impact on tissue engineering. Similarly, achievements within the field of tissue engineering have widespread effects in related areas. If the goals of repair and regeneration of damaged or diseased organs are accomplished, or if functional tissue can be engineered *ex vivo* for the replacement of damaged organs, the implications of that success will be innumerable.

1.1.3 Principles

When discussing principles of tissue engineering, it is prudent to define what exactly we mean by the term. Langer and Vacanti defined tissue engineering in the following way:

> Tissue engineering is an interdisciplinary field that applies the principles of engineering and the life sciences toward the development of biological substitutes that restore, maintain, or improve tissue function [2].

A widely accepted umbrella used to conceptualize what constitutes "biological substitutes" is the tissue engineering triad (Figure 1.1), which consists of cells, biomaterials, and exogenous bioactive factors.

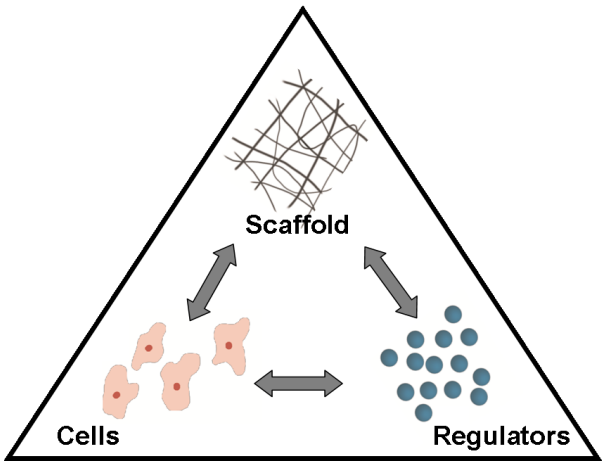

Figure 1.1: Tissue Engineering Triad. The umbrella of tissue engineering traditionally includes systems with at least two components of the tissue engineering triad, which is comprised of a biomaterial scaffold, cells, and regulators (e.g. exogenous growth factors).

In general, tissue engineering approaches involve at least two of the three constituents of the triad. Traditionally, this is represented by a biomaterial scaffold seeded with a relevant cell type and manipulated with an exogenous biomolecule (e.g.

VEGF or BMP-2) in order to reproduce or achieve some target function of the given tissue or organ. This definition can be relaxed to include biomaterial-only scaffolds that are designed to elicit a cellular response upon introduction to the host. In this case, while the "biological substitute" may include only one of the three components of the tissue engineering triad, various cell types – including progenitor cells – can be recruited to the scaffold *in vivo*, a method of *in situ* tissue engineering.

1.2 Role of biomaterials in Tissue Engineering

As an important component of the tissue engineering triad, biomaterials have been used extensively to build both two dimensional models and three dimensional constructs. Here, the importance of the extracellular matrix as a biomaterial will be discussed, the range of naturally-derived and synthetic biomaterials used in tissue engineering will be outlined and a set of examples of the applications for biomaterials as acellular, cellular and growth factor delivery scaffolds will be presented. A discussion of the challenges specific to the individual areas of tissue engineering will be left to comprehensive references [5, 6] and discipline-specific reviews, of which there are many.

1.2.1 Extracellular matrix

The extracellular matrix (ECM), which is nature's scaffold, is a complex network of structural and fibrous proteins, proteoglycans, and glycosaminoglycans, which have been implicated in the regulation of cell communication, migration, proliferation, differentiation, adhesion, and signaling [7]. Specifically, the ECM is comprised primarily

of collagen, with varying ratios of elastin, fibronectin, vitronectin, laminin, and other secreted proteins that are unique to each tissue [8]. In addition to these proteins, proteoglycans such as heparan sulfate proteoglycans (HSPGs), decorin, and dermatopontin allow for interactions between the cells and their ECM. Finally, glycosaminoglycans such as heparan sulfate, dermatan sulfate, and hyaluronic acid provide compressive strength as well as sequester and immobilize growth factors. Mimicking attributes of the architecture or composition of native ECM may allow for better manipulation of the cellular components in tissue engineered systems. Additionally, presenting an environment that closely resembles native ECM and is therefore familiar to the local cell population could promote cell infiltration and endogenous repair. For these reasons, many of the naturally-derived biomaterials commonly used in tissue engineering are ECM components.

1.2.2 Naturally-derived biomaterials

Collagen, the primary component of most ECMs, is one of the most widely used biopolymers. Depending on the application, it can take various forms, including a soft hydrogel, a fibrous sponge, or an electrospun sheet [9]. ECM components such as elastin, laminin, heparan sulfate, and hyaluronic acid have also been used extensively as scaffold materials. Other popular natural materials include chitosan, alginate, and fibrin. These natural biopolymers have the general advantage of biocompatible degradation products, as well as being inherently bioactive. Unless chemically modified, these materials will all degrade relatively quickly – an advantage or a disadvantage depending

on the application. Non-polymeric natural materials such as hydroxyapatite or calcium carbonate are more resistant to degradation and have been utilized in applications that require stiff materials, such as bone tissue engineering [10].

Naturally-derived biomaterials can be used in combination with one another, often in an attempt to more closely mimic the complex environment presented by the native ECM. One approach to harness the complexity of native ECM is to use the network secreted by cells in culture. In this way, a synthetic polymer scaffold can be used as a template on which cells can deposit ECM. If the original polymer template degrades, then eventually the construct will be remodeled to only consist of the cells and their ECM. Recently, decellularization techniques have provided the ability to start with native tissue, remove the cellular component, and then use the resulting ECM scaffold as a biomaterial scaffold. These materials have been shown to be biocompatible, as long as the decellularization protocol is effective in removal of the cellular antigens that may cause an immune response [11]. Complete decellularization of the heart with detergent solutions was first published by Ott et al. (Figure 1.2) [12]. This concept has subsequently been applied to nearly all organs and tissues [13]. Research utilizing decellularized scaffolds has involved seeding them with cells in an effort to repopulate the constructs with appropriate cell types and either encourage organization and function of adult cells or differentiation and maturation of stem/progenitor cells. In a recent example of this strategy, Petersen et al. decellularized adult rat lungs and showed that the hierarchical branching structures of airways and vasculature was retained. Pulmonary

epithelial and vascular endothelial cells were able to successfully repopulate the scaffold, indicating the potential for using this tissue engineered system for lung regeneration [14].

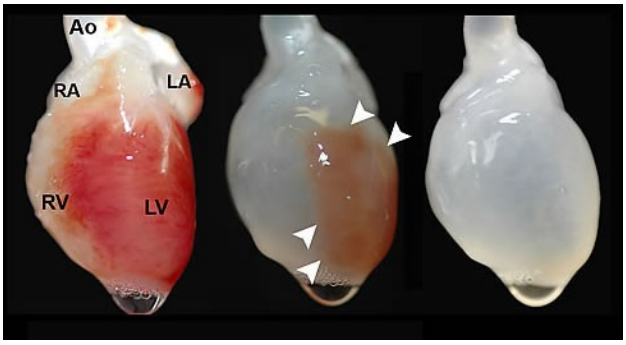

Figure 1.2: Whole Organ Decellularization. An adult rat heart is shown being decellularized with ionic detergents. The progression of decellularization is illustrated by the change in color from red/brown to a slightly translucent white, indicating the removal of blood and cellular content. The receding line of residual debris is indicated with arrows. Modified from [12] and reprinted with permission.

Not only can these decellularized ECM constructs be used as implantable, three-dimensional scaffolds, but they can also be processed into injectable materials that form gels *in situ*. Using methods modified from those first published by Freytes et al., a variety of tissues have been processed in this way, including the urinary bladder, myocardium, pericardium, adipose tissue, liver, small intestinal submucosa (SIS), and brain [15-21]. These injectable biomaterials are liquid at room temperature and form fibrous, porous hydrogels when brought to physiologic conditions of temperature, salt concentration, and pH. They are therefore potentially well-suited for minimally invasive delivery.

1.2.3 Synthetic materials

Polymers represent the bulk of synthetic materials used in tissue engineering, ranging widely from poly(lactic acid) [22], poly(glycolic acid) (PGA), poly(ethylene glycol) [23], polyurethane, polytetrafluoroethylene (PTFE), and poly(N-isopropylacrylamide) (poly(NIPAAm)), among others. One of the advantages these materials carry over natural materials includes the ability to tailor properties – stiffness, porosity, degradation, ligand density, etc. – of the material for its intended purpose. For example, synthetic polymers can be designed to be either biodegradable – by including sites that allow for hydrolysis or enzymatic cleavage – or non-biodegradable, in which case the scaffolds remain intact in the host. However, if the material does not degrade at all, there is potential for eliciting a foreign body reaction. On the other hand, another concern with synthetic polymers is the biocompatibility of degradation products.

Poly(N-isopropylacrylamide) (poly(NIPAAm)) is an interesting synthetic polymer due its physiologically relevant lower critical solution temperature (LCST) of 32-33 °C. At room temperature, poly(NIPAAm) is hydrophilic and therefore soluble in aqueous solutions as well as resistant to protein adsorption and cell adhesion. At body temperature, however, poly(NIPAAm) is hydrophobic and therefore allows for protein adsorption and cell adhesion. Taking advantage of this property, Okano and colleagues pioneered cell sheet technology by culturing cells on plates coated in poly(NIPAAm) [24, 25]. Cells are allowed to grow to confluency and produce their own extracellular matrix, at which point the temperature is dropped below the LCST. The change in hydrophobicity causes the adsorbed ECM proteins and associated cells to lift off of the

material in a sheet. Stacked cell sheets have been produced and used as thin grafts, however, due to diffusion limitations the maximum thickness that has been generated is approximately 600 μm [26, 27]. Other applications utilizing poly(NIPAAm) are found in therapeutic embolization or as *in situ* tissue engineering scaffolds since it can be kept in solution at room temperature, but when injected into the body, precipitates and forms a solid scaffold [28, 29].

1.2.4 Growth factor delivery

In addition to using biomaterials as acellular scaffolds or cellular delivery vehicles, tissue engineering scaffolds can also be used to prolong the retention and release of bioactive moieties such as growth factors. Growth factors can be used to elicit a variety of biological responses, for example, increased vascularization. Therapeutic angiogenesis via delivery of angiogenic factors such as VEGF and bFGF has specifically been investigated in a variety of disease models including myocardial and peripheral ischemia [30, 31], and wound repair [32, 33]; several reviews have been written on the topic [34-36].

1.3 Clinical translation and commercialization

In the wake of the initial tissue engineering boom in the early 1990s, many companies sprang up to commercialize the new products. Unfortunately, due to a series of underwhelming product launches, failed regulatory trials, and general lack of venture capital following the dot-com crash tissue engineering suffered a severe downturn

between 2000 and 2002. Remarkably, however, between 2002 and 2007, economic activity in the fields of tissue engineering, regenerative medicine, and stem cell therapeutics increased fivefold. By mid-2007 there were over 100 development-stage companies with more than 55 products in preclinical and clinical trials [37]. Tissue engineered products for repair of bone, cartilage, cornea, blood vessels, urinary structures, left mainstem bronchus, and skin have all proceeded to clinical trials in humans [38]. In a thorough review of the private sector involvement in the progression of tissue engineering, Lysaght et al. observes that contemporary commercial success results from identification of products that can be achieved given the current technology and regulatory guidelines [37]. It is concluded that the future of tissue engineering is bright, given the field's demonstrated resilience and the current diversity of research.

1.4 Future of Tissue Engineering

Advancement in both stem cell technologies and our understanding of disease states will inform the design of future tissue engineered systems. As discussed, since the field has such strong ties in different areas of engineering, medicine, and biology, the improvement in knowledge in a variety of areas may provide impetus for advancing the field. As our understanding of how to best manipulate progenitor and stem cells increases, scaffolds will be able to be fabricated to better achieve goals with respect to cellular organization and differentiation. Advancements in the development of smart materials – which include an ever-growing arsenal of materials sensitive to temperature, salt concentration, and pH – will also accelerate the growth of tissue engineering.

Additionally, while tissue engineering has historically been identified as applied research, a new focus on elucidating the mechanisms by which many of the tissue engineered scaffolds are effective must be undertaken. Only then will scaffolds be able to be designed and tailored under an informed set of design criteria out of which novel, relevant, and clinically translatable approaches can emerge.

1.5 Cardiac Tissue Engineering

1.5.1 Introduction

The implications of cardiac tissue engineering are widespread; more than one in three deaths in the United States alone are attributed to cardiovascular disease, and heart failure following myocardial infarction is responsible for a majority of those deaths [39]. The discovery and investigation of novel approaches to treating this difficult population will provide benefit to patients will little other recourse. The term cardiac tissue engineering will be used here to describe tissue engineered strategies for the support, repair, regeneration, or replacement of myocardial tissue (cardiac muscle) as a treatment for myocardial infarction and the prevention of heart failure.

1.5.2 Disease state

In order to understand the rationale behind the cardiac tissue engineering designs that will be discussed in this chapter, it is useful to first understand the underlying disease state. Briefly, the occurrence of events in patients with ischemic cardiomyopathy involves an initial coronary event that injures downstream tissue. The ensuing

inflammatory response leads to remodeling of the infarcted tissue, a process that can be beneficial at first, but eventually results in congestive heart failure.

1.5.2.1 Myocardial infarction and left ventricular remodeling

More specifically, myocardial infarction (MI) refers to an ischemic injury caused by the blockage of a coronary artery. These vessels provide the blood supply to the cardiac muscle and cessation of oxygen delivery causes cell death in the downstream tissue, accompanied by degradation of the associated ECM. After an initial inflammatory period, the injured region is remodeled by fibroblasts, which lay down collagenous scar tissue. Unfortunately, this non-contractile replacement cannot contribute to the pumping action of the heart. Initially, cells in the non-infarcted myocardium hypertrophy to compensate for the loss in function. This stiffens the muscle; increases in interstitial fibrosis throughout the myocardium further compound the stiffening effect which ultimately increases myocardial wall stress. Over time, this causes the infarct area to thin, further increasing wall stress. This accelerates the negative left ventricular (LV) remodeling process that leads to the development of heart failure. In the process of negative remodeling, ventricular geometries are affected – left ventricular volumes and areas measured at the end of diastole and the end of systole increase both to compensate for reduced ejection fraction and in response to the changes in wall stress. Ejection fraction, which is one measure of the heart's ability to pump blood, is often severely reduced, and can be as low at 12-20% in end-stage heart failure. Average mortality data indicates that 50% of end-stage heart failure patients die within five years of diagnosis; in

patients with coronary disease or who are older than 55, mortality is significantly higher [40].

1.5.2.2 Current treatment options

Advancements in medical therapy and percutaneous interventions have improved the prognosis post-MI considerably but the incidence of heart failure is only increasing, likely as a result of the increasing number of patients who now survive the initial attack. Currently, the only approved treatments for end-stage heart failure post-MI are left ventricular assist devices (LVADs) and total heart transplantation. The former is limited by the complications of a chronic external assist device and the inherently risky surgical procedure necessary to implant the device in a fragile patient population. While total heart transplantation may provide a solution for a few patients, there is a severe dearth of donor hearts and even for the lucky population who do receive a transplant, a lifetime of immunosuppressant drugs and the side effects thereof is not an ideal solution.

1.6 Tissue engineering approaches

1.6.1 Introduction

Initial experimental therapies involved the delivery of cells and or growth factors in simple liquid solutions. More recently, tissue engineering approaches have been explored. As discussed, classical tissue engineering strategies involve some combination of a biomaterial scaffold, a cellular component and bioactive moieties designed to achieve some functional outcome. When applied to cardiac repair post-MI, the first

application for biomaterials was as cell delivery scaffolds, utilized to enhance cell survival and retention upon implantation. This was first explored in the form of three-dimensional cardiac patches that were seeded with cells and delivered to the epicardial surface of the heart. In an effort to reduce the invasiveness of delivery, injectable biomaterials that gel *in situ* within the ventricular wall have also been investigated as scaffolds for the enhancement of cell delivery and retention. More recently, biomaterials in the form of both patches and injectable scaffolds have been investigated for use as acellular therapies, designed for *in situ* tissue engineering in which endogenous cellular infiltration and remodeling is encouraged. Cardiac patches and injectable materials have been investigated for use as cell delivery vehicles [7, 41-45] and acellular therapies [20, 41, 46, 47], as well as in conjunction with growth factors for enhanced effect [48-51]. This discussion will outline scaffold design parameters, focus on the rationale for both cellular and acellular therapies, introduce the two primary tissue engineering approaches, and summarize seminal findings. For an exhaustive assessment of *in vivo* studies utilizing biomaterials in these applications, the reader is referred to to two reviews on the use of biomaterials for MI [27, 52].

1.6.2 Design parameters

Cardiac tissue engineered scaffolds intended for the treatment of ischemic cardiomyopathy should ideally do the following: mitigate negative left ventricular remodeling, salvage at-risk cells in borderzone myocardium, provide a template for cellular infiltration, promote angiogenesis to support the tissue remodeling process, and

degrade in a biocompatible fashion. Thus, the biochemical, structural, and mechanical properties all need to be appropriate for the application. Ligand density and distribution can regulate cell attachment and degradation products of scaffold materials can either promote or retard chemotaxis into the construct. Porosity and fiber diameter are two structural considerations that can change cellular attachment and migration; pore size of approximately 30 μm has been reported as ideal for cellular and vascular infiltration [53]. Material mechanics is another consideration – with respect to cardiac tissue engineering, these mechanics can be modeled after healthy myocardium (20 kPa), or individual ECM components (0.5 – 1 kPa). The mechanics of the scaffold will affect cellular behavior, so if stem or progenitor cells are incorporated, it is possible that the mechanics of the developing heart, which is significantly more compliant than adult tissue, would be appropriate.

When designing an *in vitro* engineered cardiac patch, perfusion is an important parameter and has historically been a limiting factor. If cells are seeded throughout, constraints of diffusion prevent patches of appreciable thickness (greater than 600 um) from being successful. For *in situ* engineered systems, it is essential to have a template appropriate for the survival and retention of cells incorporated into the system or for the recruitment and organization of cells infiltrating into the scaffold. For injectable systems, gelation kinetics are an important consideration as systems that gel too quickly may not be compatible with the minimally invasive, catheter delivery methods.

1.6.3 Cellular vs. acellular scaffolds

Biomaterial scaffolds have been utilized extensively as cell delivery scaffolds, intended to provide structural support and improve survival and retention in the harsh post-MI environment [26]. In this context, a variety of biomaterials have been explored, including synthetic materials such as polyethylene glycol [23], poly(NIPAAm), and poly(glycerol-sebacate), as well as naturally-derived materials such as collagen, Matrigel™, gelatin, alginate, fibrin, and decellularized ECM. These biomaterials have served as delivery scaffolds for many cell types, including adult cells such as skeletal myoblasts, cardiomyocytes, and dermal fibroblasts as well as multi- and pluripotent cells such as bone marrow-derived mesenchymal progenitor cells and embryonic stem cells. While a wide range of materials and cell types have been combined and explored, the general results of these studies confirm the utility of biomaterial scaffolds to promote cell survival and retention *in vivo*.

In addition to their use as cell delivery vehicles and scaffolds, biomaterials have been used as acellular scaffolds. In this role, the materials provide a template for cellular infiltration and remodeling. As an *in situ* tissue engineering approach, this takes advantage of the resident progenitor and other cells already present in the given tissue. This approach may prove especially useful when the tissue has a high regenerative capacity and a larger population of progenitor cells – the urinary bladder, SIS, and the skin, for example – but the strategy can be applied in any organ, even one with a small population of resident progenitor cells, such as the heart. As noted, one of the challenges of this particular tissue engineering problem is that the heart has very little regenerative

capacity. Until recently, it was thought that all the cells in the heart were terminally differentiated. While studies have now identified a population of progenitor cells in the heart, they are in low numbers. These cells are identified as being negative for blood lineage markers (Lin-) and positive for stem cell surface markers such as c-kit, Sca-1, and MDR-1 [54]. Interestingly, in failing human hearts it was determined that there are actually more of these cells present [55]. If these cells could be recruited to the infarct area and given an environment that encouraged differentiation and organization, then some endogenous repair could potentially be elicited. Thus, an acellular treatment that promotes cell infiltration and provides an appropriate environment within the harsh infarct milieu could also elicit regeneration by taking advantage of these resident progenitor cells. A handful of studies have used immunohistochemistry to identify the presence of progenitor cells in or near the treatment region or infarct. Examples include studies involving acellular injectable scaffolds of Matrigel™ [56], an emulsion of decellularized SIS [57] , and matrix gels derived from pericardial [58] and myocardial tissue [59]. The presence of these cells indicates the potential for stem cell mobilization within the tissue.

While the techniques and materials vary greatly, one remarkable aspect these approaches have in common is that, when applied in small animal MI models, most of these tissue engineered systems show improvements in cardiac function, as measured by increases in ejection fraction (EF) or fractional shortening (FS). Other positive outcomes may include decrease in infarct size or fibrosis, increase in infarct wall thickness, and improvement in contractility or elasticity.

1.6.4 Growth factor delivery

In addition to cellular delivery vehicles and acellular biomaterial-only scaffolds, cardiac tissue engineering scaffolds for growth factor delivery have been investigated. Inducing angiogenesis may preserve endogenous cardiomyocytes and functionally contractile myocardium post-MI [60-62]. To harness this potential, tissue engineering systems have been designed to deliver these proteins to infarcted tissue. Growth factors such as VEGF and bFGF have been covalently bound to synthetic polymers such as PLGA [63] and poly(NiPAAm) [64], as well as to naturally-derived biomaterials such as collagen [65] and hyaluronic acid [34, 35, 66]. Bio-inspired self-assembling peptides [67] have also been used as growth factor delivery scaffolds. Other hybrid materials that either incorporate biomolecules that associate with growth factors natively, such as heparin or heparan sulfate [68, 69] or derivatives that include highly sulfated sugars [70] or heparin-like growth factor binding domains [71, 72] have also proved useful. Immobilization on a biomaterial scaffold has been demonstrated to be more effective than physical entrapment or bolus injection, as it increases growth factor stability and localizes the effects to the site of treatment [73]. *In vivo*, growth factors interact with sulfated glycosaminoglycans (sGAGs) that associate with ECM proteins [74]. Thus, the ECM can sequester and present growth factors to the cells in the tissue microenvironment. Recently, an injectable, acellular pericardial matrix hydrogel was shown to allow for the natural incorporation of a heparin-binding growth factor, bFGF, for prolonged release and increased vascularization in a rat MI model (data unpublished). Delivery of other

growth factors to reduce the degree of fibrosis or enhance cell survival or differentiation has also been investigated.

1.6.5 Patches

Cardiac patches, a primary tissue engineering approach for treating MI, are three-dimensional constructs fabricated *in vitro* and implanted over the infarcted tissue. In some cases, the patches are used to replace the damaged tissue after resection in a ventriculotomy. Li et al. was the first to deliver cells in a biomaterial patch; scaffolds improved cell survival and retention, but showed no improvement in cardiac function [75]. Leor et al. then used alginate to transplant fetal cardiomyocytes in a rat MI model and was successful in demonstrating improvement in both cell survival and cardiac function [76]. The first examples of cardiac patches used a variety of cell types, including stem cells and progenitor cells.

Stem cells appear in conjunction with a wide range of materials. For example, collagen scaffolds have been seeded with bone marrow-derived CD133+ cells [77], human mesenchymal stem cells [78] and human umbilical cord mononuclear cells [79] and applied in small animal infarct or cryoinjury models with varying degrees of success. In general, the application of these patches leads to increased vascularization and a maintenance or improvement in functional parameters such as EF and FS. An exciting development is the use of cell-seeded collagen patches in a phase 1 clinical trial – the Myocardial Assistance by Grafting a New Bioartificial Upgraded Myocardium (MAGNUM). In this study, a collagen patch seeded with autologous bone marrow cells

was administered to 10 patients undergoing coronary artery bypass graft (CABG) surgery in conjunction with intramyocardial injection of bone marrow cells. Results from this study indicate that the both cell injection alone and with the patch improve EF and the patient's NY Heart Association functional class at a one-year follow-up. Improvements in LV end diastolic volume and scar thickness, however, were only observed in the patients who received both patch and injection and not those who only received the bolus injection [80].

Other naturally derived materials that have been used in conjunction with stem cells include decellularized pericardial, SIS, and myocardial tissue. Mesenchymal stem cells have been seeded on decellularized pericardial tissue and used to replace tissue in a small animal ventriculotomy model with observed improvements in cardiac function [81]. Implantation of a decellularized SIS patch with and without mesenchymal stem cells, improved LV contractility and microvessel density in a rabbit MI model [82]. In addition to stem cells, many studies have used progenitor cells and ESC-derived cells. For example, Xiong et al. seeded human ESC-derived endothelial cells and human ESC-derived smooth muscle cells onto a fibrin scaffold. When implanted in a porcine model, EF improved after 7 days and maintained the improvement over 4 weeks [83]. Godier-Furnemont et al. incorporated human mesenchymal progenitor cells in fibrin and seeded them on a scaffold made from a decellularized human myocardial sheet. The scaffold was implanted over infarcts in a rodent MI model and preservation of cardiac function and an increase in vascularization was observed [84]. These results support the hypothesis that not only can a biomaterial scaffold support the survival and retention of

the cells seeded within it, but that the application of the cell-seeded patches may provide therapeutic benefit.

Acknowledging the challenges of clinical translation for strategies that rely on a cellular component, there has been recent work focused on developing acellular cardiac patches. The following examples illustrate the breadth of these approaches. Callegari et al. applied a patch made from a simple collagen sponge and showed an increase in angiogenesis compared to controls in a cryo-injury small animal model up to 60 days post-application [85]. An acellular synthetic scaffold composed of an elastic biodegradable polyester urethane urea (PEUU) developed by Fujimoto et al. (Figure 1.3) was shown to increase fractional area change, wall thickness, and capillary density 8 weeks post-implantation when compared to the control group [86]. Another synthetic scaffold used is biodegradable poly(glycolide-co-caprolactone); when implanted both with and without bone marrow-derived mononuclear cells this patch improved FS, ventricular diameters and hemodynamics after four weeks when compared to the control [87].

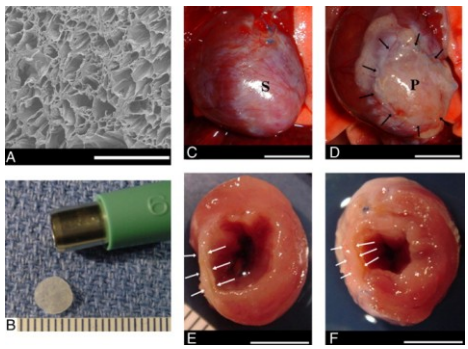

Figure 1.3: Cardiac Patch Application. Here, an elastic synthetic biodegradable cardiac patch is applied extramurally over the infarct. In (C) the infarct of a control animal is shown and compared to the applied patch, which can be seen in (D). After 8 weeks there is a marked difference in wall thickness between saline-injected control animals (E) and the patch-treated animals (F). Modified from [86] and reprinted with permission.

Hybrid patches have been also been constructed, for example, Krupnick et al. designed a patch out of a combination of poly(lactic acid) mesh, collagen type I, and Matrigel™, all of which was then reinforced with polytetrafluroethylene. They used this as both an acellular and cellular scaffold to replace ventricular tissue after ventriculotomy. Miyagi, et al. designed another hybrid system for the delivery of bone marrow MSCs and cytokines by using a combination of synthetic and natural components. Using a gelatin sponge (gelfoam) coated with poly ε-caprolactone, this group took advantage of the gelatin to promote cellular attachment as well as the synthetic component to provide structural support. When used in a small animal ventriculotomy model, the hybrid scaffold showed an improvement in cardiac function when compared to control animals and to unmodified gelatin sponge. This improvement was seen in all groups with the hybrid scaffold – alone, with or without cytokines, and with or without cells [88].

Thus, work with acellular patches as potential *in situ* tissue engineering approaches to cardiac repair has increased dramatically in the last five years and given the promising results, this area is likely to continue to expand. There is however, some dispute within the literature, as studies often have conflicting results. When investigating the effectiveness of direct cell injection compared to delivery in a poly(lactide-co-ε-caprolactone) cardiac patch, Jin et al. found that MSCs delivered via both routes were able to differentiate into cardiomyocytes. Additionally, both the direct cell injection and delivery in the patch showed similar increases in EF when compared to both saline and implantation of an acellular scaffold, which was insufficient for the preservation or

improvement of cardiac function [85]. As the body of literature increases with respect to the number of studies that specifically investigate the differences in the effects of cellular and acellular patches, it may become possible to understand how and why they differ and if one can provide more benefit. To date, the literature disagrees as to the efficacy of acellular cardiac patches, these discrepancies may be due to the differences unrelated to the scaffolds themselves – differences in the animal model, time of treatment, and length of study make it difficult to compare results across studies.

1.6.6 Injectable scaffolds

Similar to cardiac patches, injectable scaffolds have been investigated for use as cell delivery vehicles, as well as for acellular treatments or the delivery of growth factors.. A wide variety of injectable scaffolds have been investigated, including naturally derived materials such as collagen, fibrin, ECM hydrogels, and alginate as well as synthetic materials such as various polyesters as well as PEG, and poly(NiPAAm). Other materials used as injectable scaffolds for cardiac repair include self-assembling peptides [89-91] and nanofibers [92] and combination materials such as collagen-GAG hybrids. One of the most exciting advantages of developing an injectable scaffold for cardiac repair is that if the material is compatible with delivery via catheter, then the treatment could be administered via minimally invasive methods.

The potential for using an injectable biomaterial to enhance cell delivery was first demonstrated by Christman et al., by intramyocardial injection of fibrin glue – with and without skeletal myoblasts – into a small animal MI model [41, 93]. Improvements in

cardiac function as well as increases in cellular retention and survival were seen when compared to cells delivered in saline. One of the most interesting results of this study, however, was that injecting acellular fibrin demonstrated similar improvements in cardiac function. Since then, fibrin has been studied extensively as an acellular, cellular, and growth factor delivery scaffold. Marrow-derived cardiac stem cells [94], adipose-derived stem cells [95, 96], bone marrow mononuclear cells, bFGF, VEGF, hepatocyte growth factor (HGF), and transforming growth factor beta (TGFB) have all been incorporated into an injectable fibrin scaffold for cardiac repair. The results of these studies are varied – Danoviz et al. demonstrated that both an acellular injection of fibrin and an injection of adipose-derived stem cells in fibrin improved cardiac function compared to the control [95] but the cellular scaffold reduced scar area to a greater degree(51). Similarly, Zhang et al. showed that while both fibrin alone and fibrin with cells improved function compared to the control, the cellular scaffold-treated animals were significantly improved compared to the acellular scaffold. As with patches, the disagreement in literature over whether or not cellular scaffolds provide additional benefit compared to acellular scaffolds has yet to be resolved.

While Christman et al. laid the foundation with their initial work, fibrin is a two-component system comprised of thrombin and fibrinogen, which undergo a rapid gelation process when combined. To use this material in vivo, a direct injection with a Duploject™ syringe, or similar device, is required. As such, fibrin is not compatible with minimally invasive delivery methods – it would clog any catheter before reaching the myocardium. In the past few years, alginate has emerged as a biomaterial that can be

compatible with catheter delivery. After the seminal work by Leor et al., establishing alginate as a potential candidate for an injectable treatment for cardiac repair [7], it has been used extensively. Preservation or improvement in cardiac function has been observed in small animal models after injection of alginate in combination with fetal cardiomyocytes [97] and human mesenchymal stem cells [98], among others. Incorporating growth factors such as VEGF and platelet derived growth factor [99], insulin-like growth factor [100], and HGF [100] has been shown to increase neovascularization or attenuate infarct expansion and LV remodeling. Pre-clinical trials with alginate in a porcine MI model demonstrated that intracoronary injection of alginate alone could prevent or reverse negative LV remodeling. With this method, alginate is delivered into the coronary arteries and leaks through the vessels and into the myocardium [101]. Based on these successes, a "first-in-man" study was initiated to evaluate the safety and feasibility intracoronary injection of alginate in acute MI patients [102]. One of the primary limitations of alginate is that its delivery method – intracoronary injections – limits the relevant patient demographic to those whose coronary arteries can be accessed and have had a recent attack. Alginate requires excess of calcium and leaky vessels in order to form an intramyocardial gel, so it may only be used in cases of acute MI.

Decellularized ECM hydrogels reappear under this category because they can also be used as injectable scaffolds. As discussed, via methods first outlined by Freytes et al., decellularized ECM materials can be processed into an injectable scaffolds that are liquid at room temperature and form gels when brought to physiologic conditions. For cardiac

applications, ECM hydrogels derived from porcine SIS, porcine myocardium, and porcine and human pericardium have been investigated. Okada et al. investigated the efficacy of two forms of SIS-ECM hydrogels and found that one form improved fractional area change compared to both the other ECM gel and the control at 2 weeks post-treatment, and reduced infarct size and increased capillary density compared to the other ECM gel and the control at 6 weeks [103] With the rationale that a tissue-specific ECM scaffold would provide a more appropriate combination of biochemical cues, Singelyn et al. developed a myocardial matrix material derived from porcine cardiac tissue, which was shown to self-assemble into a fibrous gel upon injection [21], and preserve function in a small animal MI model [59]. Interestingly, histological staining of the self-assembled gel in vivo closely resembles the decellularized ECM prior to processing (Figure 1.4).

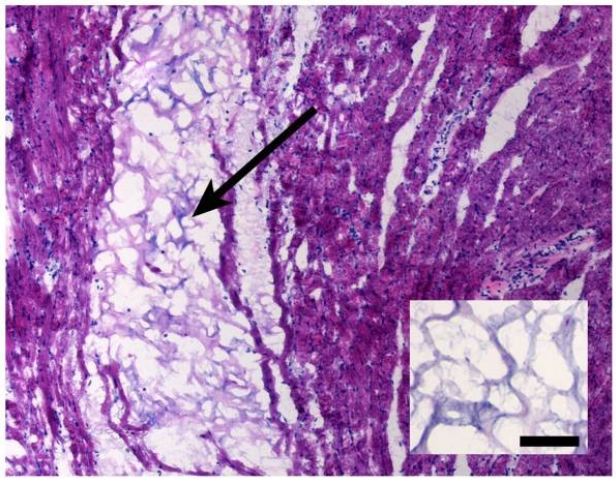

Figure 1.4: Injectable Extracellular Matrix Hydrogel. Here, a ventricular ECM derived injectable hydrogel has been injected in a healthy rat heart. Hematoxylin and eosin staining allows for visualization of the matrix injection (arrow). The inset at right shows the decellularized ECM prior to processing, which has a strikingly similar structure to the self-assembled gel *in vivo*. Modified from [21] and reprinted with permission.

When scaled up to delivery in a porcine MI model, percutaneous transendocardial catheter delivery of the myocardial matrix was successful, a benchmark for translation potential [59]. Seif-Naraghi et al. developed a potentially autologous ECM hydrogel from decellularized pericardium, establishing proof-of-concept by injecting this acellular scaffold in healthy rats and observing cell infiltration, specifically vascular cells. The authors also identified the presence of c-kit+ cells in the injection region, indicating the potential for recruiting resident progenitor cells [58]. Similarly, when an SIS-ECM suspension was injected in a rat MI model, identified a population of c-kit positive cells in the region. Additionally, the acellular injection alone promoted cell migration and improvement in cardiac function when compared to the saline control [57].

Other injectable scaffolds have been investigated; chitosan has been injected with and without cells [104, 105] as well as with bFGF [106], Matrigel has been delivered alone [56], gelatin and bFGF have been co-injected [107, 108], bio-inspired self-assembling peptides have been used to deliver insulin-like growth factor 1 and cardiomyocytes [90, 109] as well as autologous bone marrow mononuclear cells [110], these peptides have also been used for dual delivery of platelet derived growth factor and fibroblast growth factor [89].

All of the injectable scaffolds discussed thus far have been naturally-derived materials, but there have also been a number of interesting synthetic polymers used as injectable treatments. As mentioned, synthetic materials carry the advantage of being highly tunable with respect to degradation time, mechanical properties, and porosity. Additionally, the inherent batch-to-batch variability present in natural materials is

significantly reduced with synthetic polymers. Some examples of successful applications of synthetic polymers for cardiac repair include combination scaffolds based on PEG and poly(NIPAAm). As discussed, the degradation of these materials is a consideration; many synthetic scaffolds are modified to be enzymatically degraded *in vivo*. For example, matrix metalloproteinase (MMP)-degradable PEG hydrogel with thymosin B-4 and human ESCs [111] and MMP-depgradable PNIPAAM-co-acrylic acid hydrogels with bone marrow derived mononuclear cells have both been shown to improve cardiac function in small animal MI models [112].

While the exact mechanism by which these scaffolds are effective is unclear, a variety of hypotheses have been discussed, including that an appropriate degradation time may allow for resident cell in-growth and tissue remodeling, having a fibrous, porous microstructure may support the cell infiltration process, mechanical support may decrease stress on the ventricle, and finally, that degradation products of the naturally-derived materials discussed may offer biochemical cues for cellular migration and angiogenesis. Additionally, when these biomaterials serve as delivery vehicles for cellular cardiomyoplasty, there could be a synergistic effect that enhances benefit. Recently, attention has turned to elucidating these mechanisms. Ifkovits et al. investigated how material properties affect cardiac function and remodeling by injecting two different formulations of methacrylated hyaluronic acid (one at 8 kPa and one at 43 kPa) in an ovine MI model. Functional outcomes were not different between the two groups, but the stiffer hydrogel did reduce infarct area to a greater degree than the more compliant hydrogel [113].

Previously, computational modeling was used to try to predict how an injected material would affect the myocardial mechanics. Results of this work suggested that the increase in wall thickness provided by the presence of the bulk material would lead to a decrease in wall stress due to Laplace's Law and a subsequent improvement in cardiac function [114]. However, recent work by Rane et al. established that the presence of a bioinert material within the infarct wall did not prevent the negative remodeling process and was not sufficient to improve cardiac function despite increasing wall thickness [115]. Dobner et al. also injected non-degradable PEG hydrogel in order to investigate the effects on remodeling and found that by 13 weeks pathological progression was similar to that of saline [116]. Taken together, these results suggest that the structural support provided by a bulk material is insufficient to mitigate negative LV remodeling. Therefore, the biological properties, degradation properties, or other aspects of the material that encourage cell infiltration may be the mechanisms by which these materials are efficacious.

These examples represent only a few of the many promising approaches, and given the advances made over the last ten years, it is not surprising that materials have advanced both to pre-clinical large animal models and beyond to the initial stages of clinical trials [102]. Bearing in mind the goal of clinical translation, it is encouraging to see materials that are designed to be compatible with percutaneous transendocardial delivery via the catheters already in use. Alginate and the myocardial ECM hydrogel both have gelation properties conducive to these delivery methods [59, 101, 117],

potentially circumventing the need for the surgical procedures required for the placement of patches or the direct injection of other materials.

1.7 Future of cardiac tissue engineering

The past decade has seen tremendous growth in the field of cardiac tissue engineering. Most recently, injectable biomaterials have emerged as a promising alternative therapy that could potentially be delivered via minimally invasive methods, eliminating the need for risky surgical procedures. Improvement in our mechanistic understanding of both the pathophysiology of heart disease and the effect of these biomaterial-based tissue engineered approaches will drive the advancement of the field. As we begin to understand the mechanisms behind the success of these therapies, we will be able to establish true design criteria and start optimizing the strategies to meet relevant clinical needs.

1.8 Scope of the dissertation

This dissertation addresses key questions in the development of injectable biomaterial therapies for the prevention of heart failure post-myocardial infarction. With this work, a pericardial matrix hydrogel has been established as a potentially autologous biomaterial therapy for cardiac repair. To our knowledge, this was the first potentially autologous extracellular matrix derived biomaterial scaffold that may be deliverable via minimally invasive methods. The characterization described herein will inform the direction of future work with both ECM and hybrid materials, specifically with respect to

the delivery of growth factors for tissue engineering applications. The novel approach of using an ECM hydrogel for growth factor sequestration was investigated and the results will impact multiple areas of tissue engineering, as well as support the investigation of a novel growth factor candidate as a therapy for myocardial infarction. Additionally, the important issues regarding immunogenicity and safety are resolved – this information is necessary to justify the continued investigation of a variety of extracellular matrix hydrogels, as well as the translation into the clinic.

Chapter 1 provides an overview of the history and state of tissue engineering, discussed the currently available experimental therapies and their limitations, as well as introduced the design parameters for clinically relevant injectable scaffolds.

Chapter 2 describes the development and initial testing of a potentially autologous pericardial extracellular matrix hydrogel as an injectable material for cardiac repair. In these studies, processing and characterization of both human and porcine tissue was established and initial feasibility confirmed *in vivo*.

Chapter 3 describes the investigation of the hypothesis that the sulfated sugar content of an extracellular matrix hydrogel will allow for sequestration and prolonged delivery of growth factors for enhanced retention and effect *in vivo*. This hypothesis is explored using a model heparin-binding growth factor in a small animal MI study evaluating the potential for an ECM hydrogel to serve as a growth factor delivery platform by analyzing improvements in growth factor retention and its acute effects on angiogenesis.

Chapter 4 presents the results obtained from testing the hypothesis that the delivery of a novel hepatocyte growth factor peptide in an extracellular matrix hydrogel will provide enhanced benefit post-MI compared to delivery of the growth factor dimer or the ECM hydrogel alone. In this study we evaluate the therapeutic potential for delivery of HGF in the porcine pericardial matrix in a long term small animal functional study.

Chapter 5 describes our evaluation of the safety and biocompatibility of an extracellular matrix hydrogel for use in its intended application post-myocardial infarction. While the composition and behavior of most ECM hydrogels are very similar, the work presented in this chapter was done with myocardial matrix. This is also the material that is closest to clinical translation. In this chapter, data regarding safety, hemocompatibility, and the local tissue response at acute and chronic time points is presented.

Chapter 6 provides a summary and conclusion, as well as addresses study limitations and outlines recommendations for future work.

Chapter 1 is, in part, published as: Sonya B. Seif-Naraghi and Karen L. Christman. Tissue Engineering and the Role of Biomaterial Scaffolds: The Evolution of Cardiac Tissue Engineering. In (Eds. Regina Coeli dos Santos and Antonio Carvalho), Resident Stem Cells and Regenerative Therapy. Academic Press, Elsevier, Inc. 2012.

The author of this dissertation is the primary author of these manuscripts.

CHAPTER TWO:

Design and characterization of a potentially autologous injectable pericardial matrix gel

2.1 Introduction

Cardiovascular disease continues to be the leading killer in the Western world, being responsible for 1 out of every 2.8 deaths in the United States [118]. Heart failure (HF) following a myocardial infarction (MI) accounts for a majority of these deaths [118]. Lacking significant regenerative capabilities cardiac tissue is not repaired after ischemic injury [119] leading to negative left ventricular (LV) remodeling and subsequent heart failure [120]. Currently, the only successful treatment for end-stage heart failure post-MI is total heart transplantation, a treatment severely limited by a dearth of donor hearts and the risk associated with such an invasive procedure. Recently, tissue engineering approaches are providing exciting new possibilities.

Treatments such as cellular cardiomyoplasty [121, 122] and cardiac patches [123, 124] have been investigated, but each faces limitations such as poor cell retention and survival with the former or an invasive surgical procedure with the latter. Thus, there is still a need for a minimally-invasive solution that would mitigate negative LV remodeling, thereby preventing heart failure. Recent cardiac tissue engineering approaches have focused on designing injectable scaffolds for use in cellular and acellular therapies [123]. Investigated scaffold materials include fibrin [125, 126], collagen [127], alginate [128], chitosan [129], self-assembling peptide nanofibers [91, 130, 131], polyethylene glycol [23, 132, 133], Matrigel™ , and an extracellular matrix (ECM) gel derived from decellularized porcine myocardium [21]. All of these materials are injectable, but only Matrigel™ and the myocardial matrix gel mimic the extracellular matrix (ECM) with respect to complexity of biochemical composition, including proteins,

peptides, and polysaccharides that comprise the native ECM. Matrigel™, however, is limited in its clinical relevance since it is produced by mouse sarcoma cell lines and while the most attractive aspect of the myocardial matrix gel is that it provides tissue-specific ECM cues, it is also necessarily xenogeneic [21]. Although not for the application of cardiac repair, a similar injectable matrix scaffold has been made from decellularized urinary bladder matrix [134].

Porcine pericardium is another tissue commonly decellularized for use in various applications, conventionally used in gluteraldehyde-fixed bioprotheses. It is FDA approved for use in a variety of applications including stent covers [135], dural grafts [136], prosthetic valve materials [137], and in the repair of soft tissue defects [138-140]. As a fibrous sac chiefly composed of compact collagen layers interspersed with elastin fibers [141], the pericardium is generally used for its mechanical properties and convenient shape. Historically, the tissue decellularized to make patches and grafts, or produce ECM gels has been necessarily xenogeneic or allogeneic [142] as one's own small intestine submucosa, bladder, and cardiac tissue cannot be harvested in sizeable quantities without detriment. In contrast, a clinically attractive aspect of using pericardial tissue therapeutically is that the pericardium is not essential to life. No adverse consequences result from congenital absence or surgical resection [143]. During cardiothoracic surgery, the pericardium is routinely left unsutured when the procedure is complete and removing a small piece of this tissue poses little health risk to the patient. Autologous pericardium has been utilized in cardiac surgery due to its ready availability,

ease of handling, and low cost [144]. Applications have included mitral valve extension [145], aortic valve replacement [144], and even reconstruction of the left ventricle [146].

Thus, if the endogenous repair shown with porcine scaffolds – including cell infiltration and neovascularization, [11, 21, 142, 147] – can be achieved using a scaffold derived from this autologous source, it would provide a faster route to clinical translation, reducing regulatory concerns and avoiding any ethical, immunogenic, or disease transfer concerns associated with xenogeneic sources. In this work, the pericardium is identified as a potential source of autologous human ECM for use as an injectable cardiac tissue engineering scaffold. However, for the subset of patients where tissue can be collected at no additional risk, it is prudent to identify if this tissue can be processed consistently into a suitable scaffold. While the bulk of the studies discussed in this chapter were performed on a combined pool of material, it is necessary to determine if the tissue collected from any given patient could be processed and used in the same manner. It is understood that tissue composition changes with age and disease; some of the more well-documented age-related changes include the elastinization and loss of collagen in both human and porcine mitral and aortic valves [148]. While pericardial ECM composition has not been studied for age-related changes, it is not unreasonable to expect differences between patients of varied ages and pathologies. These differences may cause difficulty when working with human tissue or even prevent some human pericardial samples from being processed into injectable hydrogels.

The primary objectives of this study were to develop and characterize an injectable pericardium scaffold for cardiac tissue engineering applications. The

techniques described herein were first established with healthy, juvenile porcine tissue, but, given the attractiveness of an autologous therapy, it was of interest to determine if the same were possible with human tissue from a relevant demographic, in this case, patients with cardiovascular disease undergoing cardiothoracic surgery. In this study, the biochemical composition, *in vitro* chemoattractant potential, and *in situ* cellular infiltration of two injectable ECM scaffolds derived from decellularized porcine and human pericardial tissue are reported, demonstrating feasibility of two novel pericardial ECM gels to serve as *in vivo* scaffolds for cell recruitment and indicating proof-of-concept for an autologous biomaterial treatment for the myocardium. As a follow-up study, several human pericardium specimens were collected, processed, and compared with respect to material composition, gelation, degradation, and microstructure. In this way, we established that the inherent patient-to-patient variability would not prevent the application of this technology across a wide patient population.

2.2 Methods

All experiments in this study were performed in accordance with the guidelines published by the Institutional Animal Care and Use Committee at the University of California, San Diego and the American Association for Accreditation of Laboratory Animal Care.

2.2.1 Pericardial matrix hydrogel preparation

2.2.1.1 Tissue collection

Porcine pericardium samples were harvested from juvenile farm pigs weighing approximately 45-50 kg. Animals used for this purpose had previously been anaesthetized with isofluorane and immediately prior to harvest were euthanized with an overdose of Pentobarbital (90 mg/kg) administered intravenously. Human pericardium samples were collected from consenting patients scheduled for cardiothoracic surgery; the surgeon removed a small piece (approximately 4-5 cm^2) of tissue during surgery, in compliance with the University of California, San Diego Institutional Review Board. For the purposes of comparing human pericardium samples, specimens were selected from a wide range of patient demographics, as outlined in Table 2.2.

2.2.1.2 Decellularization

After dissecting away any adherent adipose tissue, fresh porcine and human tissues were decellularized using hypotonic and hypertonic rinses in deionized (DI) water and sodium dodecyl sulfate (SDS), an ionic detergent previously shown to decellularize pericardium [149]. Specifically, the porcine pericardium was first washed in DI water for 30 minutes, then stirred continuously in 1% SDS in phosphate buffered saline (PBS) for 24 hours, followed by a 5 hour DI water rinse. All human pericardia were first washed in DI water for 30 minutes, then stirred continuously in 1% SDS in PBS for 60-65 hours, followed by an overnight DI rinse. For both types of tissue, specimens were then removed from solution and again rinsed under running DI water. A small piece was

removed, fresh frozen in O.C.T. freezing medium, and 10 μm tissue sections were taken every 100 μm throughout the sample for verification of complete decellularization via histological analysis, as previously reported [149]. Briefly, hematoxylin and eosin (H&E) stains were performed and the tissue was examined for the absence of nuclei. For the initial fabrication and testing experiments, batched samples (multiple decellularized pericardia) were used. For the human pericardium comparison studies, 7 samples were kept separate for evaluation.

2.2.1.3 Preparation of injectable ECM

Injectable ECM was prepared via methods modified from previously published protocols for bladder [134] and myocardial matrix [21]. The decellularized pericardia (porcine and human) were lyophilized, ground into a coarse powder with a Wiley mini mill (Thomas Scientific, NJ) and then frozen until further use. Milled samples were pepsin-digested in 0.1 M HCl at a concentration of 10 mg ECM per 1 mL HCl. Pepsin (Sigma, St. Louis, MO) was used at a concentration of 1 mg/mL. The ECM powder was digested for 60-65 hours and neutralized to a pH of 7.4 with the addition of 1 M NaOH and 10x PBS. The resulting viscous solution, here called 'injectable ECM' was diluted with 1x PBS to the appropriate concentration.

2.2.2 Characterization of injectable ECM

One-dimensional gel electrophoresis was performed on human and porcine injectable ECM (7 mg/mL) compared to rat tail collagen type I (2.5 mg/mL; BD

Biosciences, San Jose, CA). The three solutions were run on a Tris-HCl, 12% polyacrylamide gel (Bio-Rad Laboratories, Hercules, CA) in Tris/Glycine/SDS buffer (Fisher Scientific, Hanover Park, IL) and 80mM reducing agent Dithiothreitol (DTT) (Invitrogen, Carlsbad, CA). NuPAGE Plus2 Prestained Standard (1x) (Invitrogen, Carlsbad, CA) was used as the protein standard; all other samples were stained with Imperial Protein Stain (Pierce, Rockford, IL). Samples were prepared and run in an XCell Surelock MiniCell (Invitrogen). GAG content of the injectable ECM was quantified using a colorimetric Blyscan glyocosaminoglycan assay (Biocolor, UK). Samples were run in triplicate.

To more fully characterize the protein content of the injectable ECM, tandem mass spectroscopy (MS/MS) was performed to identify the remaining proteins and peptide fragments. Injectable ECM samples were briefly pepsin-digested before analysis by liquid chromatography (LC)-MS/MS with electrospray ionization, using a QSTAR-Elite hybrid mass spectrometer (Applied Biosciences, Foster City, CA) interfaced to a Tempo™ nanoscale reversed-phase high-pressure liquid chromatograph (Applied Biosciences) using a 10 cm 180 ID glass capillary packed with 5 µm C-18 Zorbax^{TM} beads (Agilent Technologies, Santa Clara, CA). The buffer compositions were as follows: Buffer A was composed of 98% H_2O, 2% ACN, 0.2% formic acid, and 0.005% TFA; buffer B was composed of 100% ACN, 0.2% formic acid, and 0.005% TFA. Peptides were eluted from the C-18 column into the mass spectrometer using a linear gradient of 5–60% Buffer B over 60 min at 400 µl/min. LC-MS/MS data were acquired in a data-dependent fashion by selecting the 4 most intense peaks with charge

state of 2 to 4 that exceeds 20 counts, with exclusion of former target ions set to "360 seconds" and the mass tolerance for exclusion set to 100 ppm. MS/MS data were acquired from *m/z* 50 to 2,000 Da by using "enhance all" and 24 time bins to sum, dynamic background subtract, automatic collision energy, and automatic MS/MS accumulation with the fragment intensity multiplier set to 6 and maximum accumulation set to 2 s before returning to the survey scan. Peptide identifications were made using paragon algorithm executed in Protein Pilot 2.0 (Life Technologies, Inc, Carlsbad, CA). Detected peptide sequences were run against the swissprot databank for protein identification. Proteins were identified based on at least one peptide detected with a confidence of above 99% for that peptide identification. Additionally, a brief trypsin digest was performed on the injectable ECM samples and the LC-MS/MS repeated as described. All mass spectroscopy work was performed at the Biomolecular Mass Spectroscopy Facility at the University of California, San Diego (La Jolla, CA).

2.2.3 Migration Assay

Rat epicardial cells (RECs) (courtesy of Dr. David Bader) were cultured with Dulbecco's Modified Eagle's Medium (DMEM) with 10% FBS and 1% penicillin/streptomycin at 37 °C with 5% CO_2. These cells were grown on collagen coated plates and split 1:4 before use. Passage 6 cells were used for this study. Human coronary artery endothelial cells (HCAECs) were purchased from Cell Applications, Inc. (San Diego, CA), cultured with MesoEndo Cell Growth Medium (Cell Applications, Inc.), and split 1:2 before use; passage 6 cells were used in this study. Rat aortic smooth

muscle cells (RASMCs) were isolated as previously described [21, 150], cultured with DMEM plus 10% FBS and 1% penicilin/streptomycin at 37 °C with 5% CO_2. These cells were grown on collagen coated plates and split 1:4 before use and passage 7 cells were used. Prior to use, all cell types were serum starved for 15 hr in DMEM with 0.5% heat inactivated FBS and 1% penicillin/streptomycin. A Chemotaxis 96-well Cell Migration Assay Kit (Chemicon, Billerica, MA) was used as previously described [151, 152]. Five different chemoattractants were pipetted into the bottom well of a 96-well transwell plate: injectable human pericardial ECM at 4 mg/mL, injectable porcine pericardial ECM at 4 mg/mL, calf skin collagen Type I at 4 mg/mL, and 10% FBS in DMEM. Both the injectable ECM samples and the collagen were neutralized before use. RECs, RASMCs, and HCAECs were pipetted into the top chamber of the transwell plate and allowed to migrate toward the different solutions. Each condition was run in 5-7 wells. After a four hour incubation at 37 °C and 5% CO_2, the cells that had migrated through the membrane toward the bottom chamber were isolated, lysed and stained with Cyquant dye per the manufacturer's protocol. In order to determine if the cells preferentially migrated toward a certain chemoattractant, fluorescence was read at 480/560 in a Spectramax plate reader. Relative fluorescent intensities correspond to relative number of cells that migrated through the membrane toward any given chemoattractant.

2.2.4 Myocardial Injections

Injectable human pericardium and porcine pericardium ECM were neutralized and diluted to 6.6 mg/mL. Myocardial injections were performed as previously described

[21, 125]. Briefly, 90 µl samples were drawn up into a syringe and injected into the left ventricular free wall of adult male Harlan Sprague-Dawley rats (375-400 g) through a 30 gauge needle. The animals were euthanized and the hearts excised at either 45 minutes (human, n = 2; porcine, n = 2) or at 14-15 days (human, n = 4; porcine, n = 6). For all comparison studies, human pericardial matrix-injected animals were euthanized after 45 minutes, in order to address the question of whether or not all samples would for a gel *in vivo*.

2.2.5 Histological and Immunohistochemical Analysis

Hearts were fresh frozen and short axis cross sections were taken every 400 µm from apex to base throughout each heart. Sections were fixed with acetone and stained with hematoxylin and eosin (H&E) for histological analysis. Sections were examined under a light microscope to locate the injection region and identify the two sections in which the injection region area was largest in each heart.

Immunohistochemistry (IHC) was used to identify and quantify blood vessels that had formed in the injection region, as previously described [21]. Briefly, sections were costained with an anti-SMC antibody and FITC-labeled isolectin to identify smooth muscle and endothelial cells, respectively. The injection regions were outlined on the images and arterioles within the area were counted. c-Kit+ cells were also identified with a primary anti-c-Kit antibody (Santa Cruz Biotechnology, 1:100 dilution), and with an AlexaFluor 468 goat anti-mouse secondary antibody (Invitrogen, 1:200 dilution).

2.2.6 Rheometry

A TA instruments AR-G2 rheometer was used to test pericardial ECM gel rheological properties. Pericardial matrix gels were tested at 37°C using a 20 mm parallel plate geometry, with a 1.0 mm gap between plates. Three frequency sweeps from 0.1 to 50 rad/s were conducted with a constant strain of 2.5%, a value within the linear viscoelastic strain region (determined experimentally). Each gel was tested in triplicate, and the resulting values were averaged. Additionally, each sample was run in triplicate and a representative curve was obtained. The storage modulus (G') is reported at 1 rad/s.

2.2.7 Scanning electron microscopy

Environmental scanning electron microscopy (ESEM) was used to visualize the structure of the pericardial matrix gels. ESEM is preferred for hydrogels because a humid environment can be maintained and uncoated samples can be examined [153]. Gels were prepared for ESEM by fixation with 2.5% glutaraldehyde for two hours at 37 °C, followed by a serial dehydration in ethanol rinses (30 - 100%), as has been done previously with both decellularized tissue and gels made from natural materials [12, 16, 21, 154]. Images were taken with a Phillips XL30 Environmental SEM Field Emission microscope. Fiber diameter was evaluated by taking 20-40 measurements of fiber diameter per image. An average and standard deviations are reported for each sample.

2.2.8 In vitro degradation

To assess degradation properties of the different pericardial matrix gels, ninhydrin reactivity was evaluated after incubation with collagenase [155, 156]. Sets of 100 uL gels at 6 mg/mL (HP-A – E) or 8 mg/mL (HP-F and G) were formed overnight in microcentrifuge tubes. Collagen gels at a concentration of 2.5 mg/mL were used for comparison. Bacterial collagenase (Worthington Biomedical Corporation, Lakewood, NJ) at 100 U/mL in a 0.1 M Tris-base, 0.25 M $CaCl_2$ solution, at pH 7.4, was added to the gels. Gels were incubated with collagenase at 37 °C for 2, 4, 12, or 24 hours. Visual observations made throughout the incubation; at the end of the experiment, samples were centrifuged at 15,000 rpm for 10 min and the supernatant was reacted with 2% ninhydrin (Sigma-Aldrich) at 100 °C for 10 min. Samples were read on a BioTek Synergy 4 (BioTek Instruments, Winooski, TX) spectrophotometer at 570 nm.

2.2.9 Statistical Analysis

A two-tailed Student's t-test was performed on the *in vivo* vessel ingrowth data; one-way ANOVA was performed for migration assay data with a Holm's corrected t-test. Statistical significance was accepted at $p < 0.05$. Values are reported as the mean ± standard deviation.

2.3 Results

2.3.1 Preparation of injectable pericardial ECM

Porcine and human pericardium samples were decellularized immediately upon collection, frozen, sectioned, and stained for analysis. Decellularization was verified by histological analysis; H&E staining indicated an absence of nuclei as shown in Figure 2.1.

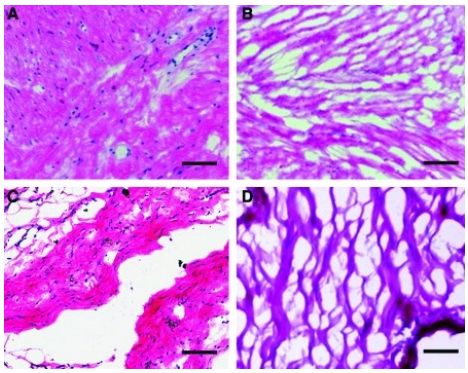

Figure 2.1: Histological analysis of pericardia. H&E stains of (A) fresh human pericardium, (B) fresh porcine pericardium, (C) decellularized human pericardial matrix, and (D) decellularized porcine pericardial matrix. Scale bar is 500 μm.

For clinical relevance, we determined percent yield for each material, as an indication of tissue source feasibility. Lyophilization of a 2-4 cm^2 piece of porcine pericardium yields approximately 20 mg of dry weight ECM; a similar sized piece of human pericardium yields 17-40 mg of dry weight ECM. Decellularized pericardium powder was partially digested with pepsin until the solution was visibly free of ECM particles, approximately 60-65 hours. This process is illustrated in Figure 2.2, with examples of pericardium at each point: fresh (Fig.2.2A), lyophilized (Fig.2.2B), milled (Fig.2.2C), and digested (Fig.2.2D).

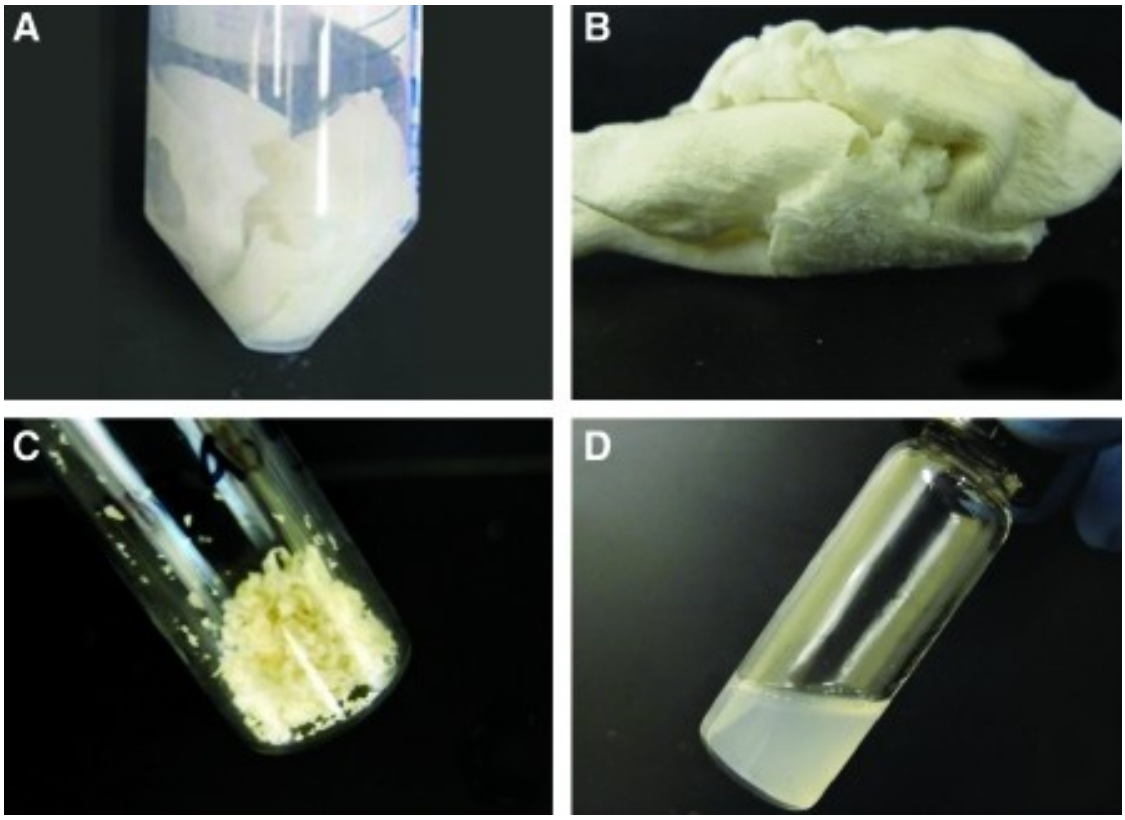

Figure 2.2: Tissue processing. Fresh human pericardium (A) was decellularized and lyophilized (B), milled into a powder (C), and then pepsin-digested (D).

2.3.2 Characterization of injectable pericardial ECM

Results of an SDS-PAGE gel comparing the protein and peptide composition of injectable human pericardial ECM, porcine pericardial ECM, and collagen indicate the presence of bands that match collagen in both pericardium samples, but also the presence of bands at lower molecular weights (Fig.2.3). This composition was investigated further with mass spectroscopy, which identified fragments of a variety of ECM proteins, outlined in Table 2.1 on the following page.

Table 2.1: ECM components identified with mass spectroscopy.

Identified Protein	HPM	PPM
Biglycan		x
Collagen I	x	x
Collagen II	x	x
Collagen III	x	
Collagen IV	x	x
Collagen V	x	x
Collagen VI		x
Collagen VII		x
Collagen VIII		x
Collagen IX	x	
Collagen X		x
Collagen XI	x	x
Collagen XII		x
Collagen XIII		x
Collagen XIV		x
Collagen XXII	x	
Elastin	x	x
Fibrillin		x
Fibrinogen	x	
Fibromodulin		x
Lumican		x
Tropoelastin	x	x

The various types of collagen reported account for fibrillar, FACIT, basement membrane, and short chain collagen, among others. Native pericardial ECM is primarily composed of collagen, elastin, and glycosaminoglycans (GAGs) [141]. The identification of an array of these fibers as well as supporting ECM proteins such as fibrillin and fibrinogen indicate that, even after processing, the injectable pericardial matrix retains a high degree of fidelity to the original ECM composition. Peptide fragments derived from proteoglycans were also identified, namely biglycan, which binds chondroitin or dermatan sulfate, lumican and fibromodulin, which bind keratan sulfate, and FACIT collagen (Type IX, XII, XIV), which associates with various GAGs. Using the Blyscan

Assay, GAG content of the injectable ECM was determined to be 125.9 ±6.6 and 136.5 ±1.1 µg GAG per mg of dry ECM for the porcine and human samples, respectively.

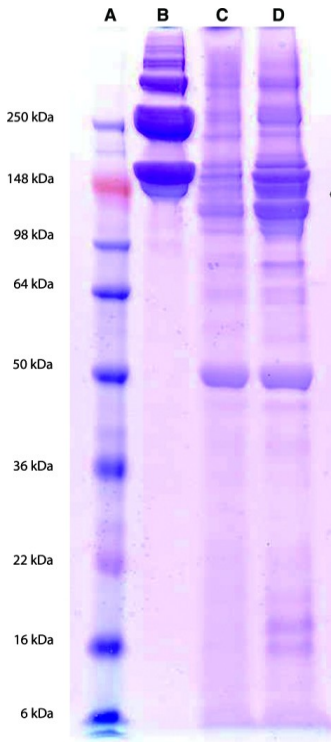

Figure 2.3: Polyacrylamide gel electrophoresis (PAGE) results. (A) Molecular weight standard. (B) Rat tail collagen Type I (2.5 mg/mL) compared to the injectable human (C) and porcine (D) pericardial ECM (7 mg/mL). Note the presence of collagen as well as several other proteins and peptides in the pericardial matrix samples.

2.3.3 In Vitro Migration Assay

Results of the *in vitro* migration assay indicated that the porcine pericardium was the preferred chemoattractant for all three cell types investigated – RASMCs, RECs, and HCAECs ($p < 0.05$). No cell type indicated a preference for the human pericardium over the positive control, FBS, which is a known chemoattractant for endothelial and smooth muscle cells [157, 158]. The level of fluorescence reported in Figure 2.4 corresponds to

the relative number of cells that have migrated through the transwell toward the different chemoattractants.

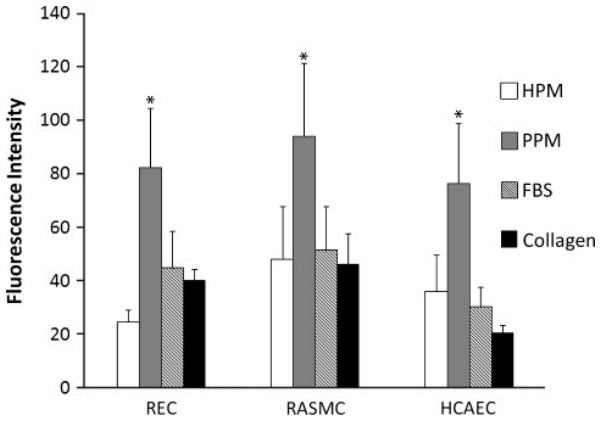

Figure 2.4: In vitro migration assay. RASMC, REC, and HCAEC migration toward injectable human pericardial matrix, porcine pericardial matrix, collagen, and 10% FBS. Values are based on fluorescence data – intensity correlates to the number of cells that have migrated through the transwell membrane toward any given solution. *$p<0.05$ compared to other groups.

2.3.4 Myocardial Injections

Injectable pericardial ECM was injected into the LV free wall of male Sprague Dawley rats at a concentration of 6.6 mg/mL. Both human and porcine pericardial ECM gelled within 45 minutes, the first time point at which hearts were excised for analysis. H&E sections (Fig. 2.5) show the area of gelled matrix *in vivo* – a fibrous, porous structure that gels interstitially, similar to findings reported for myocardial matrix [21].

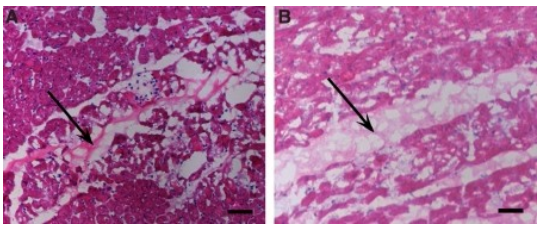

Figure 2.5: Myocardial injections: in vivo gelation. H&E stain of human (A) and porcine (B) pericardial matrix injections that have gelled *in vivo* after 45 minutes. Arrows denote matrix location, stained lighter pink than the myocardium. Scale bar is 500 μm.

Hearts were also collected after two weeks and examined for new vessel formation within the injection region. Representative images are presented in Figure 2.6 on the following page, with smooth muscle cells labeled in red and endothelial cells in green. While the migration assay data indicated that the porcine pericardium was a stronger chemoattractant *in vitro*, results from these *in vivo* studies indicate that the porcine and human pericardial matrix gels have similar potential for promoting neovascularization. Hearts injected with human and porcine pericardial ECM gels showed statistically equivalent ($p = 0.26$) number of arterioles after two weeks, 76 ± 13 vessels per mm^2 and 51 ± 42 vessels per mm^2, respectively.

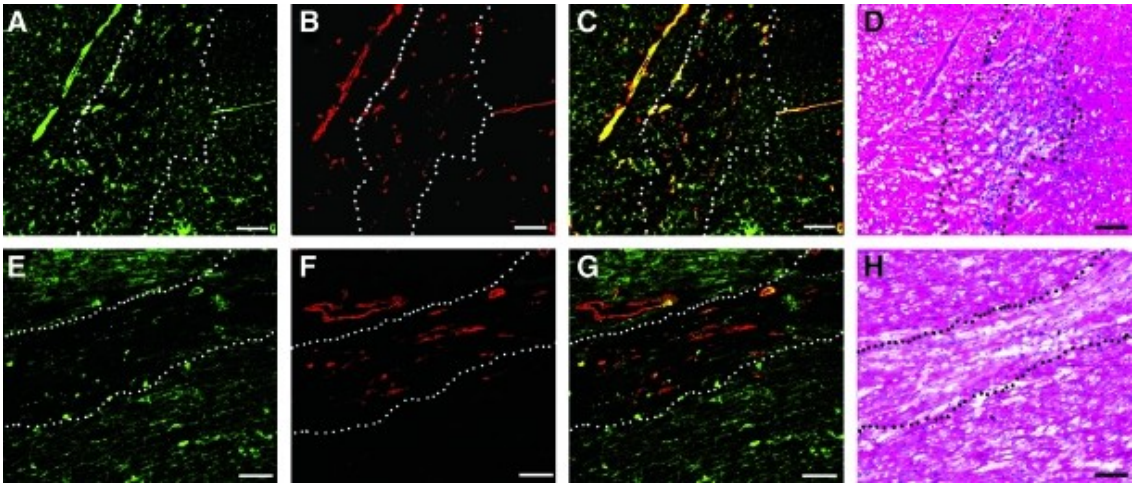

Figure 2.6: Vasculature infiltration. Fluorescent stains for vessels in the injected human (A-C) and porcine (D-F) matrix gels at two weeks. Endothelial cells are labeled green (A, D), while smooth muscle cells are labeled red (B, E). Merged images are shown in C and F. Scale bar is 100 μm. The white dotted lines indicate the area of matrix injection, as determined by H&E analysis of a nearby section.

Sections from the same injected hearts were also examined for the presence of stem cells, determined by a positive stain for c-Kit, a cluster of differentiation (CD) on the cell membrane of hematopoetic stem cells shown to differentiate into myocardial

precursors and vascular cells in the heart [54, 159]. c-Kit+ cells were found within the injection region in clusters, identifiable as green fluorescence in Figure 2.7. This phenomenon occured in very low numbers and was not quantified.

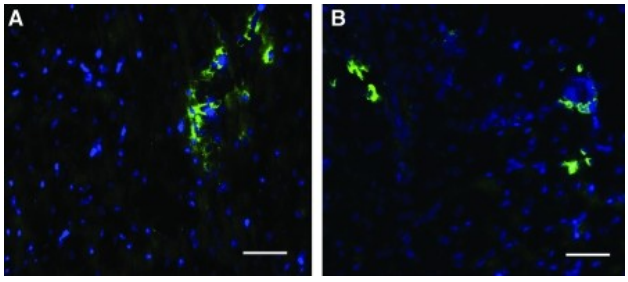

Figure 2.7: Stem cells within matrix injection region. A Hoescht stain for nuclei (blue) and c-kit (green) identifies stem cells in the human (A) and porcine (B) matrix injection regions. Scale bar is 50 μm.

2.3.5 Human pericardium comparison

2.3.5.1 Tissue collection and processing

Samples were collected from patients across a wide range of age and condition (Table 2.2). Each human pericardium sample presented differently upon gross examination. Samples varied in the amount of adipose tissue present, thickness, and size. After preparation for decellularization, all visible adherent adipose tissue was removed, as extant lipid content prevents material processing [160].

Table 2.2: Specimen Information. Information regarding the tissue sources for each sample. Mean donor age was 56 years. M, Male; F, Female; CABG, coronary artery bypass graft; PTE, pulmonary thrombo endarterectomy, AVR, aortic valve replacement.

Sample	Gender	Age	Surgery
HP-A	F	35	PTE
HP-B	M	86	CABG, AVR
HP-C	M	46	CABG
HP-D	F	59	PTE
HP-E	M	23	PTE
HP-F	M	66	CABG
HP-G	F	77	AVR

Previous results with multiple human pericardium samples demonstrated the efficacy of the decellularization method [161] and verification via H&E staining indicated a removal of nuclear material for all samples (Fig. 2.8).

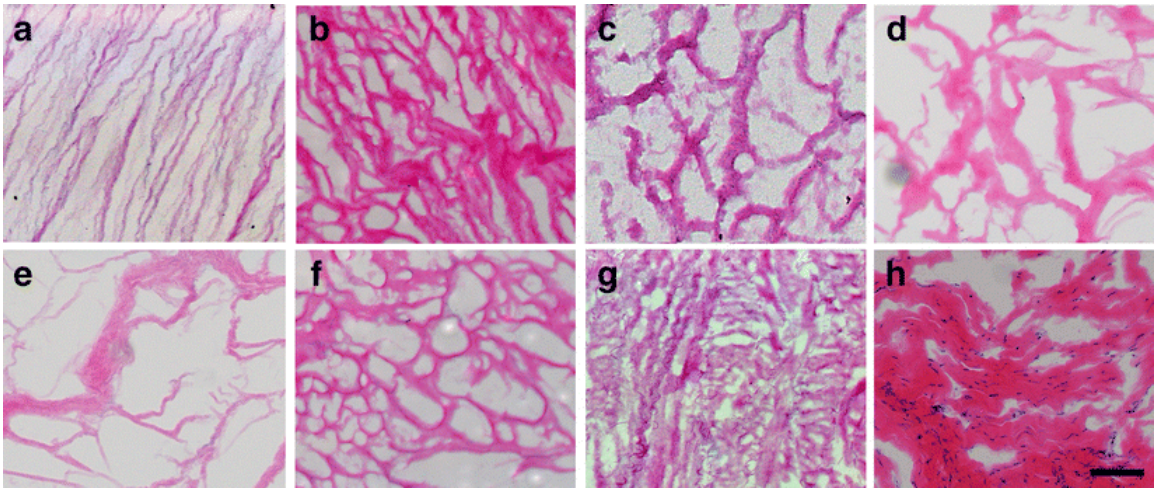

Figure 2.8: Decellularization verification. Hematoxylin and eosin staining on 10 µm sections of decellularized samples reveals a lack of nucleic material (A-G) in all seven human pericardium samples (HP-A through HP-G) compared to the section of a fresh sample of HP-A (H), scale bar is 1 mm.

After decellularization, all samples could be lyophilized and milled in a similar manner. Pepsin digestion was less consistently homogeneous than when working with porcine tissue, but with no discernable patterns between the gels. When brought to physiologic conditions, all samples except HP-F and HP-G form weak gels at a concentration of 6 mg/mL. HP-F and HP-G required a concentration of 8 mg/mL to gel *in vitro* at 37 °C. After digestion, it was observed that HP-F and HP-G were also less viscous than the other matrix materials.

2.3.5.2 Biochemical characterization

In order to elucidate potential differences in biochemical composition, the pericardial matrix materials were characterized and compared. According to a Blyscan Colorimetric GAG Assay, the human pericardial matrix samples range in sulfated GAG content from 10 ug/mg to 30 ug/mg dry ECM weight (Table 2.3). This is lower than previous results [161], perhaps due to variability in the extent of digestion seen with individual human samples. The SDS-PAGE gel pictured on the following page reveals the samples are not equal in protein content (Fig. 2.9). HP-F and HP-G do not have as defined bands and HP-D and HP-F appear to have less overall protein content, specifically less collagen I. Variable protein content is supported with the results of the ninhydrin assay described later.

Table 2.3: Glycosaminoglycan Content. Results of a colorimetric Blyscan assay for sulfated GAGs in the human pericardial matrix materials. All materials retain these carbohydrates, though the relative amount varies.

Sample	GAG (ug/mg)
HP-A	25 ± 2.7
HP-B	23 ± 3.3
HP-C	27 ± 2.3
HP-D	20 ± 4.1
HP-E	30 ± 3.2
HP-F	20 ± 7.4
HP-G	18 ± 5.5

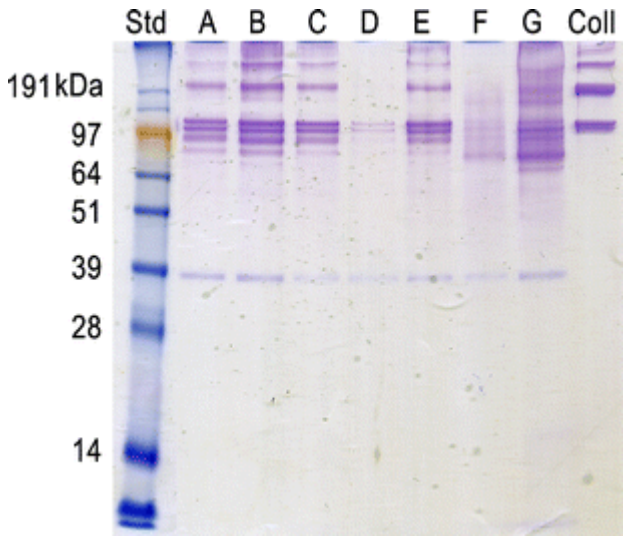

Figure 2.9: SDS-PAGE. An Imperial Protein stain of samples run on a poly-acrylamide gel indicates variable protein content, specifically lower collagen content in HP-D and HP-F.

Tandem mass spectrometry results indicate that all human pericardia samples retain components of structural ECM proteins and glycoproteins after processing (Table 2.4). These results correlate well with previously published results for human and porcine pericardia [161]. The characterization performed here indicates that the biochemical composition by mass spectrometry is comparable and while relative percentages cannot be quantified, basic components such as collagen I, collagen V, collagen VIII, elastin, fibrillin are retained across all samples. Other proteins present in most, but not all samples include collagen III, collagen IV, microfibrillar associated protein 4 (MFAP4), and procollagen I.

Table 2.4: MS/MS Results. A summary of the results of tandem mass spectrometry data is presented here. Presence of peptides identified from a wide range of ECM proteins and glycoproteins indicates the retention of these components after material processing.

Identified Protein	HP-A	HP-B	HP-C	HP-D	HP-E	HP-F	HP-G
Angiomotin			x				
Collagen I	x	x	x	x	x	x	x
Collagen II							x
Collagen III	x		x	x	x	x	x
Collagen IV	x		x	x	x	x	x
Collagen V	x	x	x	x	x	x	x
Collagen VI							x
Collagen VII	x			x	x		x
Collagen VIII	x	x	x	x	x	x	x
Collagen XI		x		x		x	
Collagen XII		x					
Collagen XIX							x
Collagen XXII	x						
Decorin				x	x		x
Dermatopontin	x			x			x
Elastin	x	x	x	x	x	x	x
Emilin							x
Fibrillin 1	x	x	x	x	x	x	x
Fibulin 2			x				
Follistatin		x					
Hemicentin					x		x
MFAP4	x		x	x	x	x	x
Procollagen I	x		x	x	x	x	x
Prolargin		x		x			
EGFR kinase substrate				x			

Some components appeared in only a few samples – collagen II, VI, XI, XII, XIX, decorin, dermatopontin, emilin, fibulin, follistatin, hemicentin, and prolargin. The extracellular matrix proteins identified include hemicentin, which forms track-like structures to facilitate directed cell movement [162]. Prolargin binds perlecan and collagens I and II [163]. Microfibrillar associated protein 4 (MFAP4) has a role in cell adhesion and intercellular interactions [164]. Fibulin-2 binds various extracellular ligands and calcium and has been shown to interact with laminin and perlecan [165-167].

Dermatopontin has a role in cell-matrix interactions and matrix assembly. Additionally, it may modify the behavior of TGF beta through interaction with decorin [168].

ECM glycoproteins and proteoglycans were also identified. Emilin (elastin microfibril interface located protein) is an ECM glycoprotein found in elastin-rich tissues; recombinant EMILIN-1 has been shown to be a very efficient ligand for cell adhesion of several cell types [169]. Follistatin, or activin binding protein, is an autocrine glycoprotein [170, 171]. Another glycoprotein, fibrillin is essential for the formation of elastic fibers – it is secreted into the ECM and becomes incorporated into the insoluble microfibrils that provide a scaffold for elastin deposition [172-174]. Decorin is a proteoglycan that consists of a protein core containing leucine repeats with a glycosaminoglycan [175] chain consisting of either chondroitin sulfate [118] or dermatan sulfate (DS); it binds to type I collagen fibrils and plays a role in matrix assembly [176]. Decorin has also been shown to influence fibrillogenesis, interact with fibronectin, epidermal growth factor receptor (EGFR) and transforming growth factor-beta (TGF-beta) [177, 178].

Other components identified include EGFR kinase substrate, which binds to EGFR and enhances EGF-dependent mitogenic signals and angiomotin, which increases migration of endothelial cells toward growth factors [179]. Peptide mass distributions were analyzed and all samples except HP-B have similar curves. HP-B is shifted to the left – there were more small peptides (< 2 kDa) resolved by the mass spectrometer than in the other samples (Fig. 2.10).

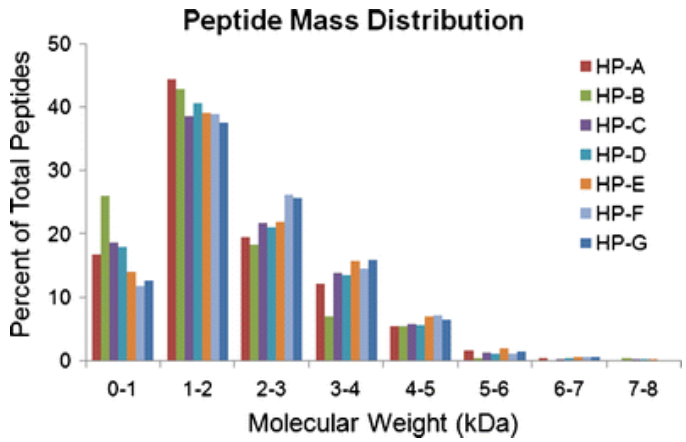

Figure 2.10: Peptide mass distribution. Precursor mass information for all peptides was derived from the MS/MS data, here binned in 1 kDa increments to identify differences in the mass distribution, such as the left-ward shift of peptides in HP-B.

2.3.5.3 Structural and mechanical characterization

After determining that there were slight variations in the biochemical composition, it was interesting to investigate if that would have any effect on the structure and mechanical properties of the materials after gelation. Electron microscopy allowed for the visualization of the fibrous microstructure of the matrix gels. Samples HP-F and HP-G did not gel *in vitro* at 6 mg/mL, so SEM was performed on gels from 8 mg/mL samples. Figure 2.11 shows representative images from the different gels, all illustrating a fibrous mesh. Fibers were on the order of 200 nm. While fiber size varied throughout each sample, the different specimens were similar when compared to each other ($p = 0.19$) implying the differences in biochemical composition did not prevent similar self-assembly.

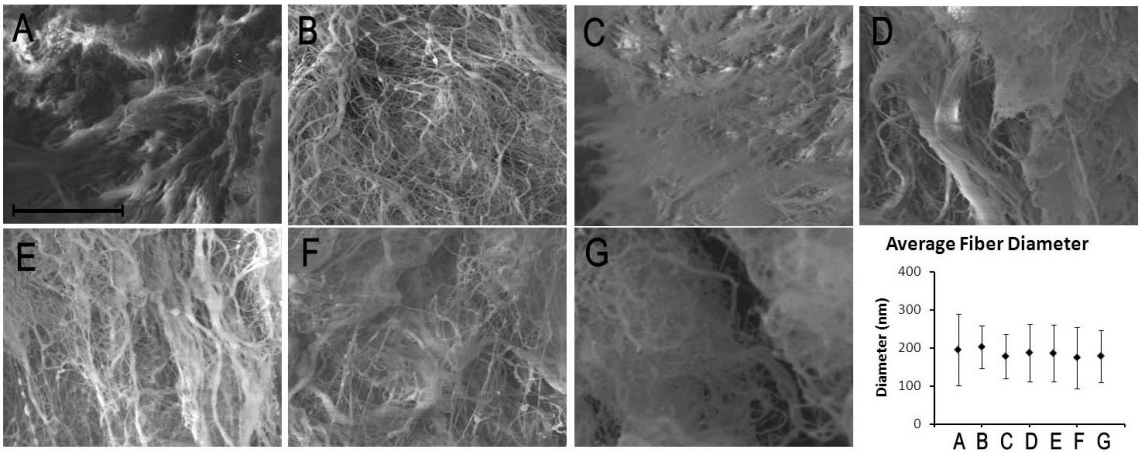

Figure 2.11: Scanning electron microscopy. ESEM images reveal a fibrous network in each sample (A-G). Quantification of fiber diameter (H) reveals no statistical difference across samples – all with approximately 200 nm fibers ($p = 0.19$). HP-A through HP-E (A-E) were gelled at 6 mg/mL and HP-F and HP-G (F, G) were gelled at 8 mg/mL. Fiber diameter data shown as mean ± standard deviation.

Parallel plate rheometry revealed that all seven samples form relatively weak gels, with average storage moduli (G') ranging from 2.1 to 6.9 Pa (Fig. 2.12) and average loss moduli (G") from 0.5 to 1.1 Pa. HP-F and HP-G did not gel *in vitro* at 6 mg/mL, so rheometry was performed on 8 mg/mL samples. These values were comparable to the other samples that formed gels at 6 mg/mL. Due to high variability within each sample, no significant differences were observed when comparing average G' ($p = 0.06$).

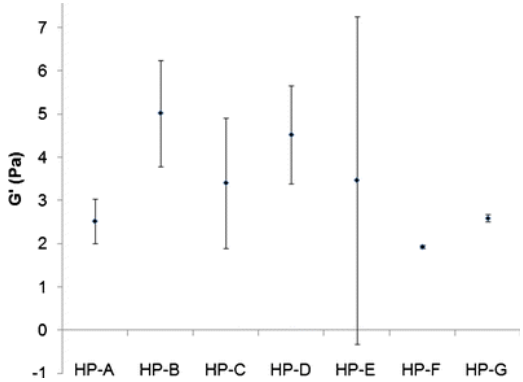

Figure 2.12: Storage modulus. Due to high variability within each matrix gel sample, all samples are statistically similar ($p = 0.06$). HP-F and HP-G were gelled at 8 mg/mL, all other samples were gelled at 6 mg/mL. Data is presented as mean ± standard deviation.

2.3.5.4 Scaffold degradation

Using a ninhydrin reactivity assay to determine the extent of degradation after collagenase treatment *in vitro* allowed for the analysis of degradation patterns in the gels formed from the different tissue samples. Collagen gels (2.5 mg/mL) were used as a control for comparison. In the presence of collagenase, ninhydrin reactivity peaked for all samples after 12 hours at 37 °C (Fig. 2.13); no further reactivity was seen at 24 hours (data not shown). Even after complete collagen degradation, remnants of the gels remained, indicating the presence of other structural ECM components. No visible material remained in the collagen gels after 12 hours. Total ninhydrin reactivity varied across the samples, implying the protein content varied. Specifically, ninhydrin reactivity was lower for HP-D and HP-F, the same samples with an observed decrease in protein content compared to the other samples on the SDS-PAGE gel. Data for the 2-hour time point for samples HP-F and HP-G were not gathered due to insufficient material.

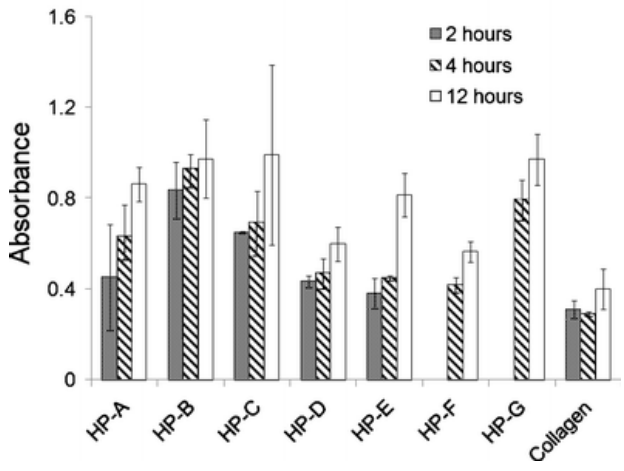

Figure 2.14: Degradation. Ninhydrin reactivity after 2, 4, and 12 hours of incubation with collagenase. Absorbance values indicates a variable protein content across the gels, though the samples degrade in a similar fashion.

2.3.5.5 *In vivo* scaffold formation

While all of the matrix samples formed gels *in vitro* at 37 °C, albeit two at a different concentration, we explored whether gelation would occur with the 6 mg/mL concentration *in vivo*. After injection in the LV free wall of a rat, H&E stained sections of excised tissue were examined for presence of the pericardial scaffold. All seven pericardial matrix samples formed porous scaffolds *in vivo* similar to what we previously reported with porcine pericardium matrix and pooled human pericardial matrix [161] (Fig. 2.15). Average pore size ranged from 25 to 35 µm, consistent with previously published work with other decellularized tissue matrices [21]. The interstitial spread of gels varied, a consistent result based on previous work with similar materials. Due to the small sample size, no conclusions could be drawn with respect to whether or not the varied collagen content or donor age contributed to the differences observed in the *in vivo* gelation.

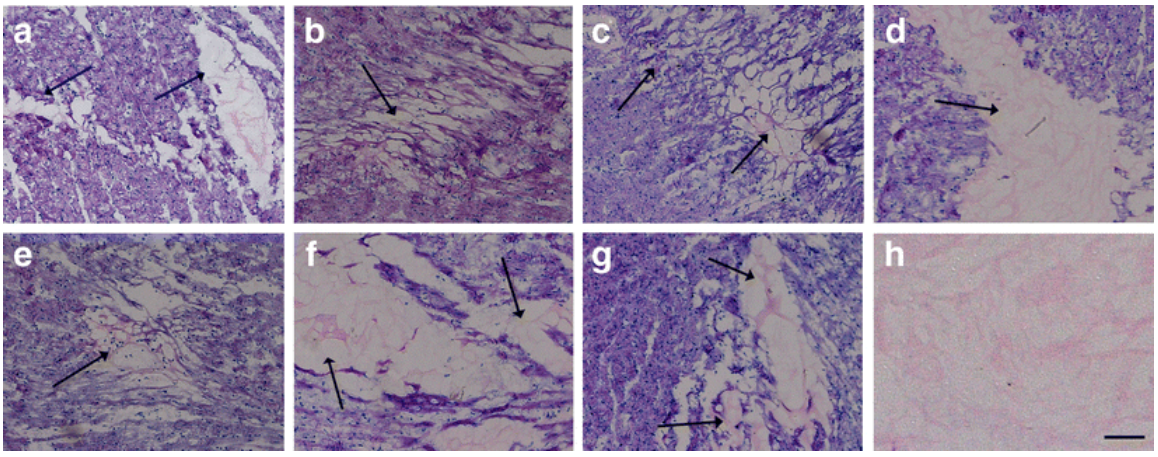

Figure 2.15: *In vivo* gelation. Hematoxylin and eosin stain of the injection region identified on a short-axis cross-section. Within 45 minutes of injection, all materials form a porous gel visible with H&E. Arrows indicate injection region. Scale bar is 1 mm (A-G); scale bar is 500 µm (H).

2.4 Discussion

In order to overcome limited endogenous repair after ischemic injury in the myocardium and prevent the negative remodeling that leads to heart failure, a clinically relevant tissue engineering solution is needed. The ideal tissue engineered scaffold would need to do the following: provide appropriate physical and biochemical cues, recruit cells to promote neovascularization and reduce fibrosis, and enhance the ability of resident and circulating stem cells to regenerate healthy cardiac tissue. Evidence of an increased number of cardiac progenitor cells present in damaged hearts [54] supports the understanding that regeneration could occur if the infarct environment were modified to be conducive to the recruitment, retention, and maturation of these cells [180]. Additionally, the ideal scaffold would be autologous and deliverable via minimally invasive methods.

Cardiac tissue engineering strategies have employed a diverse range of natural and synthetic materials, alone or in combination with various cell types, from skeletal myoblasts and cardiac fibroblasts to stem cells, in hopes of achieving regeneration [121-123, 181, 182]. What these materials attempt to provide is a 3D microenvironment, or mimic of the ECM, to encourage myocardial regeneration. The native ECM is a complex, interconnected, and interdependent network of fibrous proteins, proteoglycans, glycosaminoglycans, and other supporting molecules [7, 8, 142]. Its composition changes with age and plays a significant role in tissue development [183, 184]. By providing the necessary microenvironment, the ECM plays a role in the regulation of many cellular activities, including migration and differentiation [7, 8, 185]. In order to fulfill these roles

and promote a regenerative response, a tissue engineered scaffold must be similarly capable of providing diverse biochemical cues. As such, the use of decellularized tissue-derived materials is attractive.

Decellularized matrix materials, including sheets of porcine pericardium, have been shown to promote endothelial cell infiltration *in vitro* [186, 187]. As functional materials, decellularized ECM scaffolds can encourage endogenous repair upon implantation or injection [142]. For example, a myocardial matrix gel and cardiac patches made from small intestine submucosa and bladder matrix promote neovascularization and cell infiltration *in vivo* [11, 21, 147]. This effect is likely enhanced by the biodegradable nature of tissue-derived scaffolds; degradation products of ECM components have been shown to have chemoattractive potential [8, 151, 188-191]. Moreover, collagen- and proteoglycan-derived fragments have been shown to be chemotactic for a variety of cell types [192-194]. A major limitation however shared by all of these decellularized materials is that they are typically derived from xenogeneic or allogeneic sources. This raises concerns regarding issues such as disease transfer and immunogenicity. For these reasons, among others, an autologous approach is more attractive from a clinical perspective. Using a patient's own tissue to produce a tissue engineering scaffold that encourages similar endogenous responses – specifically neovascularization and cellular infiltration – would provide a faster route to clinical translation.

With these guidelines in mind, the pericardium was investigated for its potential as an injectable tissue engineered scaffold for cardiac repair. Porcine pericardium is a commonly used biomaterial and has been shown to be especially useful for valve

replacements [137] and wound healing applications [195, 196], thus it was a strong candidate for development as an injectable scaffold for cardiac repair. The investigation of pericardial tissue is of great clinical interest because human pericardium can be surgically resected without adverse consequences and is therefore a potential source for an autologous scaffold. The protocol and techniques described herein were first established with porcine tissue. When it was determined that an injectable matrix gel made from porcine pericardium would gel *in situ* and promote neovascularization upon injection in the LV free wall, we next investigated human pericardium, since it has the distinct advantage of being autologous. While the composition of the pericardial ECM is similar in the porcine and human specimens, the former was collected from young, healthy animals, while the latter was donated by significantly older, diseased individuals; it was thus hypothesized that these differences may reduce the chemoattractive potential and regenerative capacity of the human tissue. The results of the *in vitro* migration assay supported this hypothesis – all cell types preferentially migrated toward the porcine pericardial matrix, while no increase in migration was seen toward the human pericardial matrix with respect to the positive control, FBS. *In vivo*, however, the two materials performed similarly – the human pericardial matrix gel allowed for comparable vessel ingrowth. This is potentially due to a slight inflammatory response as a result of injection injury and the structural properties of the gelled matrix that encouraged cell infiltration, as well as other complex *in vivo* conditions not represented in the *in vitro* assay.

Clinical relevance of this material was evaluated by an array of considerations including percent yield, induction of neovascularization *in vivo*, and ease of clinical

translation. When determining percent yield, or what injection volume could be produced from a small (< 4 cm^2) piece of pericardium, this tissue size was found to be sufficient for 3 mL of injections, indicating feasibility for treating an MI. As discussed, both materials allow for cellular infiltration and arteriole formation within two weeks. With respect to ease of translation, decellularized porcine pericardium is already FDA approved for use in humans and has a well established history as a biomaterial. As a potentially autologous avenue, human pericardium can be surgically resected without adverse consequences; thoracoscopic pericardiectomy is a minimally invasive procedure for removal of the pericardium. It should be noted that while pericardial tissue comprises the functional portion of the pericardial matrix gel, for a fully autologous therapy, the pepsin used to digest the matrix should likewise be autologous. To this end, pepsin can be isolated in relevant quantities from patient gastric juice collected via nasogastric aspiration, thereby ensuring that all biological components are autologous [197]. The material developed here could be administered as an acellular scaffold, or in conjunction with cells such as adult stem cells, induced pluripotent stem cells, or other autologous cell types.

With this work, we demonstrate proof-of-concept for the use of decellularized porcine and human pericardial matrix gels as injectable scaffolds for cardiac repair. *In vitro*, porcine pericardial matrix gels promoted cellular migration while human pericardial matrix gels did not promote migration when compared to known chemoattractants [161]. Upon injection into the LV free wall of healthy rats, however, the human pericardial matrix gels facilitated a similar degree of vascular cell infiltration and arteriole formation at 2 weeks, implying the *in vivo* effect may be driven more by the

fibrous, porous structure. In these initial proof-of-concept experiments, pericardial tissue was identified as a potential source of autologous ECM for use as a biomaterial scaffold [161].

This assertion, however, that an injectable form of human pericardial tissue could be a potentially autologous scaffold for myocardial tissue engineering, requires assessment of the patient-to-patient variability. In a follow up study, seven human pericardia from a relevant patient demographic – those undergoing a thoracic surgery where the pericardium was accessed – were processed into injectable matrix materials that gel when brought to physiologic conditions. The resulting matrix gels were compared with respect to their protein composition, glycosaminoglycan content, *in vitro* degradation, *in vivo* gelation, and fibrous microstructure. In order to serve as an injectable scaffold, each matrix gel needed to be able to be processed into an injectable form, self-assemble when brought to physiologic conditions, and form a fibrous, porous network *in vivo*. By fulfilling these criteria, the matrix gels can serve as structural and biochemical scaffolds to support the infiltration of cells and revascularization of the damaged region in order to mitigate negative remodeling post-MI.

It was expected that there would be variability between the tissue samples, as the donors ranged in age and condition. Tissue changes with age, both in composition and material properties. For example, investigation of age-related changes in the mitral and aortic valve revealed that with age the collagen content of the valve decreases, the valves thicken and GAG and elastin content increase dramatically [148]. Significant age-related differences exist in the material properties of these valves as well [198]. Additionally,

while the effect of disease on the composition of pericardial ECM has not been examined, changes in the composition of pericardial fluid have been characterized. It has been shown that growth factors such as basic fibroblast growth factor (bFGF), acidic fibroblast growth factor (aFGF), hepatocyte growth factor (HGF), and vascular endothelial growth factor (VEGF) accumulate in the pericardial fluid in patients with ischemic heart disease [199]. Pericardial fluid from these patients has also been shown to have significant effects *in vitro* – accelerating growth of vascular smooth muscle cells and inducing myocardial cell and vascular endothelial cell apoptosis [199]. Several other disease states can cause inflammation in the pericardium – infections, malignancies, rheumatologic disorders, and uremia. In these cases, the pericardial fluid volume increases and composition may become purulent, exudative, or frank blood [200]. All of these changes could also affect the pericardium and unfortunately, little is understood about the composition of healthy human pericardial tissue; it is therefore difficult to ascertain the effects these disease states and the changes in pericardial fluid have on the composition of the pericardial ECM.

The characterization performed here allowed for a broad comparison of conserved proteins and glycoproteins. While a powerful tool for identification of peptides in a complex sample, mass spectrometry is limited by how well the peptides ionize, crosslinking that causes branched regions and any significant methylation. It is important to acknowledge that mass spectrometry is not an exclusive determination of composition, but it is one of the only ways to start fully characterizing complex samples. Here, we found retention of basic structural ECM components across all samples and the presence

of a variety of other protein and glycoprotein components in some of the samples, indicating retention through the material processing steps. Variation was also found in the peptide mass distribution – HP-B was shifted to the lower masses, indicating it was comprised of smaller peptides (Fig. 2.11). This may be due to an over-digestion of the sample. Since all samples were processed identically, this could be reflecting a property of the composition of HP-B, that it was prone to degradation or digestion more so than the other samples. Peptide mass distribution for HP-F and HP-G were slightly shifted toward the higher masses, indicating they were comprised of larger peptides. These slight differences may contribute to the differences in variability observed in the rheological characterization (Fig. 2.13). The reduced variability in samples HP-F and HP-G could be due in part to the decreased collagen content, the increased concentration, or the potentially shifted peptide mass distribution. If the mass spectrometry data reflects true differences between the samples, it supports the prediction that there will be patient-to-patient variability.

Mass spectrometry provides no quantification of the different proteins. Varied protein content is, however, apparent with the results of SDS-PAGE and the ninhydrin assay. Decreased collagen content in HP-F and HP-G most likely caused the need to increase the concentration from 6 mg/mL to 8 mg/mL to achieve *in vitro* gelation. However, the histological sections taken after *in vivo* injections into a healthy rat heart indicate that each pericardial matrix material can form a gel *in vivo* even at the lower concentration. This is consistent with previous work with this material and other injectable matrix materials [21, 161].

Characterization of the microstructure of gels formed *in vitro* reveals a similarly fibrous structure across all samples, implying the self-assembly process for the different matrix samples may be similar, despite differences in composition. The gels collapsed upon preparation for SEM and so porosity could not be quantified, but the average fiber diameter is not statistically different between samples. Fiber diameter has been implicated in a variety of effects *in vitro*, including cell attachment, migration, and spreading [201-203]; the similar fiber diameter in the matrix gels may imply that cell infiltration will be similarly facilitated across all samples. While it could not be quantified via SEM, the H&E stained sections illustrate the porosity of the gels formed *in vivo*; the average pore size is approximately 25-35 μm, within a range previously identified as ideal for cellular and vascular infiltration [8, 53, 204, 205]. The importance of porosity has been demonstrated repeatedly [206-211], suggesting the structure of these gels is an important factor in determining their success as injectable scaffolds.

Additionally, since degradation products have been implicated as contributing to the chemotactic nature of decellularized tissue scaffolds [151] and the degradation rate of tissue engineered scaffolds is known to affect cell infiltration [212, 213], it is important to note that the degradation patterns for the different materials are also similar. After 12 hours, no additional ninhydrin reactivity was recorded – the collagenase had fully degraded the parts of the gel it could degrade. Gels with lower total ninhydrin reactivity at 24 hours contain a relatively lower collagen concentration compared to the other gels; this was true for HP-D and HP-F, which correlates with the decreased protein content observed with SDS-PAGE. The increased ninhydrin activity compared to a 2.5 mg/mL

collagen gel indicates the presence of additional peptides in the HP samples. With respect to the pattern of degradation over time, however, all HP gels behaved similarly – partially degraded at 2 hours and 4 hours and considered fully degraded after 12 hours. The similarities observed may be due to the similar structural properties of the gels moderating enzymatic activity.

As injectable materials derived from decellularized tissue continue to be developed for use as therapies, it will be of utmost importance to determine the short and long-term effects of the materials on the host immune system. Using xenogeneic tissue raises concerns about immunogenicity, but by establishing an autologous source for a complex, tissue-derived scaffold, these concerns can be circumvented. It is important to note here that in order to be a fully autologous therapy, the pepsin used in the processing methods would need to come from the patient. This is feasible, as human pepsin has been isolated in an active form from gastric juice [214]. Relevant quantities can be acquired via minimally invasive measures during the same procedure in which pericardium is harvested.

There is no doubt that working with human tissue is less consistent than working with porcine tissue; however, we have successfully applied a protocol to decellularize, process, and gel seven different human pericardium samples with similar results. The seven donors varied broadly with respect to age and condition, allowing for the evaluation of a wide range of representative pericardia. If future results reveal that the concentration of collagen or other components is important for cellular recruitment, each sample may require optimization of ECM concentration. If it is determined that over- or

under-digestion is an important factor, this may also need to be optimized for each sample. Based on previous studies and current cardiomyoplasty clinical trials, even a conservative estimate of the quantity of pericardial tissue that can be collected (4-5 cm^2) will provide significantly more material than would be injected therapeutically, allowing material to be used for optimization.

Thus, first, we demonstrated proof-of-concept for the use of decellularized pericardial matrix gels as injectable scaffolds for cardiac repair [161]. Porcine and human pericardial ECM gels were shown to be injectable and therefore potentially deliverable via currently used, minimally invasive methods, to promote neovascularization *in vivo*, and to allow for stem cell infiltration. With the second part of this work, we examined the effects of inter-patient variability on the processing, composition, and material properties of the matrix gels. Tissue from seven patients spanning a wide range of ages and conditions was examined in order to investigate the applicability of this approach across a broad patient population. The patients were selected from a relevant demographic and the tissue was processed in an identical fashion. Comparison of the samples revealed similarities with respect to composition, rheological properties, fibrous microstructure, gelation and degradation. Collagen content varied from sample to sample; in samples with less collagen *in vitro* gelation was only achieved after raising the concentration to 8 mg/mL but all samples gelled *in vivo* at 6 mg/mL. It is concluded that, while not identical, human pericardium samples across a wide patient population can all be processed into injectable scaffolds for cardiac repair. With clinical translation as the

ultimate goal, the pericardium is a strong candidate for cardiac tissue engineering since it has potential to be an autologous therapy.

Chapter 2, in part, is published as the following two papers: Sonya B. Seif-Naraghi, Michael Salvatore, Pam Schup-Magoffin, Diane Hu, Karen L. Christman. Design and characterization of an injectable pericardial matrix gel: a potentially autologous scaffold for cardiac tissue engineering. Tissue Engineering: Part A. 2010. 16(6): p. 2017-27 and Sonya B. Seif-Naraghi, Dinah Horn, Pam Schup-Magoffin, Michael M. Madani, Karen L. Christman. Patient-to-patient variability in autologous pericardial matrix scaffolds for cardiac repair. Journal of Translational Cardiovascular Research. 2011.

The author of this dissertation is the primary author on these publications.

CHAPTER THREE:

Extracellular matrix hydrogel as a growth factor delivery vehicle

3.1 Introduction

In many disease states – myocardial and peripheral ischemia, diabetic ulcers, retinal diseases, chronic wounds, etc. – the pathology is caused by a reduced blood supply [215]. This causes cell death in the downstream tissue, followed by degradation of the associated extracellular matrix. Tissue engineering approaches, designed to mitigate the damage and promote healing or regeneration, focus on eliciting angiogenesis and remodeling of the damaged region. This remodeling can be achieved by encouraging endogenous cell infiltration into an acellular biomaterial or by delivering exogenous cells; in both cases, the goal is to encourage repair and contribute to the function of the organ. In order to do this, many tissue engineering strategies have attempted to design materials to mimic the structure and composition of the native extracellular matrix (ECM) [97, 216-218]. As has been discussed, scaffolds derived from the native ECM of decellularized tissues have been developed and used in tissue engineering applications [15-17, 21]. These materials can be used intact as three-dimensional implantable scaffolds, as well as processed into injectable hydrogels that self-assemble *in situ*. When implanted or injected *in vivo*, previous work has demonstrated that these materials provide a template for cell infiltration and neovascularization [219-221]. In the case of cardiac repair, injectable ECM-derived hydrogels from decellularized small intestinal submucosa and the myocardium have been explored [20, 21, 222]. Injected alone into an infarct in small animals, these materials promote cell infiltration and have also been shown to preserve cardiac function post-myocardial infarction (MI) [20, 222]. While the mechanisms behind their effectiveness *in vivo* have yet to be fully elucidated, it is clear

that ECM-derived hydrogels provide porous, fibrous scaffolds that allow for cellular infiltration and neovascularization in ischemic regions.

In addition to their use as biomaterial only therapies and cellular delivery platforms, tissue engineered scaffolds can also be used to deliver bioactive moieties such as growth factors. Therapeutic angiogenesis via administration of angiogenic factors, such as vascular endothelial growth factor (VEGF) and basic fibroblast growth factor (bFGF), has specifically been investigated in a variety of disease models including myocardial and peripheral ischemia [30, 31, 223-226], and wound repair [32, 33, 227-230]; a number of good reviews have been written on the topic [34, 35, 66, 215]. Restoring blood supply has been demonstrated to have positive effects; for example, using growth factors for cardiac repair has demonstrated that inducing angiogenesis may preserve endogenous cardiomyocytes and functionally contractile myocardium post-MI [60-62]. To harness this potential, growth factor delivery systems have been designed to deliver these proteins to infarcted tissue. Growth factors, such as VEGF and bFGF have been immobilized within delivery systems based on synthetic polymers such as poly(ethylene glycol) [23] [35, 231] and poly-NiPAam [232-234], as well as naturally derived polymers such as collagen [50, 65] and hyaluronic acid [34, 35, 66]. Other delivery systems involve self-assembling peptides [67] or hybrid materials. Most systems either incorporate biomolecules that associate with growth factors natively, such as heparin or heparan sulfate [68, 69] or use derivatives that include highly sulfated sugars [70] or heparin-like growth factor binding domains [71, 72]. Previous work has demonstrated the advantage of immobilization over physical entrapment or bolus

injection, as it increases growth factor stability and localizes the effects to the site of treatment [73]. Unfortunately, the modifications used to increase growth factor activity or stability may change the chemistry of many natural biopolymers and therefore change their activity *in vivo* [235]. Natively, immobilization is achieved by the interaction between growth factors and sulfated glycosaminoglycans (sGAGs) that are bound to ECM proteins [74]. In this way, the ECM sequesters and presents growth factors within the tissue microenvironment.

Processed from native extracellular matrix, a variety of ECM-derived hydrogels have been shown to retain sGAG content [15-17, 21]. As discussed, *in vivo*, the ECM sequesters growth factors; we therefore hypothesized that the sGAG content of decellularized ECM-derived hydrogels could provide a platform for enhanced retention and delivery of growth factors without additional material manipulation. While a variety of hybrid materials have been developed as growth factor delivery systems, the potential for using exogenous angiogenic factors incorporated in a decellularized ECM-derived hydrogel has yet to be investigated. To this end, we examined the delivery of a heparin-binding growth factor in our pericardial matrix hydrogel. As a model system, we explored the delivery of bFGF in the ECM hydrogel in a rat myocardial infarction model. We demonstrate that the sGAG-containing ECM-derived hydrogel enhances retention and delivery of bFGF in ischemic myocardium via ionic association with the extant sugar content, resulting in increased retention and acute neovascularization when compared to delivery of the growth factor in collagen or saline.

3.2 Methods

3.2.1 Animal experimental groups

All experiments in this study were performed in accordance with the guidelines published by the Institutional Animal Care and Use Committee at the University of California, San Diego, and the American Association for Accreditation of Laboratory Animal Care.

3.2.2 Tissue collection and decellularization

Porcine pericardia were collected from juvenile Yorkshire pigs and decellularized with sodium dodecyl sulfate (SDS), an ionic detergent previously shown to decellularize pericardium [15, 149]. After dissecting away any adherent adipose tissue, the samples were first washed in DI water for 30 min, and then stirred continuously in 1% SDS in PBS for 24 h, followed by an overnight DI rinse. Specimens were then removed from solution and agitated rinses under running DI water were performed to remove residual SDS. This protocol has previously demonstrated consistent decellularization of both human and porcine pericardial tissue samples [15, 236] .

3.2.3 Preparation of injectable ECM and collagen hydrogels

Injectable ECM was prepared via methods modified from previously published protocols for bladder [16] and myocardial matrix [21]. Decellularized porcine pericardia were lyophilized and ground into a coarse powder with a Wiley mini mill (Thomas Scientific, Swedesboro, NJ). Milled samples were frozen and stored at -80 °C until

further use. When used, aliquots were pepsin-digested in 0.1 M HCl at a concentration of 10 mg ECM per 1 mL HCl. Pepsin (Sigma, St. Louis, MO) was used at a concentration of 1 mg/mL. The ECM powder was digested for 60–65 h and then brought to physiologic pH (7.4) and osmolarity (1x PBS) by adding 1 M NaOH (1/10 of original digest volume) and 10x PBS (1/10 of final neutralized volume). Raising the pH stops pepsin activity; the enzyme is deactivated above pH 6 [237]. All processing steps, including the pepsin digestion, were performed at room temperature. The resulting liquid was diluted with 1x PBS to the 6 mg/mL before use. For gels including growth factor, bFGF (GlobalStem, Rockville, MD) was added prior to dilution to the matrix such that the final 75 μL volume contained 10 μg of growth factor. Collagen gels were prepared from rat tail collagen type 1 (BD Biosciences). Collagen was used at a pH of 7.4 and a concentration of 2.5 mg/mL. All solutions were sterile-filtered before use and all manipulation was performed in a biosafety cabinet.

3.2.4 Comparison of mechanical and structural properties

Rheometry was used to verify that the PPM and collagen gels had similar mechanical properties at these concentrations. To do so, 350 uL gels were made from each material and tested on a parallel plate rheometer with a gap height of 0.8 mm. A frequency sweep was performed at 2.5% strain, a value previously determined to be within the linear region for these materials. The storage modulus was determined and compared; both are reported at 1 rad/s. Each gel was run in duplicate and three gels from each material were tested. Scanning electron microscopy was used to verify that the fiber

density was similar. Gels were fixed in 2.5% glutaraldehyde (SigmaAldrich, Grade II, 25%, St Louis, MO) for 2 hours, dehydrated with a serial dilution of ethanol (30 – 100%), before being critical point dried in CO_2 using a Tousimis AutoSamdri 815A and sputter-coated with iridium using an Emitech K575X Sputter Coater. Samples were imaged with an FEI XL30 Ultra High Resolution Scanning Electron Microscope (UHR SEM) and images were taken at 2000x magnification. To compare fiber density, images were taken at 2,000x and the number of fibers that intersected two diagonal lines drawn across the image was quantified. This provided a method of comparing the two materials to each other and allowed us to determine if the fiber density was similar.

3.2.5 Confirmation and quantification of sulfated GAG content

Fourier transform infrared (FTIR) spectroscopy was performed to confirm the presence of carbohydrates in the material. Porcine pericardial matrix (PPM) and collagen samples were prepared as though for *in vivo* injections and then frozen and lyophilized. Transmission FTIR spectra were measured on a Nicolet Magna 550 spectrometer. An average of 64 scans were acquired, at a spectral resolution of 4 cm^{-1}. A background scan was obtained in the absence of material and the baseline was normalized for each sample after acquisition. Sulfated glycosaminoglycan (sGAG) content of the injectable ECM was quantified using a colorimetric Blyscan GAG assay (Biocolor, Carrickfergus, United Kingdom). Samples were run in triplicate.

3.2.6 In vitro retention and release

In order to evaluate if the ECM-derived hydrogel could sequester bFGF for prolonged release as compared to encapsulation in collagen, retention was first evaluated *in vitro*. Sets (n = 6) of 100 μL PPM or collagen gels were formed overnight in microcentrifuge tubes. 10 μg of bFGF was added to both materials before gelation. After gelation, the gels were rinsed to remove any bFGF not incorporated in the gels. After rinsing, 150 μL of PBS was added to each sample. The supernatant was collected and exchanged every 24 hours for 5 days, at which point bacterial collagenase (Worthington Biomedical Corporation, Lakewood, NJ) at 100 U/mL in a 0.1 M Tris-base, 0.25 M $CaCl_2$ solution, at pH 7.4, was added to the gels. Gels were incubated with collagenase at 37 °C for 4 hours to degrade the collagen. A sandwich ELISA for bFGF was performed on rinse step as well as the collected supernatant samples according to manufacturer's directions (Super-X Elisa, Antigenix, Huntington Station, NY). bFGF in the rinse was used to determine the amount of bFGF remaining in the gels. Quantification of bFGF in the supernatant samples allowed for determination of cumulative release over time, calculated as a percent of the bFGF remaining in the gels after the rinse step. A second experiment was performed by forming gels in the described manner, rinsing, and changing and collecting the supernatant after 24 hours. The gels were then incubated with collagenase for 4 hours and a sample of the supernatant was taken. To release remaining bFGF, 100 μL of a 1.5 M NaCl solution was added to each tube and incubated for 1 hour. The supernatant was sampled again and a sandwich

ELISA for bFGF was run on the supernatant samples according to the manufacturer's directions.

3.2.7 Infarct and injection surgeries

Female Sprague Dawley rats (225-250 g) were given an MI via 25 min occlusion-reperfusion of the left coronary artery using a modified previously published protocol [222]. Briefly, animals were anesthetized under 5% isofluorane and then maintained at 2.5% isofluorane for the remainder the procedure. The rats were placed in a supine position and the chests were cleaned and shaved. Using aseptic technique, the chests were then opened by performing a thoracotomy, accessing the pericardial space and using suture to temporarily occlude the left coronary artery. One week later, all rats received an injection of 75 μL of one of the following groups: bFGF in PPM, bFGF in collagen, bFGF in saline, PPM, collagen, or saline. The injection procedure was performed under isofluorane, following a well described protocol [41, 222]. Briefly, animals were placed in supine position and an incision was made from the xyphoid process along the abdomen. A small incision is made in the diaphragm to access the apex of the heart. 75 μL samples were drawn up into a syringe and injected into the LV-free wall through a 30-gauge needle. Care was taken to prevent puncture of the left ventricle. For each growth factor group, 10 μg of bFGF was used. On day 5 post-injection (day 12 post-infarct), all animals were euthanized. In order to evaluate anastomosis of the vessels formed as a result of the material and growth factor injections, before euthanasia, two

animals from each group were perfused with carboxylated red fluorescent microbeads retrograde via the abdominal aorta as previously described [238].

3.2.8 Histological and immunohistochemical analysis

After sacrifice, hearts were resected, fresh frozen in OCT, and short axis cross sections were taken every 300 μm from apex to base throughout each heart. Sections were fixed with acetone and stained with hematoxylin and eosin (H&E) to identify the infarct region. Infarct screening based on histological (H&E) analysis was done to exclude hearts with small or no infarcts; 2-3 animals were excluded per group prior to any analysis, leaving n = 6-7 remaining for each injection group. The 5 tissue sections in which the infarct region was largest were identified in each heart. These slides were examined by an experienced histopathologist who was blinded to the study groups. The slides were qualitatively scored from 1 to 5 and an average, overall score was assigned to each heart. A score of 1 is defined as a few inflammatory cells or mild inflammation; 2 as mild to moderate inflammation; 3 as moderate inflammation; 4 as moderate to severe inflammation; and 5 as severe inflammation with any necrosis.

Slides from the 5 previously identified sections were co-stained with fluorescein-isothiocyanate-labeled isolectin (1:100) (Vector Labs, Burlingame, CA) to visualize endothelial cells and anti-smooth muscle α-actin (1:50) (Dako, Carpinteria, CA) with an AlexaFluor 488 secondary antibody (1:1000) (Invitrogen, Carlsbad, CA) to visualize smooth muscle cells. Nuclei were visualized with fluorescent Hoescht 33342. Five images were taken evenly spaced throughout the infarct region on each section. Infarct

regions were outlined and the arteriole density within the region was quantified. Any vessel that stained positive for anti-SMA and had an average lumen diameter greater than 10 μm was included. Remaining bFGF in the tissue was identified with an anti-human bFGF antibody at a dilution of 1:100 and an AlexaFluor 488 secondary antibody at a dilution of 1:1000. Anastomosis was evaluated within the relevant sections by staining with the anti-SMA antibody with an AlexaFluor 568 secondary antibody at a dilution of 1:200 to visualize the vessels in green and the fluorescent microbeads in red.

3.2.9 Statistical analysis

All data is presented as the mean ± standard error. Statistical significance was calculated by performing a one-way ANOVA followed by a Bonferroni post hoc analysis for all results with multiple groups (data presented in Figures 3.5 and 3.7). A student's T-test with a Tukey correction was used to determine statistical significance for the *in vitro* retention experiment (data presented in Figure 3.4) and the inflammation scores. Statistical significance was accepted when $p < 0.05$.

3.3 Results

3.3.1.1 Confirmation of sulfated GAG content

Sulfated glycosaminoglycans have been previously identified in ECM-derived hydrogels [15, 17, 21, 236, 239]; here both FTIR and a Blyscan assay for sGAGs were used to confirm and quantify sGAGs in the porcine pericardial matrix (PPM). The Blyscan assay indicated the PPM retained 26.5 ± 3.4 μg of sGAGs per mg dry ECM,

while no sGAGs were present by Blyscan on rat tail collagen I. These values are comparable to those found for matrix hydrogels derived from myocardial and adipose tissue [21, 160]. The FTIR spectrum for the rat tail collagen type I contained characteristic absorption bands at 1649 cm^{-1} (amide I), 1545 cm^{-1} (amide II), and 1339 cm^{-1} (amide III) [240-243]. The FTIR spectrum obtained for PPM (Fig. 3.1) indicated the presence of sulfate groups as well sugar residues [240]. Peaks in the PPM IR spectrum correlated with the characteristic spectral features of sGAGs, similar to previously published work comparing proteoglycans and collagen in cartilage [240]. Both chondroitin sulfate and heparan sulfate contain absorption bands at 1240 cm^{-1} indicative of S=O stretch of R-SO_3^{-1} and absorption bands characteristic of polysaccharides from 1200–1000 cm^{-1} (C-C-O and C-O-C stretches). Taken together, the Blyscan assay and FTIR on the PPM confirm the presence of sGAGs.

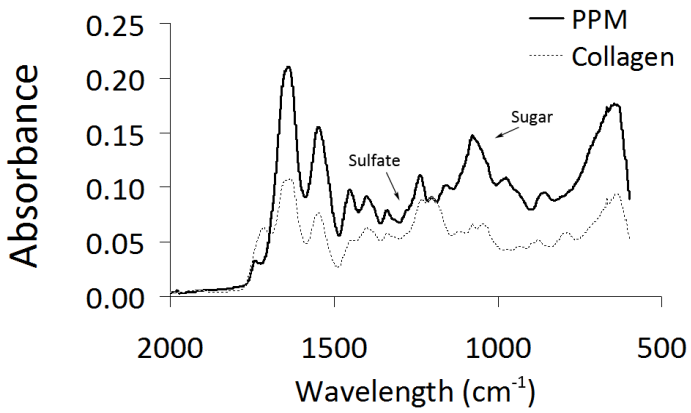

Figure 3.1: FTIR. Spectra obtained for porcine pericardial matrix and rat tail collagen, both lyophilized after pepsin digestion. Arrows denote carbohydrate peak and sulfate peak.

3.3.2 Rheometry and SEM

In order to determine that the effects observed *in vitro* and *in vivo* were due to the association of bFGF with the pericardial matrix and not simply a change in diffusion due to a difference in the structural properties, rheometry and SEM were performed on both PPM and collagen gels. The storage moduli for the PPM and collagen gels were 6.5 ± 1.7 Pa and 7.7 ± 0.7 Pa, respectively, values which are not significantly different from each other (Fig. 3.2). Loss moduli for the PPM and collagen gels were 1.3 ± 0.3 and 0.9 ± 0.2 Pa, respectively. Fiber diameter was analyzed from images taken at 20,000x (Fig. 3.3) – fibers ranged widely in both materials, most were on the order of hundreds of nanometers, similar to other work with these hydrogels [236, 244]. There were approximately 2.5 ± 0.3 and 2.2 ± 0.2 fibers per linear micron in the PPM and collagen, respectively.

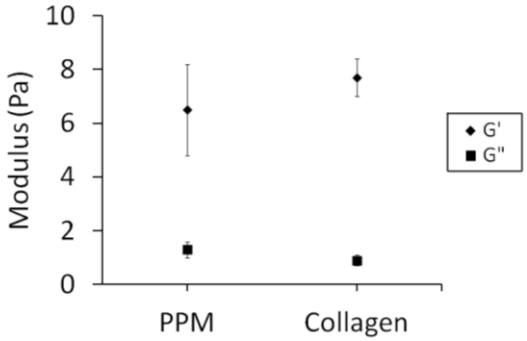

Figure 3.2: Rheometry. Storage and loss moduli reported at a frequency of 1 rad/s. The two materials are not statistically different, though there is more variability within the pericardial matrix.

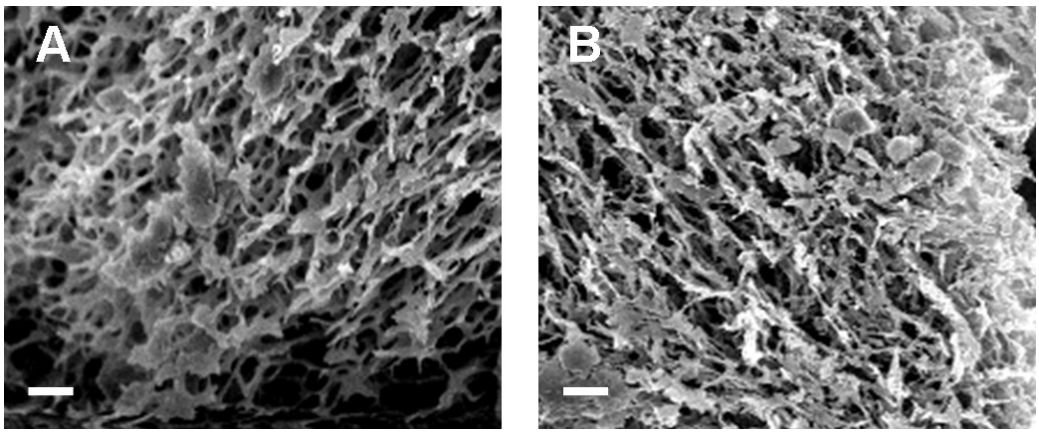

Figure 3.3: Scanning electron microscopy. Representative images of the microstructure of gels composed of (A) PPM at 6 mg/mL and (B) collagen at 2.5 mg/mL. Fiber diameter and density were similar between the two materials. Scale bar is 2 μm.

3.3.3 bFGF retention *in vitro*

To evaluate whether the processed pericardial matrix would retain its native growth factor binding capability, an *in vitro* study was first performed. bFGF was encapsulated in either PPM or collagen gels, and release was determined via ELISA. The incorporated bFGF diffused out of the collagen gels quickly compared to the PPM gels; cumulative release from the collagen gels reached 73.5 ± 0.62% by the fifth day (prior to treatment with collagenase), while only 27.8 ± 4.1% of the bFGF was released from the PPM gels (Fig. 3.4A). After collagenase treatment, the collagen gels were completed degraded and the cumulative release reached 82 ± 2.9%; however, an intact structure remained with the PPM gels and cumulative release only increased to 33 ± 4.1%. To confirm that bFGF was still bound to the remaining components of the PPM gels, a high ionic strength buffer (1.5 M NaCl) was employed, which releases growth factors that bind electrostatically to sulfated sugars [245]. Similar to the previous experiment, gels were rinsed and the supernatant was sampled after 24 hours, followed by sequential

incubation with collagenase and NaCl. As expected, the addition of 1.5 M NaCl did not change the cumulative release from collagen gels (84.5 ± 6.5% to 85.0 ± 6.3%). The salt did, however, release remaining bFGF from the PPM gels – cumulative release reached 82 ± 4.1% (Fig. 3.4B).

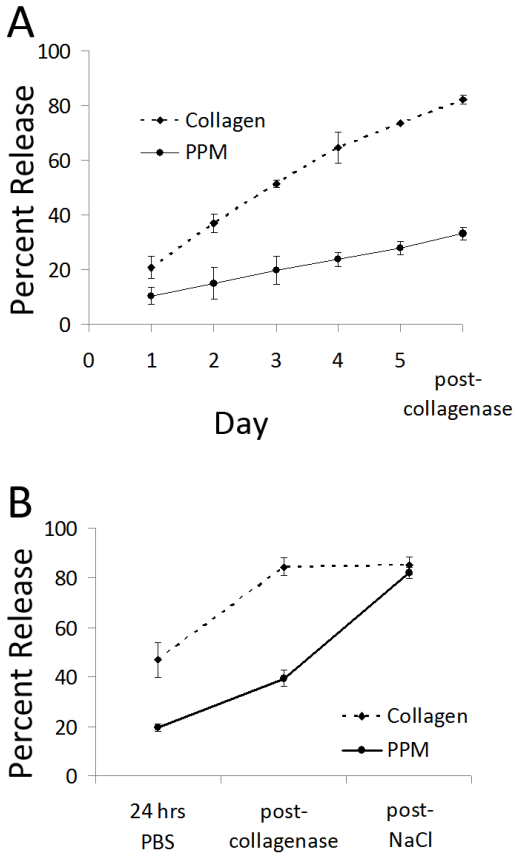

Figure 3.4: In vitro binding and release. (A) Cumulative release of bFGF from porcine pericardial matrix and collagen gels *in vitro* over 5 days, followed by a 4-hour collagenase incubation. (B) Release with 1.5 M NaCl; cumulative release of bFGF from porcine pericardial matrix and collagen gels. Here, incubation with 1.5 M NaCl allowed for release of bFGF from pericardial matrix gels. *$p < 0.05$ compared to PPM at the same timepoint.

3.3.4 bFGF retention *in vivo*

After first establishing the ability of the ECM-derived hydrogel to enhance growth factor retention *in vitro*, we next explored whether the PPM gel could enhance

delivery of bFGF in the setting of myocardial infarction. Here, of the 80 Sprague Dawley rats that received a myocardial infarction, 54 survived the initial surgery and were injected on day 7 post-MI with either PPM, collagen, or saline with or without bFGF (n = 9 per group). Upon histological analysis of tissue sections from the hearts, which were resected 5 days post-injection (12 days post-MI), hearts with no infarct, or a small infarct, were excluded from the study and no further analysis was done on that tissue. A total of 16 animals were excluded, after which the sample distribution was as follows: bFGF in PPM, n = 6, bFGF in collagen, n = 7, bFGF in saline, n = 6, PPM, n = 6, collagen, n = 7, and saline, n = 6.

Analysis of the tissue sections obtained after sacrifice five days post-injection indicated increased retention in the bFGF in PPM group compared to bFGF in saline ($p < 0.05$); due to high variability, other differences were not significant, though retention trends upward from delivery in saline to collagen to PPM. Thus, at five days post-injection, a significantly increased amount of bFGF was retained in the tissue when injected in the ECM-derived hydrogel when compared to a bolus injection in saline, with a trend towards increased retention when compared to delivery in collagen.

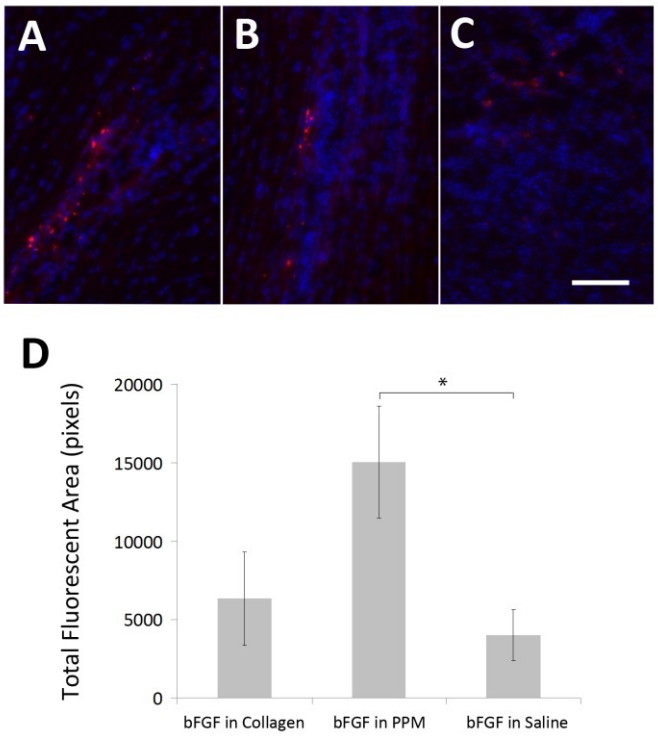

Figure 3.5: In vivo retention. Visualization of bFGF (red) retention in the infarct region in animals injected with bFGF in PPM (A), bFGF in collagen (B), and bFGF in saline (C) *in vivo* after 5 days. Quantification of bFGF in the three groups (D) via total fluorescent area (n = 6-7). Scale bar is 25 μm. *$p < 0.05$.

3.3.5 Enhanced neovascularization in vivo

Beyond establishing the binding and retention of bFGF injected in an ECM-derived hydrogel, the ultimate goal of investigating this growth factor delivery system was to determine if additional activity can be achieved by delivering growth factors through inherent sGAGs in the material. In this case, we assessed the ability of this system to enhance bFGF-mediated neovascularization in ischemic myocardium. Here, acute vascularization was examined 5 days post-injection (12 days post-MI) to determine if the extended retention of bFGF had a significant effect on vessel formation (Fig. 3.6). Quantification of arteriole density showed that only bFGF in PPM significantly increased

arteriole density within the infarct region ($p < 0.05$) when compared to the controls (Fig. 3.7). Injecting bFGF in PPM resulted in a statistically significant increase in arteriole density (arterioles/mm^2) with respect to injecting bFGF in collagen, bFGF in saline, PPM, collagen, or saline. This increase was approximately 112% higher than when bFGF was delivered in collagen. After binning the data into diameter ranges, it was observed that the majority of vessels (70-75%) had average diameters of 10-25 μm; injecting bFGF in PPM produced a significantly greater number of arterioles both in this range and in the 25-50 μm range compared to the other groups (Fig. 3.7).

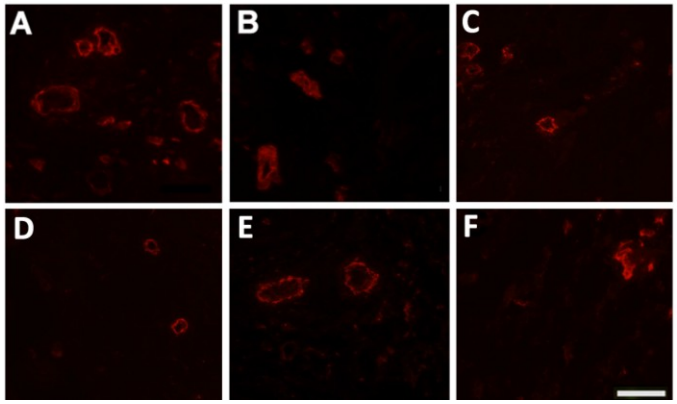

Figure 3.6: Neovascularization. Arterioles (red) in infarct regions of animals injected with bFGF in PPM (A), bFGF in collagen (B), bFGF in saline (C), PPM (D), collagen (E), and saline (F). Scale bar is 200 μm.

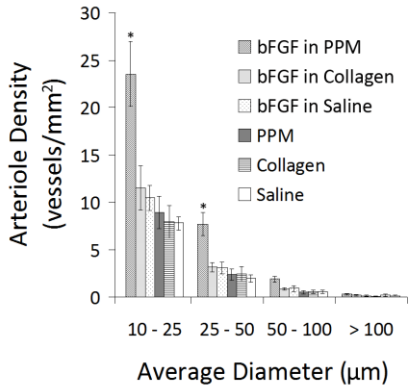

Figure 3.7: Arteriole density. Graphical representation of the arteriole density binned by vessel diameter. Majority of vessels are 10-25 μm in diameter. *$p < 0.05$ compared to all other treatment groups.

The increase in vessels alone is not sufficient to establish increased vascularization of the infarct region – the vessels must be perfused and delivering blood to the damaged region. We therefore confirmed the existence of anastomosed neovasculature by the presence of perfused microbeads within the arterioles formed in the infarct region. Presence of microbeads indicated that vessels formed through the delivery of bFGF in PPM were in fact functional (Fig. 3.8).

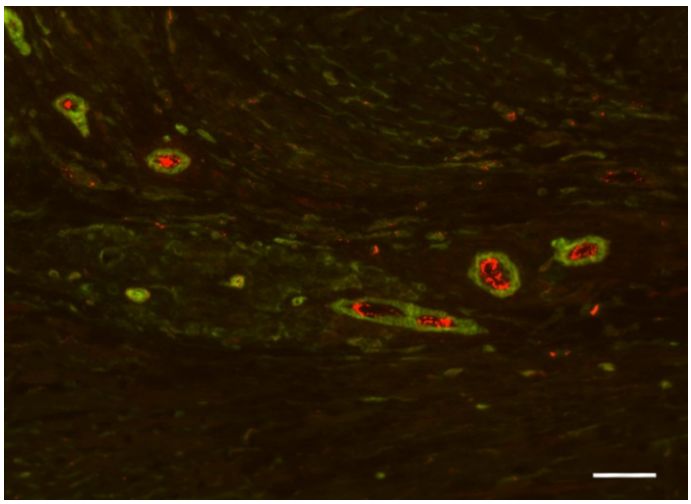

Figure 3.8: Functional vessels. Anastomosis is shown by red beads in vessels formed in the infarct of an animal injected with bFGF in PPM. Scale bar is 50 μm.

In order to assess the potential influence of inflammation on our neovascularization results, we performed a semi-quantitative assessment of tissue sections from each group. The result of a blinded pathologist's score of the tissue indicated that injection of growth factor in any form – alone, with collagen, or with pericardial matrix – caused an increase in the inflammation score (from mild/moderate to moderate/severe) that was statistically significant compared to the saline-injected hearts ($p < 0.05$). Injection of the materials alone showed a trend toward increased

inflammation (from mild/moderate to moderate), but the degree was not statistically significant compared to the saline-injected hearts or to each other.

3.4 Discussion

Growth factor delivery systems have been designed from a variety of materials – both inert and bioactive. These systems are diverse and numerous, taking the form of injectable microspheres [48], implantable patches [50, 246], and *in situ* gelling scaffolds [93, 97, 217]. *In vivo*, growth factor delivery is achieved via sequestration in the native extracellular matrix. Through binding to sulfated glycosaminoglycans linked to ECM proteins, growth factors can be immobilized for presentation or stored for future release [36]. When designing tissue engineering approaches that mimic this system, important design parameters include providing for prolonged presentation and release of the incorporated growth factors, as well as a fibrous, porous template that allows for cellular infiltration and remodeling. A wide array of materials have previously been investigated for encapsulation of angiogenic factors for therapeutic delivery [35], including synthetic materials such as poly(lactide-co-glycolide) (PLG) [63] and poly-NiPAam co-polymers [64], as well as natural materials such as alginate [247, 248], fibrin [230, 249], collagen [250], gelatin [251], and chitosan [252-254], among others. Often, a material that has been demonstrated to be a useful scaffold for a certain tissue engineering application will be modified to deliver growth factors in order to enhance the therapeutic effect. Common modifications include crosslinking the material or covalently attaching growth factors [50, 246] or growth factor-binding molecules such as heparin [255]. Previous

work has shown that when angiogenic growth factors are immobilized on a scaffold, angiogenic potential is enhanced [65, 256]. Unfortunately, the modifications used to increase growth factor activity or stability may change the chemistry of many natural biopolymers and therefore change their activity *in vivo* [235]. ECM-derived hydrogels processed from decellularized tissue have shown great promise as scaffolds for tissue repair, but their potential as growth factory delivery systems had not been previously explored. These matrix hydrogels have been demonstrated to retain components of the native ECM, including proteins, glycoproteins, and glycosaminoglycans [15, 17, 21, 236, 239]; implying the possibility of employing the same method for sequestration and delivery observed in the native tissue microenvironment. With this work, the natural incorporation of a heparin binding growth factor, bFGF, in a pericardial matrix hydrogel was explored.

Confirmation of the sulfated GAG content in the PPM gel was performed by comparing the FTIR spectra obtained for PPM and collagen and identifying a sulfate peak and a sugar peak (Fig. 3.1), similar to previous work comparing proteoglycans and collagen in cartilage [240]. A Blyscan sulfated glycosaminoglycan assay allowed for quantification of the sGAG content, which was comparable to matrix hydrogels derived from myocardial and adipose tissue [21, 160]. While bFGF diffused readily out of the collagen gels over 5 days *in vitro,* significant release of bFGF from the PPM gels was only observed after the addition of NaCl (Fig. 3.4b), indicating that the growth factor was bound to the matrix through electrostatic means, presumably through the sGAGs in the material. A portion of bFGF did diffuse out of the PPM gel over 5 days, indicating that

some of the growth factor was simply encapsulated in the material instead of bound. Upon the addition of collagenase, additional bFGF was removed as the collagen structure was degraded; however, the remaining components of the gel, which were visible in an intact 3D structure, retained a significant amount of growth factor that was dissociated upon the further addition of NaCl. These *in vitro* results with enhanced retention were further validated by the increased retention *in vivo*, quantified five days post-injection (Fig. 3.5d). This data, taken in conjunction with the similar mechanical and structural properties of the two materials, indicates that the growth factors are likely associating with the extant binding domains in the decellularized ECM hydrogel.

Using biomaterials for immobilization and prolonged release of angiogenic factors has been shown to enhance their activity; in this study, injection of bFGF in pericardial matrix was the only treatment group to significantly increase acute neovascularization compared to controls (Fig. 3.7). Additionally, a significantly greater density of large-diameter vessels (25-50 μm) were identified in the infarcts in these animals (Fig. 3.7), indicating a maturation of the vasculature. These results may be due to the extended presence of bFGF in the injected PPM or an increase in stability or activity due to immobilization on the PPM scaffold. There may also be synergistic effects with the addition of bFGF to the matrix hydrogel. Inflammation is known to influence neovascularization, and the inclusion of bFGF [257, 258] and GAGs [259] as well as differences between allogeneic and xenogeneic material sources could influence this process. We therefore obtained a semi-quantitative score of the inflammation in each group. While an increase in the degree of inflammation was observed with injection of

all groups with a growth factor (bFGF alone, bFGF in collagen, and bFGF in pericardial matrix) when compared to the saline injection, there was no significant difference in the inflammatory response of either material alone (pericardial matrix or collagen) when compared to saline or each other. Thus, while an increase in inflammation may be one of the mechanisms by angiogenesis is enhanced [260], since the inflammatory response was not significantly different among the growth factor groups, it is likely not the major contributing factor in the increased arteriole density observed when bFGF is delivered with the pericardial matrix.

It is important to note that while other studies have shown extant growth factor content (bFGF and VEGF) in decellularized matrix materials after processing, the quantity is on the order of picograms per milligram of dry weight ECM [261]. While we previously did not identify bFGF in the PPM using mass spectrometry [15], any potential extant bFGF content should be masked by the much larger quantity added to the injection. Additionally, the control pericardial matrix injection did not show a significant increase in arteriole density compared to collagen or saline, indicating the material alone does not enhance neovascularization over other injections at this time point.

Given the potential for hemangioma formation [262-264], where vascular tissue proliferates without being connected to the host vasculature, it was important to determine if using the pericardial matrix hydrogel to deliver bFGF would result in anastomosis of the blood vessels formed in the infarct region. This was done by perfusing red fluorescent carboxylated microspheres retrograde before euthanasia. Red fluorescence in the vessels formed in the infarct region for all bFGF groups indicated that

the vessels were connected to the host vasculature (Fig. 3.8), supporting the feasibility of the pericardial matrix as a delivery system for bFGF. Importantly, even though the high concentration of bFGF injected did not cause hemangioma formation, it would still be necessary to optimize the loading dose of growth factor for any application. In previous studies utilizing bFGF for treatment post-MI, the administered dose varied greatly, from 30 mg injected with 3 mg of heparin sulfate in a canine model [265], 110 mg daily intracoronary bolus injection also in a canine model [266], or a total of 5 ug incorporated in heparin-sepharose-alginate beads in a porcine model [48]. Further investigation with ECM-derived hydrogels will be necessary to determine the maximum loading capacity for a heparin-binding growth factor. This value will vary for matrix hydrogels derived via different methods and from different tissues as it will depend on the concentrations of growth factor-binding motifs in the processed materials.

Injectable matrix hydrogels derived from different tissue sources have been previously explored as therapies for the prevention of heart failure post-myocardial infarction [220]. Intramyocardial injection of hydrogels derived from porcine myocardium and small-intestinal submucosa has been demonstrated to preserve ejection fraction post-MI while saline-injected control animals continue to decline [20, 222]. While the exact mechanism behind this success has not yet been elucidated, it may be that the fibrous microstructure provides a template for cell infiltration and vascularization [209, 210, 267] or that degradation may promote cell in-growth and tissue remodeling [220, 268]. ECM-derived hydrogels are of special clinical interest as they are deliverable via catheter and therefore could potentially be administered via minimally invasive

methods [222]. While long-term studies with this growth factor delivery system will be necessary to evaluate its effect on cardiac function and remodeling post-MI, with this work, we have established proof-of-concept for using an ECM-derived hydrogel to enhance retention and delivery of a heparin-binding growth factor.

Chapter 3 is a reprint of the following manuscript: Sonya B. Seif-Naraghi, Dinah Horn, Pam Schup-Magoffin, Karen L. Christman. Extracellular matrix derived hydrogel enhances retention and delivery of a heparin-binding growth factor in ischemic myocardium. Acta Biomaterialia. 2012.

The author of this dissertation is the primary author of this manuscript.

CHAPTER FOUR:

Effect of novel growth factor delivery system on cardiac function post-myocardial infarction

4.1 Introduction

As mentioned previously, one of the experimental therapies for myocardial infarction is cell transplantation. The success of cellular cardiomyoplasty, however, is thought to be due in large part to paracrine signaling. In fact, intramyocardial delivery of cytokines produced by mesenchymal stem cells (MSCs) has been shown to be more important for improvement in post-infarction cardiac function than the transplanted cells [269]. These studies support the emerging idea that stem cell therapy may enhance myocardial repair and cardiac function due to paracrine mechanisms, rather than regeneration of new cardiomyocytes via differentiation of transplanted cells. Thus, the move toward identifying the important paracrine factors and finding ways to make them clinically relevant and feasible for translation has become an important investigation. One cytokine that has emerged as a strong candidate is hepatocyte growth factor (HGF).

Originally identified as a mitogenic factor for hepatocytes, HGF has been demonstrated to be anti-apoptotic, pro-angiogenic, and anti-fibrotic *in vitro* and *in vivo*. After identification, HGF was also found to be a key cytokine secreted by mesenchymal stem cells. Additionally, after acute MI, elevated levels of HGF secreted in the infarct region have been correlated to less severe ventricular enlargement and improved cardiac function [270]. This, in conjunction with support for finding useful paracrine factors lead to the pursuit of HGF as a therapeutic. Since then, HGF has been shown to be cardioprotective – protecting endogenous cardiomyocytes from acute ischemic death during infarction [271, 272], *in vitro* it has been shown to improve cardiomyocytes survival under oxidative stress [272, 273]. Recently, HGF has been applied in animal

models of chronic heart disease and has been shown to provide benefit even in ischemic cardiomyopathy following old MI or hereditary cardiomyopathy [274-276]. In those cases, the main mechanisms appeared to be a hypertrophic effect on cardiomyocytes as well as angiogenic and antifibrotic actions. Finally, HGF has been used in clinical trials – delivered via gene transfer [277, 278] or direct delivery of recombinant human HGF (rh-HGF) via intracoronary infusion [279], or intramyocardial injection.

As experimental approaches to treating myocardial infarction are investigated, it will continue to be very important to maintain an understanding of whether or not the therapies will be able to translate to the clinic. While HGF has previously demonstrated promise in vitro and in vivo with anti-apoptotic, anti-fibrotic, pro-angiogenic, and cardioprotective properties, it continues to be very expensive to manufacture. Thus, despite the promise, use in humans was not reasonable. However, with the recent development of a mutant HGF dimer made via inexpensive recombinant methods, clinical translation may be feasible. Dr. Jennifer Cochran's lab has recently developed methods for fabricating a highly potent peptide that recapitulates a portion of full length human recombinant HGF. They have demonstrated initial in vitro efficacy – their peptide causes endothelial cell scattering similar to full length rh-HGF. The peptide binds to heparin, and pre-aggregation with heparin enhances its effects.

Immobilization of growth factors enhances effect via increasing stability and activity. It provides a more similar environment to the native one, where growth factors are bound to sulfated sugars in the extracellular matrix. A variety of scaffold materials have been investigated for use in growth factor delivery systems. Ideally, the scaffold

would be deliverable via minimally invasive methods, and therefore injectable. As extensively discussed in Chapter 3 of this dissertation, there are a variety of injectable biomaterials that have been used to deliver a variety of cytokines. Common strategies are covalently linking the growth factor to the scaffold, using heparin or heparin sulfate proteoglycans in combination with other materials, or simply encapsulation. We were the first to demonstrate that an injectable ECM hydrogel could sequester heparin-binding growth factor for prolonged delivery and enhanced effect *in vivo*. The initial work with basic fibroblast growth factor (bFGF) and the porcine pericardial matrix (PPM) laid the foundation for moving forward with other growth factors, as a platform for investigating other potential therapies for myocardial infarction.

Given the recent success with using decellularized ECM hydrogels as heparin-binding growth factor delivery vehicles, it was hypothesized that the delivery of the novel HGF dimer in the injectable matrix scaffold would provide enhanced benefit in an ischemic injury by increasing angiogenesis, decreasing fibrosis, and salvaging myocardial cells. In this work, a small animal occlusion-reperfusion model of myocardial infarction was used to investigate the effect of delivery of the HGF peptide in an ECM hydrogel derived from pericardial tissue. As this HGF dimer has been made via low-cost recombinant methods, clinical translation is no longer prohibitively expensive; this work provides the first insight into whether or not this growth factor has potential as a therapy for ischemic diseases.

4.2 Materials and methods

All experiments in this study were conducted in accordance with the guidelines established by the Institutional Animal Care and Use Committee at the University of California, San Diego and the American Association for Accreditation of Laboratory Animal Care and were approved by the Institutional Animal Care and Use Committee at UCSD (A3033-01). All efforts were made to mitigate any pain and suffering experienced by the animals.

4.2.1 Extracellular matrix preparation

Porcine pericardial ECM matrix was prepared as previously described in Chapters 2 and 3 [58]. Briefly, decellularized porcine pericardium was lyophilized and milled into a powder and stored frozen. Prior to use the milled samples were pepsin-digested and neutralized to a pH of 7.4 at room temperature. This injectable form of the ECM was then diluted in 1X PBS to a concentration of 6 mg/ml for injection into animals.

4.2.2 HGF dimer preparation and characterization

An agonist was designed for the c-met receptor, based on the N-terminus and the first five Kringle domains of full length HGF. This NK5 peptide was then dimerized and tested in vitro for scatter factor activity. It was found to be a potent agonist and...

4.2.2.1 Cell culture assays

Scatter factor; in vitro stuff

4.2.2.2 Heparin column

The HGF dimer was run on a heparin column to establish that the peptide did, in fact, bind to heparin before using it *in vivo*. This work was done by Cassie Liu of the Cochran Lab at Stanford University.

4.2.3 In vitro binding

To confirm that the heparin-binding peptide would, in fact, associate with the ECM-derived hydrogel for prolonged release as compared to encapsulation in collagen, retention was evaluated *in vitro*. Sets (n = 6) of 200 μL PPM or collagen gels were formed overnight in microcentrifuge tubes. 10 μg of HGF dimer was added to both materials before gelation. After gelation, the gels were rinsed to remove any bFGF not incorporated in the gels. After rinsing, 200 μL of PBS was added to each sample. The supernatant was collected and exchanged every 24 hours for 5 days, at which point bacterial collagenase (Worthington Biomedical Corporation, Lakewood, NJ) at 100 U/mL in a 0.1 M Tris-base, 0.25 M $CaCl_2$ solution, at pH 7.4, was added to the gels. Gels were incubated with collagenase at 37 °C for 4 hours to degrade the collagen. To release remaining bFGF, 100 μL of a 1.5 M NaCl solution was added to each tube and incubated for 1 hour. A Ni-HRP detector molecule allowed for identification of the HGF, which has a His-tag to which nickel binds. HGF in the rinse was used to determine the amount of dimer remaining in the gels. Quantification of HGF in the supernatant samples

allowed for determination of cumulative release over time, calculated as a percent of the remaining dimer in the gels after the rinse step.

4.2.4 Rat occlusion-reperfusion model

Left coronary artery temporary occlusion was performed on female Sprague Dawley rats (225-250 g) under aseptic conditions, as previously described in Chapter 3. Briefly, the heart was exposed using a left anterior thoracotomy, and the artery was occluded for 25 minutes using a 6-0 silk suture at 1-2 mm below the left atrial appendage. The chest was closed and the animals were allowed to recover. ECG was continuously monitored for detection of arrhythmias. Buprenorphine was administered subcutaneously at 5 mg/kg to prevent post-operative pain and Ringer's Lactate (3 cc) was given subcutaneously to the animals to prevent dehydration.

4.2.5 Echocardiography

Transthoracic echocardiography was performed one week post-MI to screen for the presence of an infarct and perform baseline measurements of cardiac function. Animals were anesthetized using 5% isoflurane and then maintained at the lowest level of isoflurane necessary to maintain anesthesia during the imaging procedure (1-1.5%). Parasternal long axis and short axis images were obtained by an experienced sonographer using a GE Vivid i system with a 12 MHz transducer. At the time of imaging, a qualitative assessment of infarct size (very small, small, medium, large, very large) was recorded for screening purposes. Animals identified as having no MI or a very small MI

were excluded from the study and did not receive an injection. Echocardiographic measurements were performed again 5 weeks post-MI. For all included animals the following parameters were measured: LV internal diameter, areas and volumes based on Method of Disk (MOD) and Area-length (A-L). Ejection fraction (EF), fractional area change (FAC) and fractional shortening (FS) were calculated using LV volumes, areas and lengths respectively. End-point comparison of cardiac function between groups and pre-injection/post-treatment comparison with in each group. The heart rate of the animals was continuously observed and the ECG was carefully monitored during image acquisition to ensure there were no noticeable arrhythmias. An experienced sonographer who was blinded to the treatment groups performed all image acquisition and analysis.

4.2.6 Injection surgery

The animals were randomized one week after MI, and injected with either 75 μl of ECM (n = 8), HGF in ECM (n = 9), HGF in saline (n = 10), or saline (n = 12) (control). The rats were anesthetized at 5% isofluorane, intubated and maintained at 1.5 to 2.5% for the entire surgical procedure. A lateral incision was made in the abdominal region below the xyphoid process, followed by an incision through the diaphragm. The pericardium was partially removed and the anterolateral portion of the heart was exposed. An injection of material or saline was administered using a 27 G needle into the infarct wall. Presence of the injection was verified by temporary discoloration of the tissue. The chest was then closed and the animal was allowed to recover. To prevent post-operative

pain in the animals, buprenorphine was administered at 5 mg/kg subcutaneously and Lactate Ringer's were given to prevent dehydration as was done in the MI surgery.

4.2.7 Histology and immunohistochemisty

Animals were sacrificed immediately after post-treatment echocardiography (5 weeks post-MI) by an IP injection of Fatal Plus (sodium pentobarbital, 936 mg/kg). Hearts were immediately excised and arrested in a solution containing 25 mM $NaHCO_3$, 2 mM $CaCl_2$, 5 mM Dextrose, 2.7 mM $MgSO_4$, 22.8 mM KCl, 121.7 mM NaCl, 20 mM 2,3 butanedione monoxime. They were subsequently fresh frozen in Tissue-Tek O.C.T. freezing compound and sectioned using a cryostat into 10 μm slices with slides taken every 0.42 mm. The slides were stained with Masson's trichrome to visualize the infarct region, which is high in collagen content (blue). Images were acquired and analyzed using AxioVision software. Wall thickness was calculated as previously shown [280]. Scar thickness calculated using 3 mid-infarct slides.

Scar area percentage was calculated as the ratio of the infarct area to total LV area (septum included) multiplied by 100. All areas were obtained by outlining the respective regions on three 1X trichrome stained images spaced evenly through the infarcted region of the heart. Infarct size was assessed over three slides evenly spaced through the infarct as previously shown [281]. The average of the ratio of the endocardial infarct length to the endocardial circumference and the ratio of the epicardial infarct length to the epicardial circumference multiplied by 100 was taken as the infarct size.

To assess arteriole density, immunohistochemistry staining was done on three slides evenly spaced through the infarct region, according to previously described methods [21, 125, 282]. Briefly, the sections were fixed with acetone, incubated with anti-smooth muscle actin antibody and then stained with Alexa Fluor 568 anti-mouse antibody. Images were taken with a 10x objective (100x magnification) and vessels in the range of 10 μm to 100 μm in the infarct were quantified with Axiovision.

Sections were also stained for macrophage infiltration. M0 macrophages were identified with a mouse anti-rat CD68 antibody (AbD Serotec, Raleigh, NC) and M2 macrophages were identified with a mouse anti-rat CD163 antibody (Santa Cruz Technologies, Santa Cruz, CA). Both primary antibodies were used at a dilution of 1:100. A horseradish peroxidase conjugated anti-mouse IgG secondary antibody was used at a dilution of 1:500 (Millipore, Billerica, MA). The reaction was visualized with a metal enhanced diaminobenzidine (DAB) substrate kit (Thermo Fisher Scientific, Rockford, IL) according to manufacturer's instructions. Stained sections were imaged using a 20x objective (200x magnification). The infarct was identified and 3-5 evenly spaced images were taken on three slides evenly spaced through the infarct. Macrophages in each field of view were counted and averaged per area for each heart. A ratio of M2 to M0 macrophages was calculated.

4.2.8 Statistical analysis

Differences between baseline and post-treatment echocardiographic measures were assessed using a paired two-tailed t-test. All other statistical analysis was performed

using one-way Analysis of Variance (ANOVA) followed by Bonferroni's multiple comparison test. All measurements were reported mean ± SEM. Significance was accepted at $p < 0.05$.

4.3 Results

4.3.1 In vitro binding and release

By making gels with HGF dimer combined with PPM (6 mg/mL) or collagen (2.5 mg/mL) and monitoring the release from the gels over time the in vitro binding capability of the PPM was established. Results of this experiment show the HGF dimer diffusing out of the collagen gel within the 5 day study, followed by nearly complete release after collagenase incubation. No change was seen after addition of a high salt solution. In the PPM with growth factor gels, however, there is a slight release of dimer into the supernatant, followed by a small efflux after the collagenase incubation but only until after the NaCl incubation does the rest of the dimer associated with the matrix get released (Figure 4.1).

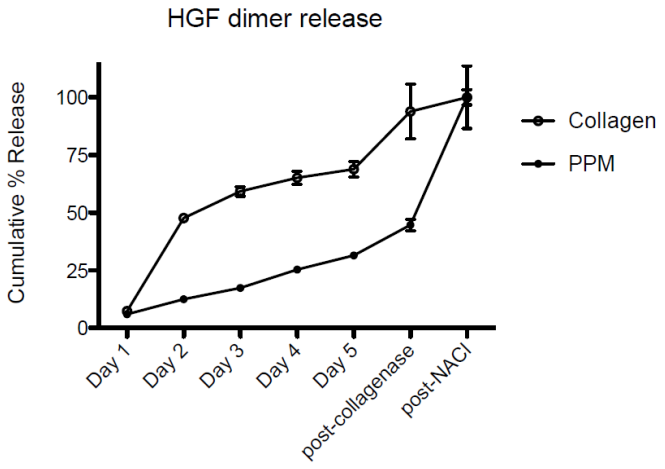

Figure 4.1: In vitro binding. A relatively rapid diffusion of HGF dimer is observed out of the collagen gels (open circles) while a slow release is seen out of the PPM gels (solid circles). Nearly complete release out of the collagen gels is seen post-collagenase incubation, while a high concentration NaCl solution is needed to fully dissociate the HGF dimer from the PPM gels.

This data is corroborated with the heparin column experiment run by Cassie Liu in the lab of Dr. Jennifer Cochran at Stanford University. Cassie prepared the HGF dimer used in this study and found that it binds to a heparin column (data not shown), eluting off the column with a high concentration salt solution (~1.5 M NaCl).

4.3.2 Cardiac function

After establishing the potential for prolonged delivery of the HGF dimer in the ECM hydrogel, an intial cardiac functional study in small animals was carried out. Here, an in vivo study was performed using a rat occlusion-reperfusion myocardial infarction model to assess the effect of the material and growth factor delivery on global cardiac function. A set of animals underwent the MI surgery, after an initial echo screening, all animals identified with an infarct were injected with one of the following four groups:

porcine pericardial matrix (PPM), HGF dimer in saline (HGF), HGF dimer in the pericardial matrix (PPM+HGF), and saline as a control. Baseline echocardiographic measurements taken at screening were compared to final measurements taken 4 weeks post-injection prior to euthanasia. After the baseline and screening echocardiography 41 animals underwent injections of PPM (n = 9), HGF (n = 10), PPM+HGF (n = 10) and saline (n = 12) injections. Three animals from the saline group were additionally excluded due to lack of infarction upon histological analysis and one animal in the HGF group died before the end of the study.

Table 4.1: Functional parameter measurements. Significance indicated by asterisks on the post-injection values represent a statistically significant change over the course of the study within the group (based on paired Student's t-test).

Functional parameter	Saline		PPM		PPM+HGF		HGF	
	Pre-	Post-	Pre-	Post-	Pre-	Post-	Pre-	Post-
EF	59.50±7.70	54.601±14.52	59.65±8.43	60.42±6.11	60.13±5.65	64.45±5.91	60.00±8.51	56.61±9.23
ESV	0.107±0.031	*0.142±0.057	0.124±0.031	0.131±0.018	0.112±0.021	0.125±0.033	0.168±0.093	0.332±0.063
EDV	0.274±0.101	*0.325±0.090	0.305±0.040	0.339±0.047	0.290±0.068	0.347±0.046	0.289±0.086	0.185±0.115
LVAd	0.652±0.112	*0.710±0.119	0.672±0.042	0.731±0.073	0.660±0.100	0.731±0.044	0.649±0.122	0.723±0.072
LVAs	0.372±0.074	*0.430±0.083	0.403±0.051	0.420±0.037	0.391±0.051	0.410±0.054	0.469±0.140	0.439±0.047
FS	33.79±6.70	32.03±9.44	32.44±7.85	30.88±8.38	36.89±5.54	39.72±8.75	32.89±5.022	34.33±9.45
LVIDd	0.615±0.076	*0.657±0.08	0.649±0.036	0.651±0.049	0.632±0.062	0.689±0.048	0.672±0.043	0.658±0.059
LVIDs	0.403±0.053	*0.445±0.08	0.437±0.049	0.449±0.049	0.398±0.050	0.416±0.068	0.447±0.040	0.429±0.046
LVAs	0.115±0.044	0.149±0.056	0.112±0.034	0.130±0.035	0.088±0.023	0.105±0.039	0.143±0.056	0.133±0.042
LVAd	0.282±0.058	0.319±0.102	0.301±0.046	0.328±0.061	0.287±0.048	0.322±0.070	0.326±0.043	0.338±0.066
FAC	0.593±0.127	0.511±0.116	0.631±0.083	0.605±0.081	0.691±0.076	0.682±0.078	0.532±0.269	0.607±0.087

Functional outcomes were measured using echocardiography and post-treatment measures were compared to baseline (Table 4.1). Saline-injected control animals declined slightly, but significantly, with respect to LV volumes, areasm and diameters (ESV, EDV, LVAs, LVAd, LVIDs, LVIDd) though not with respect to ejection fraction or fractional area change (Figure 4.2). No other group changed significantly with respect to LV geometry measurements. Infarction was confirmed using histological analysis (Figure 4.4). Significantly, there was an increase in the fractional area change in the PPM+HGF group over the course of the study (Figure 3); no other group changed with respect to this parameter. This, taken with the trend toward lack of decline in other parameters, supports the potential for HGF delivery in PPM as a growth factor delivery scaffold for cardiac repair.

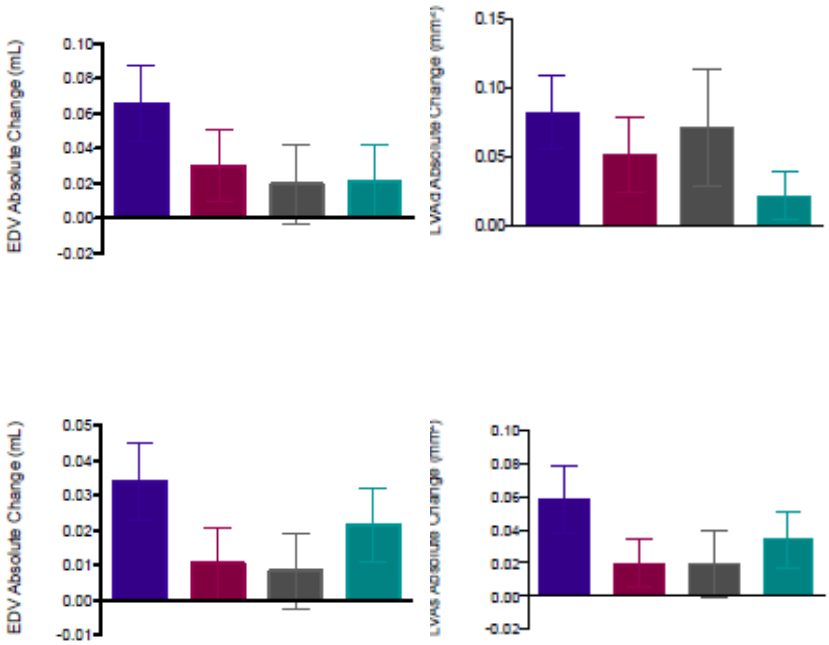

Figure 4.2: Cardiac functional parameters. The absolute change in measured or calculated functional parameters including end diastolic volume (A), end systolic volume (B), left ventricular area in diastole (C), and left ventricular area in systole (D). No endpoint analysis indicated significant differences, all significant differences are within groups pre- to post-injection.

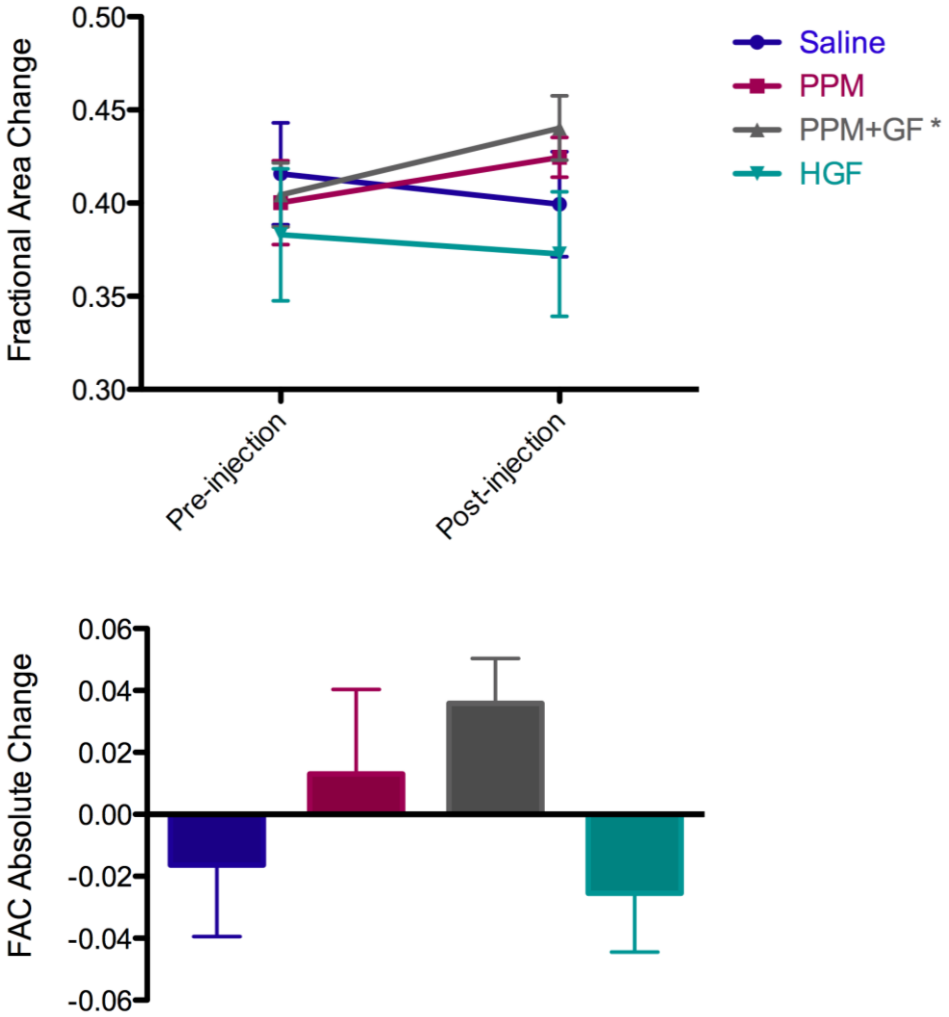

Figure 4.3: Fractional area change. Injection of the HGF dimer in pericardial matrix significantly improved fractional area change (*$p < 0.05$). Though no significant differences were observed in the absolute changes, the trend is nicely illustrated.

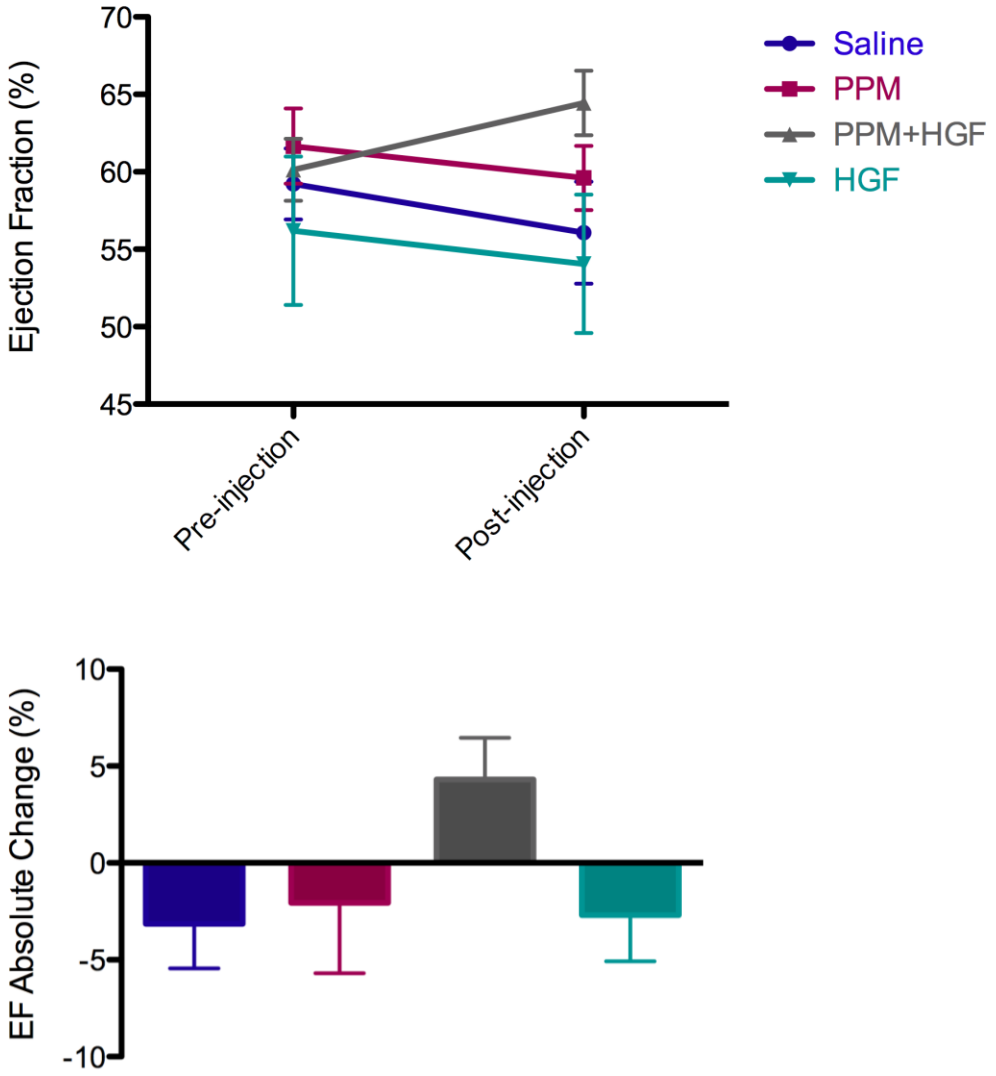

Figure 4.4: Ejection fraction. Though not significant, similar trends to the improvement in FAC were seen in ejection fraction results.

4.3.3 Histology

After euthanasia, hearts were resected and cryo-sectioned for histological analysis. There were no significant differences in scar area, infarct size, or wall thickness among any of the groups; representative Masson's trichrome images are presented in Figure 4.4.

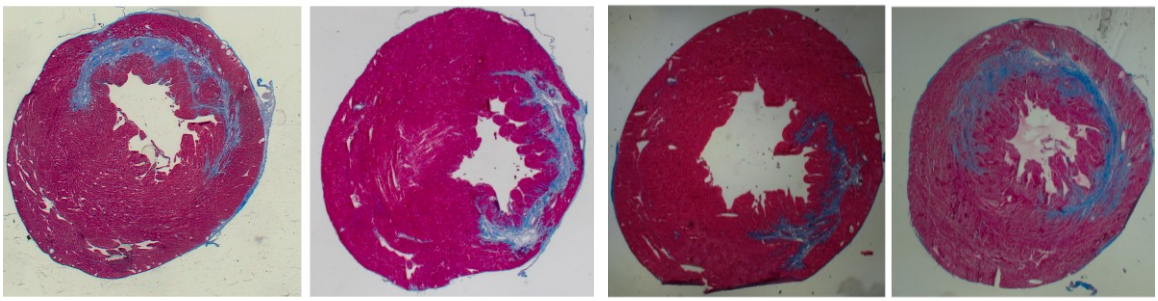

Figure 4.5: Masson's Trichrome. Histological images of hearts injected with saline (A), PPM (B), PPM+HGF (C), and HGF dimer alone (D).

4.3.4 Neovascularization

In addition to investigating changes in global cardiac function, tissue level changes give important insight into the mechanism by which cardiac function is preserved or improved after delivery of the dimer in the ECM hydrogel. Here, we assessed the ability of this system to enhance HGF-mediated neovascularization in ischemic myocardium. Arteriole density was quantified and compared to determine if delivery of HGF dimer in PPM had a significant effect on vessel formation. Quantification of arteriole density showed that only HGF in PPM significantly increased arteriole density within the infarct region ($p < 0.05$) when compared to the controls (Figure 4.6). Injecting the HGF dimer in PPM resulted in a statistically significant increase in arteriole density (arterioles/mm^2) with respect to injecting HGF in saline, PPM alone, or saline alone. There was a slight, but not significant increase after delivery of the HGF dimer alone compared to the PPM and saline controls.

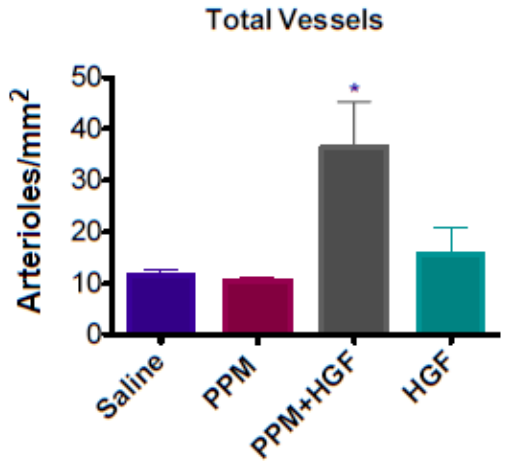

Figure 4.6: Arteriole density. Quantification of arterioles in the infarct region indicates the HGF in ECM hydrogel results in significantly greater vascularization (*$p < 0.05$). Administration of the HGF peptide alone may have had a slight effect, though it was not significantly greater than the ECM hydrogel alone or the saline control.

4.3.5 Interstitial fibrosis

One of the properties that makes HGF attractive as a therapeutic for ischemic diseases is its role in the mitigation of fibrosis. To evaluate if the HGF dimer had an effect on fibrosis in the myocardium, images taken of Masson's trichrome-stained hearts at 200x magnification were analyzed for the percentage of collagen present. In the borderzone and intra-infarct areas, there were no clear difference observed, likely due to low animal numbers and some staining and freezing artefact. However, when interstitial fibrosis in the remote myocardium was evaluated, a small trend toward reduction of fibrosis in the hearts treated with PPM+HGF was observed (Figure 4.7). Though not statistically significant, this is a promising trend. The study is limited by the relatively low number of animals; additionally, greater effects may be seen if if the tissue were evaluated at different time points.

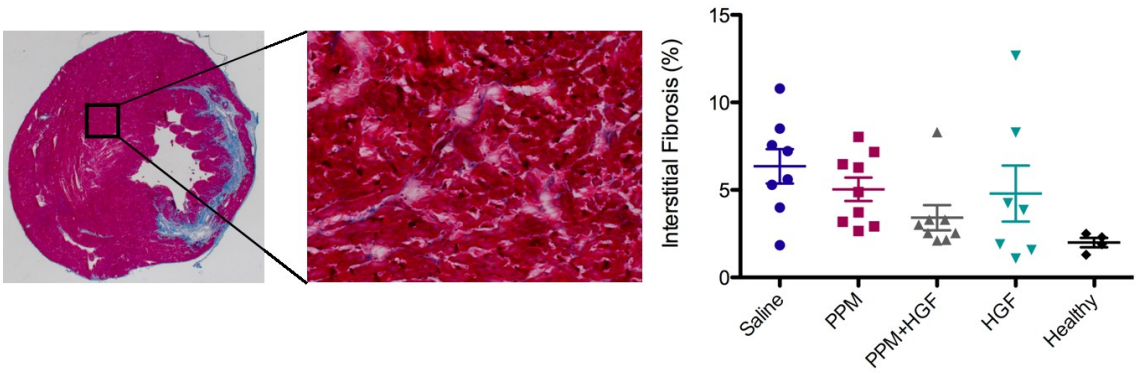

Figure 4.7: Interstitial fibrosis. Quantification of the percent collagen content of high power field of view in the remote myocardium (along the septal wall). No significant differences were observed, though the data does cluster lower for PPM+HGF. Healthy hearts were evaluated as well, and have 3.2 + 0.4% collagen content.

4.3.6 Cellular response to injection

In order to continue investigating the local tissue response – the cell infiltrate was analyzed. All infarcts had a degree of cell infiltration. After evaluating the vascular cell component, immunohistochemical staining was done to identify and quantify macrophages, myofibroblasts, and Troponin T-positive cardiomyocytes in the infarct region. As discussed, there was an increase in neovascularization in the hearts of animals that received HGF dimer.

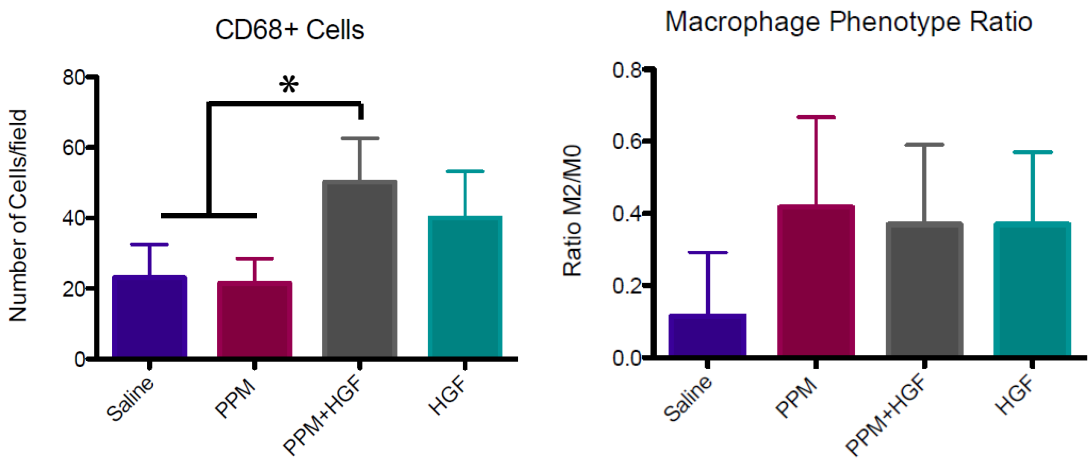

Figure 4.8: Macrophages. Immunohistochemical staining of 68+ macrophages (M0, pan-macrophage) allowed for quantification of the average number of macrophages per high powered (400x magnification) field of view in the infarct region (A). Both HGF groups had increased numbers of macrophages compared to saline and the PPM alone controls and the PPM+HGF had a statistically significant difference ($p < 0.05$). Identification and quantification of CD163+ pro-remodeling macrophgaes (M2 phenotype) allowed for the calculation of M2:M0 ratio for each group (B), indicating the degree to which the macrophage response is pro-inflammatory or pro-remodeling. No statistical differences were observed in these data.

Additionally, all treated groups – those that received PPM alone, HGF dimer alone, or the dimer in PPM – had an increase in the ratio of M2 phenotype macrophages over injection of saline alone (Figure 4.8). The ratio observed is similar to that found in studies with other decellularized ECM materials [283].

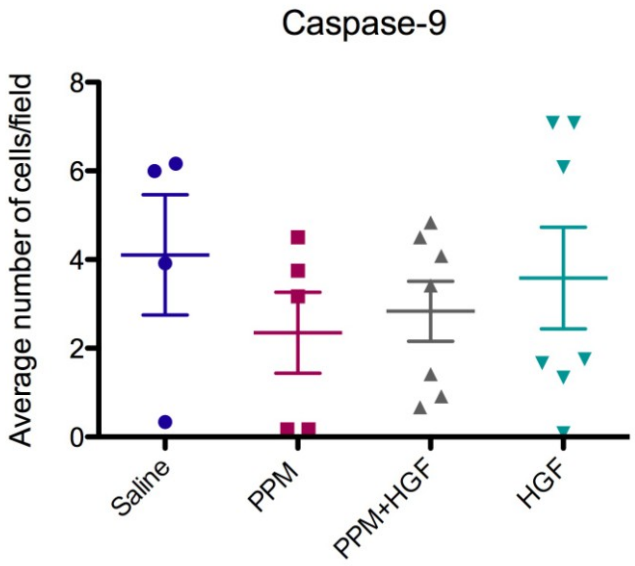

Figure 4.9: Caspase-9 quantification. Apoptotic cells are identified with caspase-9 positive staining. Quantification of the average number of cells per high power (400x magnification) field of view yielded inconclusive results with no clear trends.

Finally, antibodies for Ki-67 and caspase-9 allowed for visualization of proliferating (Figure 4.9) and apoptotic cells (Figure 4.10), respectively. Quantification of the number of cells of interest per field of view yielded insignificant results – there were minor differences, but no clear trends.

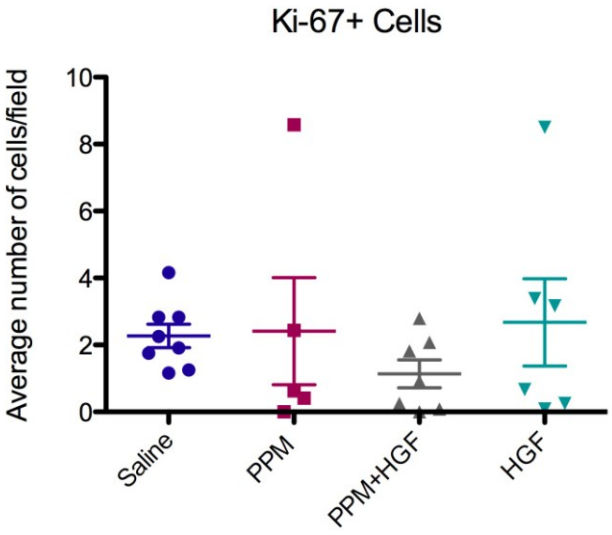

Figure 4.10: Ki-67 Immunohistochemistry. Identification of proliferating cells was done with Ki-67+ staining. Quantification of the average number of cells per high power (400x magnification) field of view yielded inconclusive results with no clear trends.

In addition to proliferative and apoptotic cells, cardiac-specific Troponin-T positive cells and myofibroblasts in the infarct region were quantified, however this analysis yielded no conclusive results, as the variability was too high to see any clear differences. (Fig 4.11)

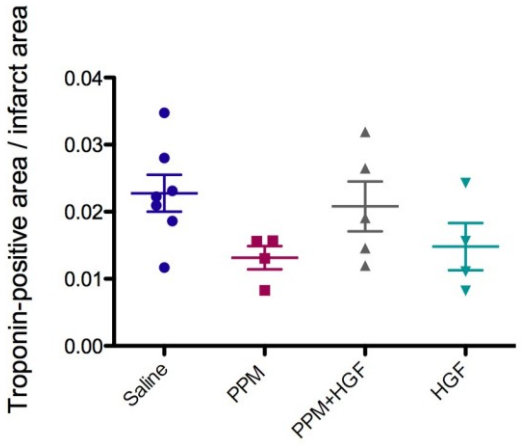

Figure 4.11: Troponin-T Immunohistochemistry. Quantification of total area of positive Troponin-T staining divided by the infarct area for each slide. No significant differences were observed

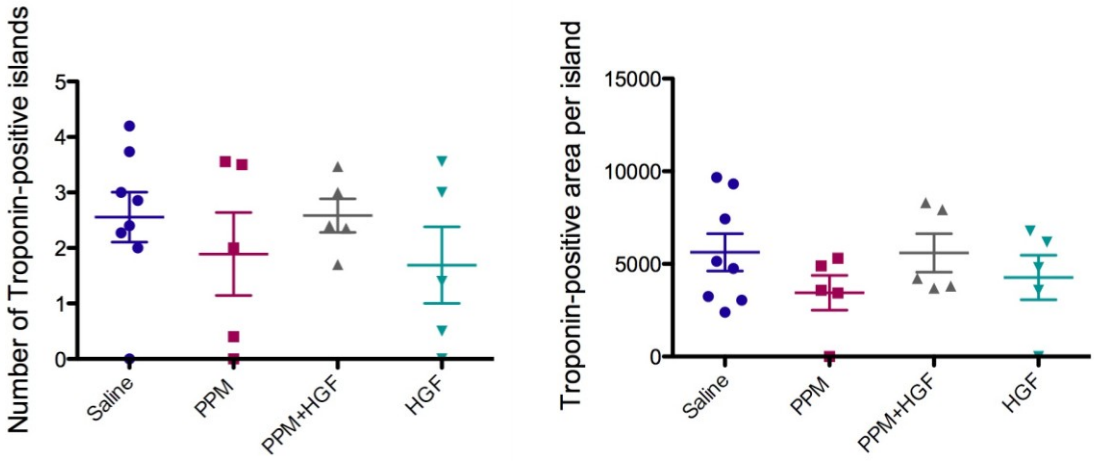

Figure 4.12: Additional Quantification of Troponin-T Immunohistochemistry. In these graphs, the number of troponin-T positive cardiomyocytes islands and the average region size for these islands is quantified. No significant differences were observed.

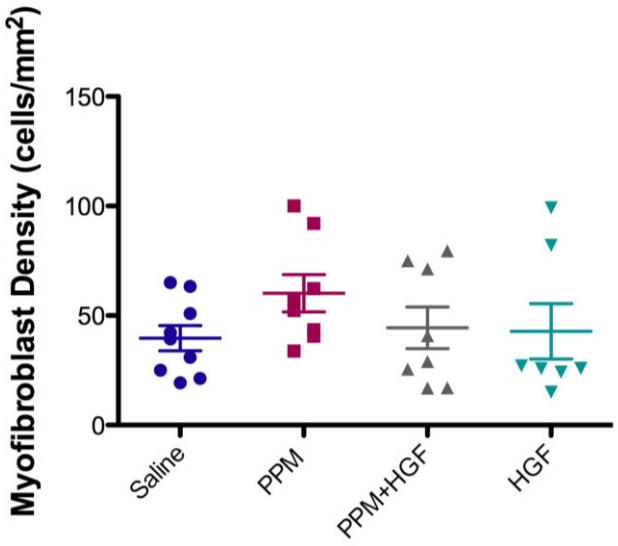

Figure 4.13: Myofibroblast Immunohistochemistry. Myofibroblasts were quantified based on non-vascular alpha smooth muscle actin staining. No significant differences were observed.

4.4 Discussion

In the wake of encouraging cell transplantation studies, a flurry of activity around understanding the mechanism by which the implanted cells contributed to the positive results showed that it was very likely via paracrine signaling rather than any physical contribution to bulking the muscle or rebuilding lost myocardium. Thus, in an effeort to simplify the therapeutic approach, the individual paracrine factors responsible for the positive outcomes are starting to be identified and evaluated. One such factor is hepatocyte growth factor (HGF) – initial success with this growth factor in increasing angiogenesis and reducing fibrosis in the liver led to its use in ischemic diseases such as peripheral artery disease and myocardial infarction. Though pre-clinical studies have been successful, and some work with HGF has moved into the clinic, recombinant human HGF (rh-HGF) has remained extremely expensive to manufacture. Thus, when a novel HGF dimer was designed in the lab of Dr. Jennifer Cochran at Stanford University, the potential for harnessing the therapeutic potential of HGF became a much more realistic – and clinically reasonable – goal. This is the first in vivo work with this peptide, in which its effects on global cardiac function as well as the local response at a tissue and cellular level was evaluated.

Building upon previous work with a model heparin-binding growth factor, bFGF, we established the ability of the ECM hydrogel to sequester and prolong delivery of a novel HGF dimer. The HGF dimer was characterized extensively in the lab of our collaborators – it was demonstrated to be nearly as effective as full length rh-HGF with respect to endothelial cell scatter *in vitro*. This effect is enhanced when complexed with

heparin, indicating that the dimer binds to heparin. This property was confirmed via a heparin column. Sequestration of HGF dimer in the ECM hydrogel was confirmed via *in vitro* release experiments (Figure 4.1).

Results from the small animal functional study support our original hypothesis, that the delivery of the HGF dimer in the pericardial matrix would be beneficial post-MI – preserving or improving cardiac function, increasing vascularization, and reducing fibrosis. While saline-injected animals declined significantly over the course of the study in various measures of cardiac function, specifically the measures of geometry including: end diastolic volume (EDV), end systolic volume (ESV), left ventricular area in diastole (LVAd), and left ventricular area in systole (LVAs). These declines were not seen in any of the treated groups. In fact, delivery of HGF dimer in PPM improved FAC significantly over the course of the study (Figure 4.3). Though the saline-injected animals did not decline in ejection fraction or fractional area change (FAC), the observed changes in geometry indicate that negative remodeling was occurring as a result of the infarct injury. This, paired with the presence of an infarct upon histological examination, support the validity of this data. End-point analysis of all parameters did not provide any significant findings – power was limited by relatively low animal numbers and the inherent variability of small animal echocardiography. Though preliminary, the results of the functional study support the potential for the HGF dimer to be beneficial post-MI.

One of the main effects of the c-met receptor and HGF is to increase angiogenesis and reduce fibrosis. In fact, when endogenous HGF is blocked – infarct size and mortality rates increase significantly in small animal occlusion-reperfusion studies [284].

Here, our data supports the conclusion that the HGF dimer acts similarly – arteriole density in the infarct region of hearts that received HGF in PPM was significantly increased over controls. There was a slight, but non-significant increase with the delivery of the growth factor alone and no observed increase with the delivery of the matrix material alone. These findings are consistent with previous work with the PPM and bFGF presented in Chapter 4. With respect to fibrosis – there was an apparent, but not significant decrease in interstitial fibrosis as measured by collagen content in the septal wall in animals that had received the PPM+HGF injection. Thus, delivery of the HGF dimer in the extracellular matrix hydrogel significantly enhances its angiogenic effect and may increase anti-fibrotic effects *in vivo*. This may be due to the prolonged presence of the HGF dimer sequestered in the pericardial matrix, as no clear benefit was conferred when the dimer was delivered in saline. Additionally, enhanced activity of the dimer has been observed *in vitro* when complexed with heparin, it is likely the ECM hydrogel is providing a similar platform for complexation of the HGF dimer, presenting it to endogenous cells in a manner similar to how endogenous HGF is sequestered in the native cardiac ECM.

The limitations of this study include a relatively small sample size and the use of conventional echocardiographic imaging instead of MRI, limiting the power and reducing the ability to distinguish true differences in the functional data. The lack of clear trends with respect to Ki-67+ and caspase-9+ cell populations is very likely due to the time point at which the analysis was performed – by 4 weeks post-injection there may no longer be an observable effect on apoptosis or proliferation. Evaluating at an acute point

– 24 hours up to 3 days post-injection would be a more appropriate time point to catch these differences. Though dose response was not specifically evaluated in this initial study, it is of great interest and will have to be investigated before establishing the HGF dimer as a potential therapeutic for myocardial infarction. Additionally, though the results of this study are encouraging and warrant further investigation into its use for cardiac repair, its effect on other ischemic diseases should also be evaluated. The scope of HGF is not limited to myocardial infarction; clinical trials for intravenous perfusion of rh-HGF for fulminant hepatitis [285] as well as intramuscular injection of HGF and HGF-encoding plasmids for critical limb ischemia [286] are currently underway.

In conclusion, with this work we have laid the foundation for moving forward with a novel HGF dimer delivered in an ECM hydrgoel. Promising results of small animal studies indicate that delivery of the HGF dimer in a pericardial matrix may provide benefit post-MI by increasing angiogenesis and reducing interstitial fibrosis. Future studies evaluating the appropriate dose and timing of the treatment and analysis will also allow for a more thorough investigation of the potential mechanisms by which these positive outcomes are achieved. Additionally, in collaboration with the Cochran lab, it will be important to identify how closely the HGF dimer mimics rh-HGF in vitro with respect to cardioprotective effects under hypoxic conditions, as that will provide additional insight into the mechanism by which the dimer is effective. With this work, a novel HGF dimer is established as a promising candidate for future investigation in conjunction with an ECM hydrogel, and may widen the scope of applicability of HGF as a treatment – by significantly reducing the cost and improving delivery.

Chapter 4, in part, is in preparation for submission for publication as: Sonya B. Seif-Naraghi, Aboli Rane, Vaibhav Bajaj, Shirley Zhang, Oi Ling Kwan, Pam Schup-Magoffin, Rebecca Braden, Anthony DeMaria, Karen L. Christman. Extracellular matrix hydrogel as growth factor delivery system for prolonged release of novel HGF dimer in a small animal model of myocardial infarction.

The author of this dissertation is the primary author of this manuscript.

CHAPTER FIVE:

Clinical translation: Safety and biocompatibility of extracellular matrix hydrogels for cardiac repair

5.1 Introduction

As discussed, experimental approaches to mitigate negative remodeling and prevent HF include LV restraints, cardiac patches, *in situ*-gelling biomaterials, and cellular cardiomyoplasty or cell transplantation. Most work has shown that many different methods and materials can provide maintenance or improvement in functional parameters in small- and some large-animal models. However, the majority of these approaches will not transition to minimally invasive delivery in the clinic – patches require a thorocotomy for epicardial placement and even most existing injectable biomaterials are not compatible with cardiac catheter procedures, which require the material to be in the catheter during a 30 minute to 1 hour long procedure or delivered via coronary infusion.

Notably, percutaneous delivery of alginate and a cardiac extracellular matrix hydrogel developed in our lab have been shown to be feasible in large-animal models [101, 222]. Leor *et al* demonstrated success with intracoronary infusion of calcium-crosslinked sodium alginate in pre-clinical work in swine [101], which led to delivery in a small Phase I/II study in acute MI patients [102], and is currently in use in a Phase II clinical trial for prevention of LV remodeling and congestive HF in patients with ST-segment elevation MI and who have had successful percutaneous coronary intervention [287]. We previously developed an injectable ECM hydrogel derived from porcine myocardial tissue [21], which self-assembles into a porous and fibrous scaffold upon injection into tissue and demonstrated that injecting this ECM hydrogel post-MI in a rodent model mitigated LV remodeling and preserved ejection fraction [222]. Recently,

feasibility for transendocardial delivery and efficacy in a clinically relevant large animal model was also established (data unpublished). Transendocardial delivery, commonly used for cell transplantion in the heart [101, 288-292], is considered by many to be the preferred method of catheter delivery [293-295], as it allows for direct intramyocardial delivery, improves retention, and does not require access to the coronary vessels, a potential concern in the affected population.

As discussed, extracellular matrix materials have emerged as a promising class of naturally-derived biomaterial scaffolds [142, 296]. While the components of various ECMs are similar, the specific biochemical composition of these materials vary with the source, with each ECM having a specific ratio of different proteins and sugars [185, 297]. In fact, using tissue-specific ECM has been shown to have enhanced effects on cell survival and differentiation *in vitro*. [298-300]. It follows that the most appropriate scaffold to replace the damaged ECM after a MI would be derived from myocardial tissue. However, using tissue-specific ECM hydrogels are necessarily xenogeneic, except in the notable case of soft-tissue repair with adipose ECM. Thus, while the porcine myocardial matrix hydrogel developed in our laboratory provides tissue-specific cues and has recently been used successfully in pre-clinical large animal studies, many unanswered and critical questions in regards to clinical translation remained from this initial work, namely to address the biocompatibility and safety of this material. Concerns regarding the use of xenogeneic material in humans was part of the original rationale for investigating an autologous tissue source.

Biocompatibility of injectable xenogeneic extracellular matrix hydrogels has been indirectly supported in the literature [21, 301] and the immune response to decellularized ECM grafts placed subcutaneously has been explored [302-304],. What is missing is work exploring the site-specific tissue response to these materials over an extended time course and an attempt to understand the differences in the host response to xenogeneic compared to allogeneic ECM scaffolds. Additionally, the safety of the proposed delivery method has not been confirmed with respect to hemocompatibility and the thrombo-embolic potential of these materials. With this work, we explore the inflammatory response to xenogeneic and allogeneic materials, and establish the safety and biocompatibility of the myocardial matrix in rodent studies.

5.2 Methods

All experiments in this study were performed in accordance with the guidelines published by the Institutional Animal Care and Use Committee at the University of California, San Diego, and the American Association for Accreditation of Laboratory Animal Care.

5.2.1 Preparation of injectable ECM hydrogels

Ventricular porcine myocardium was decellularized using sodium dodecyl sulfate (SDS) as previously described [21, 222, 244]. An injectable myocardial ECM hydrogel was then prepared via previously described methods [21, 222, 244], which were modified from a previously published protocol for bladder ECM [16]. Non-decellularized porcine

myocardial matrix was prepared according to the same protocols except that the fresh tissue was directly processed without decellularization.

5.2.2 Small animal surgery protocol

Female Sprague Dawley rats (225-250 g) were used in the small animal cellular infiltration response study and direct injection safety study. Animals were anesthetized with 5% isoflurane and then maintained at 2.5% isoflurane for the remainder the procedure. Using aseptic technique, injections into the left ventricular free wall were performed, following a well-described protocol [41, 93, 222]. Briefly, animals were placed in supine position and an incision was made from the xyphoid process along the abdomen. A small incision was made in the diaphragm to access the apex of the heart. 75 μL samples were drawn up into a syringe and injected into the LV free wall through a 30-gauge needle. For all injections, 75 μL of material or saline was used. For the cellular infiltration study, the following three materials were used: non-decellularized porcine myocardium (NDM), injectable porcine myocardial matrix (PMM), and saline. On days 1, 3, 7, 14, 28, 56, and 112 post-injection, three animals per group were euthanized.

For the direct injection safety study, only porcine myocardial matrix (PMM) was examined and 75 μL of material or saline was injected directly into the lumen of the LV. The animals were revived and maintained for six hours after the procedure and before euthanasia. After an injection of 400 uL of FatalPlus, the animals were perfused with PBS followed by 10% buffered formalin. After perfusion, the following organs were removed: spleen, brain, lung, heart, kidneys, liver, and skeletal muscle.

5.2.3 Histological analysis

For the direct lumen-injected rats, tissue was fixed, paraffin embedded, and then sectioned for histological analysis. For tissue in the biocompatibility study, hearts were fresh frozen in Tissue Tek O.C.T and cryosectioned. All tissue was analyzed in a blinded fashion by experienced pathologists. For direct injection animals, H&E stained sections were examined for evidence of acute ischemia as well as edema, hemorrhage, and inflammation in each organ. In the biocompatibility study, 3 H&E stained slides representing the largest portion of the affected region from each rat heart were evaluated with a single score per animal (absent = 0, minimal = 1, mild = 2, moderate = 3, marked = 4) with respect to infiltrating multinucleated giant cells, polymorphonuclear cells (PMNs), lymphocytes, large mononuclear cells, and spindle cells.

5.2.4 Platelet activation

In order to determine the potential consequences of the injectable matrix escaping in to the bloodstream, the effect of the injected matrix on platelets was first investigated. This was done via a standard platelet activation test in the Clinical Hematology Laboratory at the University of California, San Diego. Whole human blood was slowly spun down (200 rcf, 10 minutes) to collect platelet-rich plasma (PRP), some of which was transferred to collection vials. The remaining samples were further spun down to collect plasma (600 rcf, 10 minutes) and the supernatant was transferred to another set of collection vials. The collected PRP was tested for cell density, to make sure it contained at least 100,000 cells/mL. PRP (180 μL) was added to four capillary vials with small stir

bars and placed in a spectrophotometer that monitored optical density (OD). At baseline, OD is normalized to 100%, using pure plasma as the reference point for 0%. After normalization, 20 μL of one of the following agonists was added to each vial: adenosine diphosphate (ADP), epinephrine, arachnidonic acid (AA), and collagen. This allowed for testing the baseline platelet activity and ensuring sample viability. Four new vials with PRP were prepared and normalized before adding myocardial matrix directly to the PRP in each vial. The optical density was monitored for at least 5 minutes to determine if any activation occurred (as noted by a decrease in turbidity). After that time, the four agonists were added to the vials (one agonist per sample) to determine if the material caused platelet inhibition. A conservative estimate of the amount of material that could end up in the left ventricle was calculated based on the event that 200 μL was injected directly into the left ventricle over a 30 second period, in a patient with an average stroke volume of 80 mL and a heart rate of 60 bpm, with an additional margin of 20%. In this way, the "standard concentration" referred to herein is a ratio of 1:10,000 (injected material:blood). This experiment was repeated with material added at concentrations equal to 1x and 2.5x that estimate. This is equivalent to ratios of 1:10,000 and 1:4,000. Each test was performed with internal quadruplicate samples and then repeated. After the final data set had been collected, a control run was repeated in order to ensure platelet activity was maintained throughout the duration of the experiment.

5.2.5 Clotting times

The concern of causing a hypercoagulable state was addressed here by determining the effect of the material on the intrinsic and extrinsic coagulation pathways. The plasma collected from the blood sample used for the platelet activation (spun down at 600 rcf for 10 minutes) was used to test the activated partial thromboplastin time (APTT) and the prothrombin time [295]. Clotting times were first determined for unaffected plasma to ensure the sample was appropriate. Myocardial matrix was added to human plasma in ratios of 1:10,000 and 1:2,500. 1x PBS was used as a control and each test was performed in duplicate for each experimental group.

5.3 Results

5.3.1 Local tissue response

Building upon the work to establish efficacy in the large animal model (cite), we examined the safety and biocompatibility of using xenogeneic myocardial matrix for MI treatment. This was approached in three ways – first by examining the local tissue response to both xenogeneic and allogeneic myocardial matrix at acute and chronic timepoints, then performing direct injections of the xenogeneic myocardial matrix into the lumen of the LV, and finally by testing the effect on clotting times and platelet activation. The first approach provided insight into the host response towards the injected myocardial matrix; inflammatory cell infiltration at acute and chronic timepoints was evaluated in rats. Healthy animals received LV wall injections of porcine myocardial matrix (PMM), rat myocardial matrix (RMM) saline, and a non-

decellularized porcine myocardial matrix (NDM) and euthanized for histological evaluation after 1, 3, 7, 14, 28, 56, and 112 days (n = 2-3 per timepoint per group). All animals survived the injection surgery and showed no signs of stress or discomfort throughout the prescribed maintenance time. No animals had to be euthanized prior to the intended date. Due to freezing artifact, some tissue could not be analyzed and the data shown here is a composite score from 2 or 3 hearts per timepoint per group. RMM is not pictured and appeared very similar to PMM.

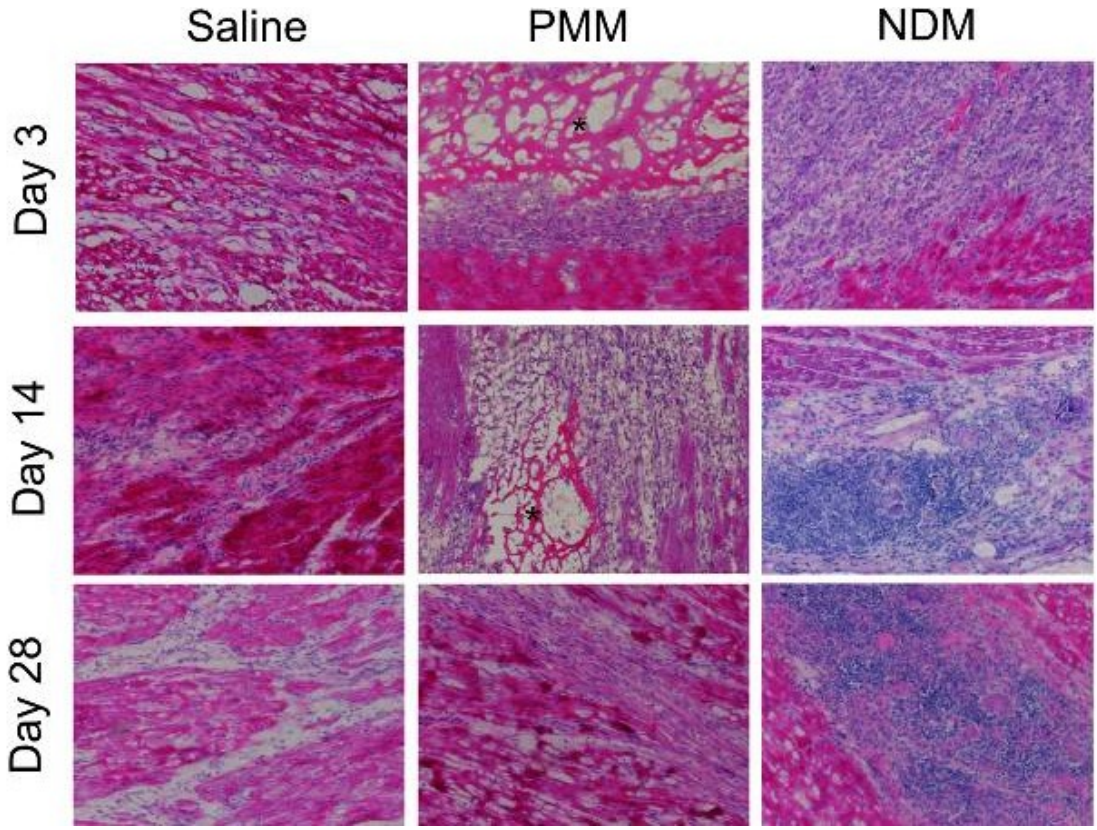

Figure 5.1: Cell infiltration histology in rats. Representative images of histological sections of rat hearts injected with saline, porcine myocardial matrix (PMM), and non-decellularized matrix (NDM) at days 3, 14, and 28. Of interest is the presence of chronic inflammation and multinucleated giant cells identifiable in the NDM groups at days 14 and 28. Also, note that the matrix (as indicated by the pink stained porous and fibrous network) is completely degraded by 28 days. All images are taken at 200x.

The myocardial matrix was identifiable in tissue sections on days 1, 3, and 7. In 1 of 2 hearts evaluated, porcine myocardial matrix was still present at 14 days, in 1 of 2 hearts evaluated, rat myocardial matrix was still present at 14 days; both materials were completely degraded in all hearts by 28 days (Fig. 5.1). Pathology scores for polymorphonuclear cells (PMNs) (Fig. 5.2A), lymphocytes (Fig. 5.2B), large mononuclear cells (Fig. 5.2C), spindle cells (Fig. 5.2D), and multinucleated giant cells (Fig. 5.2E) were assigned based on degree of cellular infiltration, where absent = 0, minimal = 1, mild = 2, moderate = 3, and marked = 4. Trends observed in this data include an acute inflammatory response in all groups, characterized by an early peak in infiltrating PMNs. Lymphocytes are a dominant cell type in the NDM group, but appear to a lesser degree in the saline, PMM, and RMM groups at all timepoints. Large mononuclear cells (macrophages) are present throughout the duration of the inflammation in all groups, though are more dominant in the NDM group at early timepoints compared to the saline, PMM, and RMM groups. Spindle cells – fibroblasts, myofibroblasts, and cardiomyocytes – become dominant in the saline-, PMM-, and RMM-injected groups after two weeks. Importantly, multinucleated giant cells are only observed in the NDM group and there is no indication of chronic inflammation in the PMM-, RMM-, or saline-injected groups (Fig. 5.5).

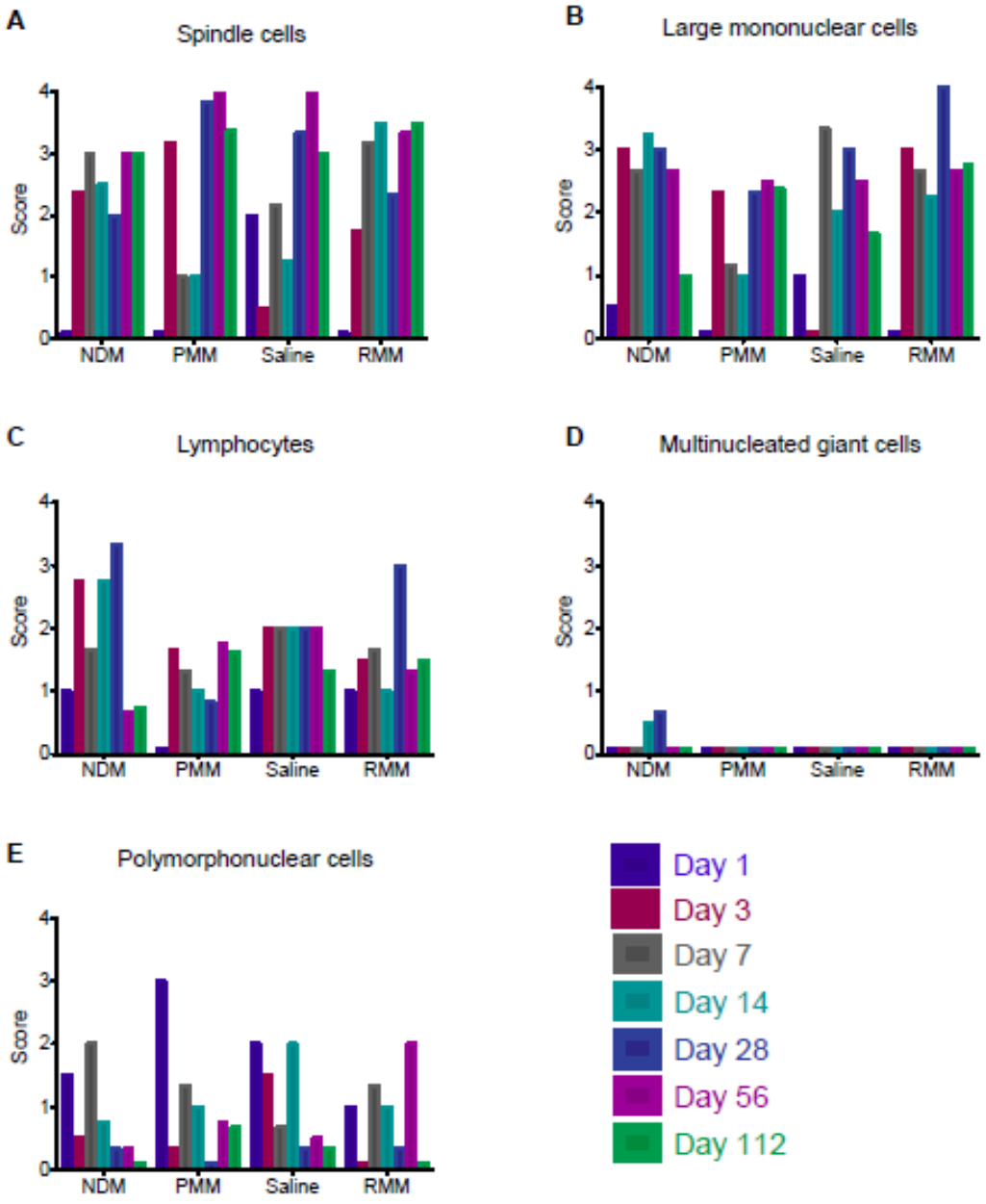

Figure 5.2: Biocompatibility assessment in rats. Average score for infiltration and degree of inflammation with respect to (A) polymorphonuclear cells (PMNs), (B) mononuclear cells, (C) lymphocytes, (D) spindle cells (fibroblasts, myofibroblasts, and cardiomyocytes), and (E) multinucleated giant cells. On this scale, 0 = absent, 1 = minimal, 2 = mild, 3 = moderate, and 4 = marked. Indications of chronic inflammation are only present in the non-decellularized matrix (NDM) injected animals, and not in the myocardial matrix (PMM) or saline-injected animals.

5.3.2 Direct injection into the LV lumen

As mentioned, the second approach to verifying the safety of this treatment was via direct injection into the lumen of the LV in rats. It is known that leakage occurs with transendocardial injection, so it is important to understand what the hemocompatibility and thrombo-embolic potential of the material would be in the event that the material enters systemic circulation. Rats that received direct injections of myocardial matrix (n = 4) or saline (n = 2) into the lumen of the LV were revived and observed for 6 hours. All rats recovered normally and showed no signs of stress or discomfort prior to euthanasia. The pathology report showed that histological examination of kidneys, heart, brain, spleen, liver, and skeletal muscle found no signs of acute ischemia or thrombus, and the degree of edema, hemorrhage, and inflammation was minimal for both groups and not different between saline- and matrix-injected animals. There was a moderate degree of edema and inflammation in the lungs, but it was similar between saline- and matrix-injected animals and attributed to trauma associated with the surgical procedure (Fig 5.8). Thus, direct injection of myocardial matrix into the lumen of the LV does not result in gelation and subsequent embolization of the material, nor does it cause clot formation downstream. This provides further evidence of the safety of the myocardial matrix for delivery via endocardial injection, a limitation of other biomaterials that have the potential to be thrombo-embolic [218].

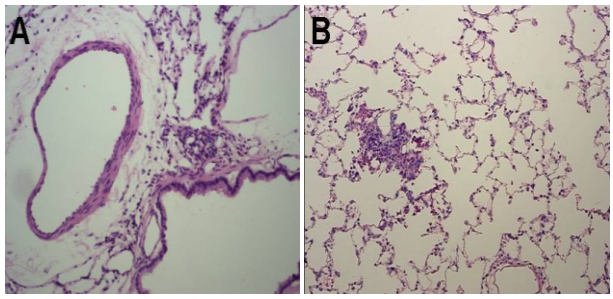

Figure 5.3: Histological assessment of lungs in small animal safety study. Analysis of hematoxylin and eosin stained sections of lungs from rats that received an injection of saline (A) or myocardial matrix (B) directly into the lumen of the left ventricle indicated some edema, inflammation, and hemorrhage attributed to the surgical procedure. Magnification is 100x.

5.3.3 Hemocompatibility

Finally, in addition to investigating the potential for these materials to gel in the bloodstream or cause embolization and downstream damage, we examined the interaction between the injected matrix and human blood with respect to clotting times and platelet activation. For these studies, myocardial matrix was evaluated at different concentrations – the "standard" concentration reflects a conservative estimate (1:10,000) of the amount of matrix that would be injected into the bloodstream if the needle disengaged from the endocardium during injection. Addition of the myocardial matrix to human plasma had no effect on activated partial thromboplastin time (APTT) or prothrombin time [295]; at both the standard concentration (1:10,000) and a higher concentration (4 times, or 1:2,500), APTT and PT remained within reference ranges (Table 2).

Table 5.1: Clotting Times

ECM:plasma	PT	APTT
Ratio	Seconds	Seconds
Control	11.65 ± 0.071	26.3 ± 0.0
1:10,000	11.75 ± 0.071	25.7 ± 0.141
1:2,500	11.75 ± 0.071	27.5 ± 0.566

Additionally, exposure of platelet-rich-plasma (PRP) to myocardial matrix at standard estimates did not cause platelet activation, indicated by a constant turbidity (Fig. 5.7A). A "high" concentration (2.5 times the standard concentration, or 1:4,000) was also tested; at this concentration, minimal platelet activation was observed, indicated by the dip in turbidity after 3 minutes (Fig 5.7B); however, this level is not clinically relevant. Exposure to myocardial matrix did not inhibit platelet activation at any concentration; the addition of agonists after 5-10 minutes resulted in normal platelet activation, indicated by the sharp decrease in turbidity. After four hours, the quality of the sample was verified by repeating the controls, which still showed normal activation curves (Fig 5.7C). These data support the hemocompatibility of the myocardial matrix.

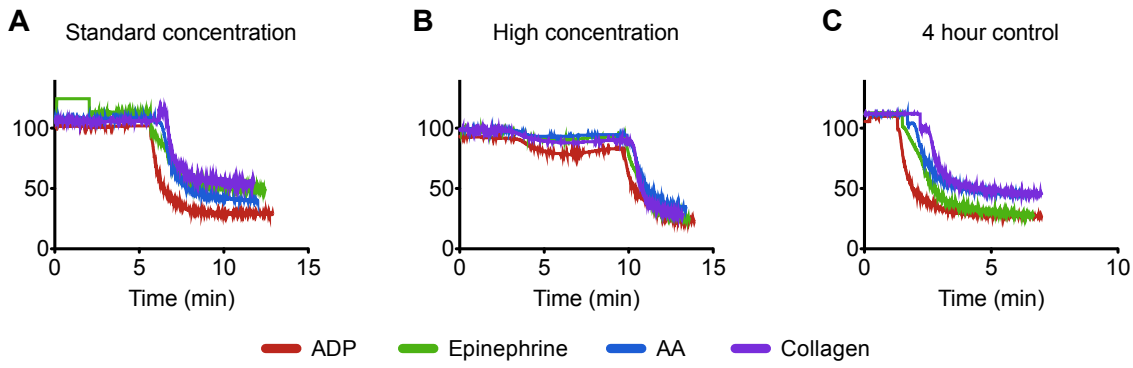

Figure 5.4: Platelet activation. Addition of myocardial matrix to human platelet-rich-plasma was done at a standard concentration (A) and a high concentration (B) and the samples were evaluated for at least five minutes. Upon observing no activation in the standard concentration samples, agonists (ADP, epinephrine, arachnodonic acid (AA), and collagen) were added and the activation response was observed to be normal. At a high concentration, minimal platelet activation was observed before 5 minutes, indicated by the slight dip in turbidity. After the samples plateaued, agonists were added at 10 minutes and normal activation was observed. In (C), a control was performed after four hours to ensure normal activity of the samples and validity of the data; response to agonists was normal.

5.4 Discussion

Confirming the success of previous small animal work [222], efficacy and feasibility of using myocardial matrix has been demonstrated in a clinically relevant porcine MI model (data unpublished), where both the pathophysiology and the administration mimic what would be observed and performed in humans [305]. Before implementing this biomaterial therapy in clinical studies, thorough exploration of its safety and biocompatibility is important and this work specifically addresses questions that remained after the small animal work, including the responses to allogeneic and xenogeneic ECM in rodents, how the inflammatory process changed over time, effects of leakage into the LV lumen, and potential concerns with hemocompatibility. Leor et al, in pre-clinical work with alginate injections in swine, postulated that these biomaterials should 1) gel at the infarct site only; 2) have rapid, controllable gelation without detrimental effects on myocardial function and remote organs; 3) provide sufficient tissue-bulking properties to support damaged myocardium; 4) be biodegradable; 5) nonimmunogenic; and 6) nonthrombogenic [101]. In the present study, we complete the argument for an injectable myocardial matrix hydrogel to fulfill these requirements, building on previous research showing biomaterial injection can improve cardiac function, prevent negative left ventricular remodeling, and salvage cardiomyocytes after MI in a porcine model.

Decellularized matrix materials have been utilized as “nature’s platform” for a variety of applications [12, 142, 306], and injectable hydrogels derived from SIS and pericardium have both been investigated for cardiac repair in rodent models [20, 51].

While the pericardium is a potentially autologous source for an ECM hydrogel, the myocardial matrix described here is the only tissue-specific ECM hydrogel available for cardiac repair – the other possible candidates are derived from the tissue of different organs. Since the extracellular matrix is specific to each tissue [142, 307], the myocardial ECM can potentially provide appropriate cues for infiltrating cells. *In vitro*, biochemical cues from the myocardial matrix have been shown to promote maturation of human embryonic stem cells [298], and cardiac differentiation and survival of cardiac progenitor cells [300]. It is known that there are more cardiac progenitor cells in failing hearts [180], so by mitigating the harsh infarct milieu, the injected ECM may also provide a more appropriate environment for circulating stem cells to encourage repair and regeneration [222]. In the rat MI model, we observed larger clusters of surviving cardiomyocytes in the infarct area at 1 week post-injection, which we postulated was a result of improved cardiomyocyte survival [222]. In the porcine model, we observed a markedly thickened zone of muscle-like cells with areas of neovascularization at the endocardium 3 months post-injection (unpublished data). This may be a combination of preserved endogenous cardiomyocytes and newly formed cardiomyocytes, as we previously observed proliferative cardiac-specific troponin T positive cells and c-kit positive cells within the matrix in the rat MI 1 week post-injection [222]. Other materials, such as self-assembling nanofibers in combination with delivery of VEGF, have also shown newly formed cardiomyocyte-like cells post-material injection [92].

As Leor et al. postulated, there are a number of important design considerations that must be met for injectable biomaterials to be useful and relevant treatments for MI.

One consideration not specified, but crucial to clinical translation is the delivery method. While several injectable biomaterials have shown promising results in small animals [308], few have been translated to percutaneous delivery in large animals, thus limiting their relevance for translation to the clinic as a minimally invasive cardiac treatment. To date, the only other material to be delivered in a large animal MI model is alginate [101]. The myocardial matrix is the second material to be delivered percutaneously in a large MI model and the first material to be delivered via a transendocardial approach. Transendocardial delivery is considered by many to be the preferred method of catheter delivery [293-295, 309]. This method allows for guided, direct intramyocardial delivery, which increases biomaterial retention in the tissue and does not require access to the coronary vessels, which reduces the risk of embolization. Additionally, the coronary access required for intracoronary delivery is often compromised in the target patient population.

With mounting evidence that injecting the myocardial matrix provides benefit post-MI in preclinical trials, establishing a firm understanding of the host response and interaction to the material is critical. Evaluation of the local tissue response to decellularized ECM biomaterials injected in the myocardium has not been previously conducted. Determining the extent of acute and chronic inflammatory responses provides a better understanding of how the biomaterial is interfacing with the host tissue. While some initial inflammation is requires to promote healing [310], any chronic inflammation could be detrimental to the success of the therapy and ultimately the health of the patient. In this study, a healthy animal model provided an un-impeded view of the inflammation

caused by injecting the myocardial matrix in the myocardium. Performing this study in rats also provided the ability to evaluate a xenogeneic model. Previous work by Allman et al. evaluated subcutaneous implantation of decellularized extracellular matrix materials in rats, demonstrating that the immune response to xenogeneic ECM is Th-2 mediated, characterized by an M2 macrophage phenotype indicative of remodeling rather than rejection [306, 311]. The increased presence of spindle cells, which include fibroblasts, myofibroblasts, and cardiomyocytes, in the xenogeneic and allogeneic myocardial matrix injected groups compared to the control groups supports a reparative remodeling response [142, 147]. Interestingly, this is corroborated by the cardiomyocyte-like populations identified in the matrix-injected pigs (data unpublished). Additionally, signs of chronic inflammation – persistent lymphocyte presence and the appearance of multinucleated giant cells – were only observed in the non-decellularized positive control and not the matrix- or saline-injected animals. This implies the response to cellular debris is both more severe and may be associated with rejection or a foreign body response, rather than the remodeling response seen with decellularized matrix materials, consistent with previously published work with decellularized grafts [283]. It may also be that the pepsin-digestion cleaves the alpha-gal epitope and reduces the severity of the immune response that way, though further investigation would be required to evaluate that hypothesis. Additionally, the inflammation observed in response to an injected ECM hydrogel is reduced due to the fact that the material degrades relatively quickly. The degradation products are all biocompatible byproducts and after the 10-14 days, the material is no longer a bulk scaffold. This is in contrast to a patch or graft that is

intended to perservere in the host tissue. As Leor postulated, an injectable biomaterial therapy for MI must be biodegradable and non-immunogenic; here we support these claims for both xenogeneic and allogeneic myocardial matrix, demonstrating degradation of the material between 14 and 28 days and an appropriate inflammatory response that may promote remodeling. Importantly, no clear differences could be drawn between the porcine and rat-derived ECM hydrogels. This supports previous conclusions regarding the conservation of ECM components across species and the general biocompatibility of the decellularized materials.

An important criterion for translation is lack of thrombogenicity and in this work we demonstrate myocardial matrix to be non-thrombogenic upon direct injection into the LV lumen. The lack of post-procedural distress in rats indicated no major event and the pathology report showed no difference in tissue morphology in peripheral organs in both matrix- and saline-injected animals. It is therefore probable that any organ damage observed was caused by the surgical procedure itself. This is apparent in the lungs, where the edema identified (Fig. 5.8) is thought to be due to ventilator pressure. The myocardial matrix is immediately diluted upon injection into the bloodstream, and therefore likely does not have a chance to self-assemble and is quickly degraded and cleared. In contrast, a synthetic or naturally-derived biomaterial that gels very quickly or causes protein aggregation could cause detrimental clot formation in the LV or peripheral vasculature [218]. Proof of hemocompatibility, however, is more than simply determining thrombogenicity of an injected material - it is also essential to understand potential effects or interactions between the matrix and the host blood. Clotting times are

an important clinical parameter, especially for patients under medical management for cardiovascular diseases. Herein, the myocardial matrix was shown to be hemocompatible in human blood, as there was no change in clotting times with the addition of the of material and no platelet activation with the addition of the standard material concentration. The slight activation observed with the high concentration of myocardial matrix is expected, as collagen is a significant component of ECM hydrogels [222] and an agonist. Addition of known agonists after the four hour experimental window confirmed that the PRP maintained the expected response to the four different agonists, validating data gathered throughout the experiment. It should be noted that the human blood used was from a healthy adult male under no medication, while the patients receiving this treatment clinically will be under significant medical management, specifically an anti-coagulant or thrombin-inhibitor. Thus, the potential for causing coagulation is unlikely, rather a potential concern arises that a degree of platelet activation could reduce the patient's ability to clot and increase the risk of bleeding. The concern that the injected material would shorten or lengthen the PT or APTT to values associated with increased risk for thromboembolism or bleeding [312], respectively, has been addressed by the results of this study, as the values did not significantly change and stayed well within the reference range for both parameters.

While the data generated are exciting and support the safety of this biomaterial therapy, there are limitations to this work. Within this work, care was taken to establish the safety of the decellularized porcine myocardial matrix material in a xenogeneic setting, through injections in a rat model and additional studies with human blood.

Despite the intentional focus on the xenogeneic response the biocompatibility and safety studies, it should be noted that the large-animal model referenced throughout this chapter used a porcine-model and thus, the material in this case is allogeneic. This work, taken in conjunction with the previous small- and large-animal studies [222], provides a foundation to support translation of this technology from large-animal preclinical studies to Phase 1 clinical trials in humans.

Chapter 5, in part, is submitted for publication as: Sonya B. Seif-Naraghi*, Jennifer M. Singelyn*, Michael A. Salvatore, Kent Osborn, Jean Wang, Jessica A. DeQuach, Unatti Sampat, Oi Ling Kwan, Monet Strachan, Jonathon Wong, Pam Schup-Magoffin, Rebecca Braden, Kendra Bartels, Adam Kinsey, Mark Preul, Nabil Dib, Anthony DeMaria, Karen L. Christman. Safety and efficacy of an injectable extracellular matrix hydrogel for treating myocardial infarction in pre-clinical animal studies. *co-authors contributed equally.

The author of this dissertation is the primary author of this manuscript.

CHAPTER SIX:

Summary and future work

6.1 Summary and conclusions

As medical management and surgical tools advance, a growing number of patients survive initial cardiac attacks. Unfortunately, a large proportion of this population then goes on to develop heart failure (HF), for which the five-year survival rate after diagnosis is only 50% [313]. Thus, there is a pressing clinical need for new therapies to prevent progression of the negative left ventricular remodeling that follows myocardial infarction (MI) and leads to HF [314]. During an MI, a blockage in a coronary artery causes death of cells in the downstream tissue. This is followed by degradation of the associated extracellular matrix (ECM) and an acute inflammatory response. Due to the limited regenerative capacity of the myocardium, the injury is resolved with formation of a dense collagenous scar. Though initially beneficial, as it stiffens the damaged region and prevents ventricular rupture, the noncontractile replacement cannot contribute to the pumping function of the heart and over time, leads to a pathology in which remote myocardium hypertrophies to compensate, the infarct wall continues to thin, the ventricle dilates, and ultimately cardiac output is insufficient to sustain systemic metabolic activity [315]. The only successful treatments for end-stage heart failure are total heart transplantation and left ventricular (LV) assist devices; however, the former is limited by a severe lack of donor organs, the latter relies on chronic use of an external device, and both require invasive, inherently risky surgical procedures.

Experimental approaches to mitigate negative remodeling and prevent HF include LV restraints, cardiac patches, *in situ*-gelling biomaterials, and cellular cardiomyoplasty or cell transplantation. Interest in LV restraints has waned considerably over the past 5

years as focus has turned toward more targeted, biodegradable strategies. Cellular cardiomyoplasty has been used experimentally in the clinic with some success [316-320], however, this technique continues to be limited by poor cell survival and retention post-implantation [27, 268]. The most attractive aspect of cell transplantation is its percutaneous catheter delivery, which is a minimally invasive procedure. Cardiac patches and injectable materials have been investigated for use as cell delivery vehicles [7, 41-45] and acellular therapies [20, 41, 46, 47], as well as in conjunction with growth factors for enhanced effect [48-51]. Investigated scaffold materials vary widely and several thorough reviews have been written on the subject [27, 308, 321]. Most work has shown that many different methods and materials can provide maintenance or improvement in functional parameters in small- and some large-animal models. However, the majority of these approaches will not transition to minimally invasive delivery in the clinic – patches require a thorocotomy for epicardial placement and most existing injectable biomaterials are not compatible with cardiac catheter procedures,,which require the material to be in the catheter during a 30 minute to 1 hour long procedure or delivered via coronary infusion.

Biomaterial therapies for the treatment of myocardial infarction and heart failure will continue to be pursued and over the next few years we will see more experimental therapies move in to clinical trials. With the rapid advancement of medical science, it is likely that all acceptable therapies will need to be deliverable via minimally invasive means. Thus, injectable biomaterials that can be administered via catheter will only become more attractive. As experimental approaches for treating myocardial infarction

move toward clinical trials, there are still only two approaches that have demonstrated utility in this approach. Alginate, which has been delivered via intracoronary injection, has gone into clinical trials. The decellularized myocardial matrix used in Chapter 5 and referenced throughout this dissertation, will likely enter clinical trials in the coming year. Alginate, as discussed in Chapter 5, has unique limitations that may narrow its applicability in the patient population – for example, requiring coronary access and potentially only being relevant in acute MI due to the need for free calcium. Decellularized materials hold such promise as scaffolds moving forward – the innate biochemical complexity, microstructures that recapitulate native extracellular matrix, biocompatible degradation products, and the potential for tissue-specific or autologous therapies.

The overall goal of this dissertation work was to investigate extracellular matrix hydrogels for cardiac repair. Through this work, we designed a decellularization and processing protocol to fabricate porcine and human pericardial matrix hydrogels. Upon characterizing the material, the presence of sulfated glycosaminoglycan content was established, similar to many other ECM hydrogels. From this point, we hypothesized that if we could natively associate growth factors with the ECM hydrogel, it could be used as a growth factor delivery system *in vivo*. We tested this hypothesis first with bFGF in an acute study evaluating enhancement of bFGF retention and neovascularization. After this successful study, we undertook a full functional study and demonstrated that a novel HGF peptide could be delivered with an ECM hydrogel to enhance cardiac function, increase angiogenesis, and decrease fibrosis post-MI. This body of work supports the

utility of ECM hydrogels, specifically the potentially autologous pericardial matrix hydrogel investigated herein.

Thus, with this work we have demonstrated, both *in vitro* and *in vivo*, that the porcine pericardial matrix hydrogel, with its sulfated sugars, has the ability to sequester bFGF. By relying on the sGAG component of the ECM-derived hydrogel to bind bFGF, the angiogenic growth factor was bound and presented in a manner similar to growth factors in the native ECM. In a rodent MI model, intramyocardial injection of bFGF in PPM was the only group to demonstrate enhanced acute neovascularization post-MI when compared to controls. We have demonstrated the potential use of a decellularized ECM-derived hydrogel as a growth factor delivery system for tissue engineering applications. While bFGF was used as the model growth factor in this study, other heparin-binding growth factors could be incorporated in a similar fashion.

We built upon these findings in Chapter 4, using the pericardial matrix to deliver a novel HGF dimer, demonstrating its potential as a therapeutic post-MI. In this work, we established the foundation for moving forward with this new peptide, as it was found to improve or preserve cardiac function in the small animal occlusion-reperfusion model. Specifically, injecting the HGF dimer with PPM improved the fractional area change and increased angiogenesis in the infarct region. Given the promising trend seen with interstitial fibrosis, it is possible the peptide possesses the anti-fibrotic properties of full length HGF. Additionally, the findings of these studies imply that the sulfated GAG content in other ECM-derived hydrogels would provide a platform for the incorporation of heparin-binding growth factors. This incorporation can be achieved without additional

chemical modification and could allow for prolonged delivery of the growth factors to the site of application.

Finally, as the goal of this work is to investigate extracellular matrix hydrogels – to understand their utility as tissue engineering scaffolds, their interaction with the host system, and their future with respect to clinical use – understanding the immune response and addressing safety concerns is an imperative task. As the evidence for benefit in pre-clinical large animal studies continues to amass and support the initiation of clinical trials, having a better understanding of the inflammatory response, as well as safety, hemocompatibility, and biocompatibility were all important. The work done in Chapter 5 to address these concerns established the safety of the xenogeneic material in a rat model, the safety with respect to thromb-embolic potential upon escape into the bloodstream. Importantly, clotting times and platelet activation were unaffected after exposure to a conservative estimate of the amount of injectable material that may end up in the bloodstream during the procedure. A long-term study evaluating the cellular infiltration in the myocardium demonstrated, for the first time, that the presence of the xenogeneic material did not cause any chronic inflammation. While the pericardial matrix is a unique material that is exciting due to its potential as an autologous therapy, it is a niche therapy. Evaluating the safety and biocompatibility of the myocardial matrix provided a great deal of insight not only into that specific material but a general understanding that can be extended to ECM hydrogels as a whole – at least when processed in a similar manner. As this material will go in to clinical trials next year, these studies form the backbone of supporting its safety *in vivo*.

6.2 Limitations and future work

There are several limitations in design of the studies presented in this dissertation, as well opportunities for future work. In Chapter 4, the functional study results are limited by the relatively low animal numbers. Additionally, if MRI had been available, that would have been a more sophisticated imaging modality that may have provided more consistent results. Histological and immunohistochemical analyses would have been greatly improved with more animals in each group and even more information could have been gathered if an earlier time point were evaluated – by one month post-injection, the intial cellular response can no longer be captured, as evidenced by the lack of clear trends in apoptotic or proliferative cells.

The work that comprises this chapter is only a starting place for answering the questions raised. Given the promising results, it would be useful and necessary to do follow-up animal studies in which the dose response to the HGF dimer delivered in an ECM hydrogel is studied. If greater effects are garnered with a higher dose of the growth factor, or similar results are seen with significantly less growth factor, this information would inform the translation of this potential therapy. Additionally, timing of both delivery and analysis would be interesting to investigate. For example, it would be of great interest to the field to establish if the therapy is effective in both acute MI and chronic MI. Evaluating the effect of delivery of the HGF dimer in an ECM hydrogel on the local tissue response and cellular infiltration at different time points after injection would also provide useful insight into the potential mechanisms by which these therapies are effective. Finally, before a true argument for using Dr. Cochran's HGF dimer in the

clinic could be made, a long-term large animal functional study would need to be performed in pigs.

Finally, the scope of this work is not limited to cardiac repair. Establishing ECM hydrogel delivery of heparin-binding growth factors, specifically this HGF dimer, will have implications in other fields. It has great promise for potential use in other applications, such as in critical limb ischemia, and this work opens a great deal of possibilities for future study. Investigation of other ECM hydrogel preparations from different tissues – specifically the myocardial matrix and skeletal muscle matrix – should be done in order to assess the possibility of using various scaffolds to deliver various growth factors for tissue engineering applications. Moving forward, the same characteristics that make the HGF dimer delivery in PPM attractive and potentially effective – specifically the reduction of fibrosis and increase in angiogenesis – are useful and potentially therapeutic properties in a wide range of ischemic diseases.

REFERENCES

1. Viola, J., Lal, B., and Grad, O., *The Emergence of Tissue Engineering as a Research Field.* The National Science Foundation, 2003.

2. Langer, R. and J.P. Vacanti, *Tissue Engineering.* Science, 1993. **260**(5110): p. 920-926.

3. Cohen, S., et al., *Design of synthetic polymeric structures for cell transplantation and tissue engineering.* Clin Mater, 1993. **13**(1-4): p. 3-10.

4. Odedra, D., et al., *Endothelial cells guided by immobilized gradients of vascular endothelial growth factor on porous collagen scaffolds.* Acta biomaterialia, 2011.

5. Atala, A. and R.P. Lanza, *Methods of tissue engineering*. 2001, San Diego, CA: Academic Press. xli, 1285 p.

6. Lanza, R.P., R.S. Langer, and J. Vacanti, *Principles of tissue engineering*. 3rd ed. 2007, Amsterdam ; Boston: Elsevier / Academic Press. xxvii, 1307 p.

7. Leor, J., Y. Amsalem, and S. Cohen, *Cells, scaffolds, and molecules for myocardial tissue engineering.* Pharmacol Ther, 2005. **105**(2): p. 151-63.

8. Lutolf, M.P. and J.A. Hubbell, *Synthetic biomaterials as instructive extracellular microenvironments for morphogenesis in tissue engineering.* Nat Biotechnol, 2005. **23**(1): p. 47-55.

9. Glowacki, J. and S. Mizuno, *Collagen scaffolds for tissue engineering.* Biopolymers, 2008. **89**(5): p. 338-44.

10. van Hout, W.M., et al., *Reconstruction of the alveolar cleft: can growth factor-aided tissue engineering replace autologous bone grafting? A literature review and systematic review of results obtained with bone morphogenetic protein-2.* Clin Oral Investig, 2011. **15**(3): p. 297-303.

11. Robinson, K.A., et al., *Extracellular matrix scaffold for cardiac repair.* Circulation, 2005. **112**(9 Suppl): p. I135-43.

12. Ott, H.C., et al., *Perfusion-decellularized matrix: using nature's platform to engineer a bioartificial heart.* Nat Med, 2008. **14**(2): p. 213-21.

13. Crapo, P.M., T.W. Gilbert, and S.F. Badylak, *An overview of tissue and whole organ decellularization processes.* Biomaterials, 2011. **32**(12): p. 3233-43.

14. Petersen, T.H., et al., *Tissue-engineered lungs for in vivo implantation.* Science, 2010. **329**(5991): p. 538-41.

14. Petersen, T.H., et al., *Tissue-engineered lungs for in vivo implantation.* Science, 2010. **329**(5991): p. 538-41.

15. Seif-Naraghi, S.B., et al., *Design and characterization of an injectable pericardial matrix gel: a potentially autologous scaffold for cardiac tissue engineering.* Tissue engineering. Part A, 2010. **16**(6): p. 2017-27.

16. Freytes, D.O., et al., *Preparation and rheological characterization of a gel form of the porcine urinary bladder matrix.* Biomaterials, 2008. **29**(11): p. 1630-7.

17. Young, D.A., et al., *Injectable hydrogel scaffold from decellularized human lipoaspirate.* Acta biomaterialia, 2011. **7**(3): p. 1040-9.

18. Dequach, J.A., et al., *Decellularized Porcine Brain Matrix for Cell Culture and Tissue Engineering Scaffolds.* Tissue Eng Part A, 2011.

19. Sellaro, T.L., et al., *Maintenance of human hepatocyte function in vitro by liver-derived extracellular matrix gels.* Tissue engineering. Part A, 2010. **16**(3): p. 1075-82.

20. Okada, M., et al., *Differential efficacy of gels derived from small intestinal submucosa as an injectable biomaterial for myocardial infarct repair.* Biomaterials, 2010. **31**(30): p. 7678-83.

21. Singelyn, J.M., et al., *Naturally derived myocardial matrix as an injectable scaffold for cardiac tissue engineering.* Biomaterials, 2009. **30**(29): p. 5409-16.

22. Hamamoto, H., et al., *Allogeneic mesenchymal precursor cell therapy to limit remodeling after myocardial infarction: the effect of cell dosage.* The Annals of thoracic surgery, 2009. **87**(3): p. 794-801.

23. Shirahata, A., K.L. Christman, and A.E. Pegg, *Quantitation of S-adenosylmethionine decarboxylase protein.* Biochemistry, 1985. **24**(16): p. 4417-23.

24. Okano, T., et al., *A novel recovery system for cultured cells using plasma-treated polystyrene dishes grafted with poly(N-isopropylacrylamide).* J Biomed Mater Res, 1993. **27**(10): p. 1243-51.

25. Yamada, N., et al., *Thermo-responsive polymeric surfaces; control of attachment and detachment of culture cells.* Macromol Chem Rapid Commun, 1990. **11**: p. 571-76.

26. Sarig, U. and M. Machluf, *Engineering cell platforms for myocardial regeneration.* Expert Opin Biol Ther, 2011. **11**(8): p. 1055-77.

27. Christman, K.L. and R.J. Lee, *Biomaterials for the treatment of myocardial infarction.* Journal of the American College of Cardiology, 2006. **48**(5): p. 907-13.

28. Stile, R.A., W.R. Burghardt, and K.E. Healy, *Synthesis and characterization of injectable poly(N-isopropylacrylamide)-based hydrogels that support tissue formation in vitro.* Macromolecules, 1999. **32**(22): p. 7370-7379.

29. Lee, B.H., et al., *In-situ injectable physically and chemically gelling NIPAAm-based copolymer system for embolization.* Biomacromolecules, 2006. **7**(6): p. 2059-2064.

30. Carmeliet, P. and E.M. Conway, *Growing better blood vessels.* Nature biotechnology, 2001. **19**(11): p. 1019-20.

31. Asahara, T., et al., *Synergistic effect of vascular endothelial growth factor and basic fibroblast growth factor on angiogenesis in vivo.* Circulation, 1995. **92**(9 Suppl): p. II365-71.

32. West, D.C., et al., *Angiogenesis induced by degradation products of hyaluronic acid.* Science, 1985. **228**(4705): p. 1324-6.

33. Fournier, N. and C.J. Doillon, *Biological molecule-impregnated polyester: an in vivo angiogenesis study.* Biomaterials, 1996. **17**(17): p. 1659-65.

34. Soker, S., M. Machado, and A. Atala, *Systems for therapeutic angiogenesis in tissue engineering.* World journal of urology, 2000. **18**(1): p. 10-8.

35. Zisch, A.H., M.P. Lutolf, and J.A. Hubbell, *Biopolymeric delivery matrices for angiogenic growth factors.* Cardiovasc Pathol, 2003. **12**(6): p. 295-310.

36. Patel, Z.S. and A.G. Mikos, *Angiogenesis with biomaterial-based drug- and cell-delivery systems.* J Biomater Sci Polym Ed, 2004. **15**(6): p. 701-26.

37. Lysaght, M.J., A. Jaklenec, and E. Deweerd, *Great expectations: private sector activity in tissue engineering, regenerative medicine, and stem cell therapeutics.* Tissue Eng Part A, 2008. **14**(2): p. 305-15.

38. Vacanti, J., *Tissue engineering and regenerative medicine: from first principles to state of the art.* J Pediatr Surg, 2010. **45**(2): p. 291-4.

39. Lloyd-Jones, D., et al., *Heart Disease and Stroke Statistics-2010 Update A Report From the American Heart Association.* Circulation, 2010. **121**(7): p. E46-E215.

40. Strickman, N.E., *The Pathogenesis and Prognosis of End-Stage Heart-Disease.* Texas Heart Institute Journal, 1987. **14**(4): p. 346-350.

41. Christman, K.L., et al., *Fibrin glue alone and skeletal myoblasts in a fibrin scaffold preserve cardiac function after myocardial infarction.* Tissue engineering, 2004. **10**(3-4): p. 403-9.

42. Simpson, D., et al., *A tissue engineering approach to progenitor cell delivery results in significant cell engraftment and improved myocardial remodeling.* Stem Cells, 2007. **25**(9): p. 2350-7.

43. Pozzobon, M., et al., *Human bone marrow-derived CD133(+) cells delivered to a collagen patch on cryoinjured rat heart promote angiogenesis and arteriogenesis.* Cell Transplant, 2010. **19**(10): p. 1247-60.

44. Kellar, R.S., et al., *Scaffold-based three-dimensional human fibroblast culture provides a structural matrix that supports angiogenesis in infarcted heart tissue.* Circulation, 2001. **104**(17): p. 2063-8.

45. Hamdi, H., et al., *Cell delivery: intramyocardial injections or epicardial deposition? A head-to-head comparison.* Ann Thorac Surg, 2009. **87**(4): p. 1196-203.

46. Badylak, S.F., et al., *The use of extracellular matrix as an inductive scaffold for the partial replacement of functional myocardium.* Cell transplantation, 2006. **15 Suppl 1**: p. S29-40.

47. Kochupura, P.V., et al., *Tissue-engineered myocardial patch derived from extracellular matrix provides regional mechanical function.* Circulation, 2005. **112**(9 Suppl): p. I144-9.

48. Harada, K., et al., *Basic fibroblast growth factor improves myocardial function in chronically ischemic porcine hearts.* The Journal of clinical investigation, 1994. **94**(2): p. 623-30.

49. Ruvinov, E., J. Leor, and S. Cohen, *The promotion of myocardial repair by the sequential delivery of IGF-1 and HGF from an injectable alginate biomaterial in a model of acute myocardial infarction.* Biomaterials, 2011. **32**(2): p. 565-78.

50. Miyagi, Y., et al., *Biodegradable collagen patch with covalently immobilized VEGF for myocardial repair.* Biomaterials, 2011. **32**(5): p. 1280-90.

51. Seif-Naraghi, S.B., et al., *Injectable extracellular matrix derived hydrogel provides a platform for enhanced retention and delivery of a heparin-binding growth factor.* Acta Biomater, 2012.

52. Rane, A.a.K.L.C., *Biomaterials for the Treatment of Myocardial Infarction: A five-year update.* Journal of the American College of Cardiology, 2011.

53. Ratner, B.D., *A paradigm shift: biomaterials that heal.* Polymer International, 2007. **56**(10): p. 1183-1185.

54. Beltrami, A.P., et al., *Adult cardiac stem cells are multipotent and support myocardial regeneration.* Cell, 2003. **114**(6): p. 763-76.

55. Kubo, H., et al., *Increased cardiac myocyte progenitors in failing human hearts.* Circulation, 2008. **118**(6): p. 649-657.

56. Ou, L., et al., *Intracardiac injection of matrigel induces stem cell recruitment and improves cardiac functions in a rat myocardial infarction model.* J Cell Mol Med, 2011. **15**(6): p. 1310-8.

57. Zhao, Z.Q., et al., *Improvement in cardiac function with small intestine extracellular matrix is associated with recruitment of C-kit cells, myofibroblasts, and macrophages after myocardial infarction.* J Am Coll Cardiol, 2010. **55**(12): p. 1250-61.

58. Seif-Naraghi, S.B., et al., *Design and Characterization of an Injectable Pericardial Matrix Gel: A Potentially Autologous Scaffold for Cardiac Tissue Engineering*, in *Tissue Eng Pt A*. 2010. p. 2017-2027.

59. Singelyn, J.M., et al., *Catheter-deliverable hydrogel derived from decellularized ventricular extracellular matrix increases endogenous cardiomyocytes and preserves cardiac function post-myocardial infarction.* Journal of the American College of Cardiology, 2011. **accepted**.

60. Lei, Y., et al., *Therapeutic angiogenesis. Devising new strategies based on past experiences.* Basic Res Cardiol, 2004. **99**(2): p. 121-32.

61. Henry, T.D., et al., *The VIVA trial: Vascular endothelial growth factor in Ischemia for Vascular Angiogenesis.* Circulation, 2003. **107**(10): p. 1359-65.

62. Haider, H., et al., *Angiomyogenesis for cardiac repair using human myoblasts as carriers of human vascular endothelial growth factor.* J Mol Med, 2004. **82**(8): p. 539-49.

63. Richardson, T.P., et al., *Polymeric system for dual growth factor delivery.* Nat Biotechnol, 2001. **19**(11): p. 1029-34.

64. Garbern, J.C., et al., *Delivery of basic fibroblast growth factor with a pH-responsive, injectable hydrogel to improve angiogenesis in infarcted myocardium.* Biomaterials. **32**(9): p. 2407-16.

65. Shen, Y.H., M.S. Shoichet, and M. Radisic, *Vascular endothelial growth factor immobilized in collagen scaffold promotes penetration and proliferation of endothelial cells.* Acta Biomater, 2008. **4**(3): p. 477-89.

66. Goncalves, L.M., *Angiogenic growth factors: potential new treatment for acute myocardial infarction?* Cardiovasc Res, 2000. **45**(2): p. 294-302.

67. Kim, J.H., et al., *The enhancement of mature vessel formation and cardiac function in infarcted hearts using dual growth factor delivery with self-assembling peptides.* Biomaterials. **32**(26): p. 6080-8.

68. Sakiyama-Elbert, S.E. and J.A. Hubbell, *Controlled release of nerve growth factor from a heparin-containing fibrin-based cell ingrowth matrix.* Journal of controlled release : official journal of the Controlled Release Society, 2000. **69**(1): p. 149-58.

69. Pieper, J.S., et al., *Loading of collagen-heparan sulfate matrices with bFGF promotes angiogenesis and tissue generation in rats.* Journal of biomedical materials research, 2002. **62**(2): p. 185-94.

70. Freeman, I., A. Kedem, and S. Cohen, *The effect of sulfation of alginate hydrogels on the specific binding and controlled release of heparin-binding proteins.* Biomaterials, 2008. **29**(22): p. 3260-8.

71. Sakiyama, S.E., J.C. Schense, and J.A. Hubbell, *Incorporation of heparin-binding peptides into fibrin gels enhances neurite extension: an example of designer matrices in tissue engineering.* The FASEB journal : official publication of the Federation of American Societies for Experimental Biology, 1999. **13**(15): p. 2214-24.

72. Sakiyama-Elbert, S.E. and J.A. Hubbell, *Development of fibrin derivatives for controlled release of heparin-binding growth factors.* Journal of controlled release : official journal of the Controlled Release Society, 2000. **65**(3): p. 389-402.

73. Miyagi, Y., et al., *Biodegradable collagen patch with covalently immobilized VEGF for myocardial repair.* Biomaterials. **32**(5): p. 1280-90.

74. Iozzo, R.V., *Proteoglycans : structure, biology, and molecular interactions*. 2000, New York: Marcel Dekker. ix, 422 p.

75. Li, R.K., et al., *Survival and function of bioengineered cardiac grafts.* Circulation, 1999. **100**(19): p. 63-69.

76. Leor, J., et al., *Bioengineered cardiac grafts - A new approach to repair the infarcted myocardium?* Circulation, 2000. **102**(19): p. 56-61.

77. Pozzobon, M., et al., *Human Bone Marrow-Derived CD133(+) Cells Delivered to a Collagen Patch on Cryoinjured Rat Heart Promote Angiogenesis and Arteriogenesis.* Cell Transplant, 2010. **19**(10): p. 1247-1260.

78. Simpson, D., et al., *A tissue engineering approach to progenitor cell delivery results in significant cell engraftment and improved myocardial remodeling.* Stem Cells, 2007. **25**(9): p. 2350-2357.

79. Cortes-Morichetti, M., et al., *Association between a cell-seeded collagen matrix and cellular Cardiomyoplasty for myocardial support and regeneration.* Tissue Eng, 2007. **13**(11): p. 2681-2687.

80. Chachques, J.C., et al., *Myocardial Assistance by Grafting a New Upgraded bioartificial Myocardium (MAGNUM Trial): clinical results at 2 years*. European Heart Journal, 2010. **31**: p. 941-941.

81. Wei, H., et al., *Bioengineered cardiac patch constructed from multilayered mesenchymal stem cells for myocardial repair.* Biomaterials, 2008. **29**(26): p. 3547-56.

82. Tan, M.Y., et al., *Repair of infarcted myocardium using mesenchymal stem cell seeded small intestinal submucosa in rabbits*, in *Biomaterials*. 2009. p. 3234-3240.

83. Xiong, Q., et al., *A fibrin patch-based enhanced delivery of human embryonic stem cell-derived vascular cell transplantation in a porcine model of postinfarction left ventricular remodeling.* Stem Cells, 2011. **29**(2): p. 367-75.

84. Godier-Furnémont, A.F., et al., *Composite scaffold provides a cell delivery platform for cardiovascular repair.* Proc Natl Acad Sci USA, 2011. **108**(19): p. 7974-9.

85. Jin, J., et al., *Transplantation of mesenchymal stem cells within a poly(lactide-co-epsilon-caprolactone) scaffold improves cardiac function in a rat myocardial infarction model.* Eur J Heart Fail, 2009. **11**(2): p. 147-53.

86. Fujimoto, K.L., et al., *An elastic, biodegradable cardiac patch induces contractile smooth muscle and improves cardiac remodeling and function in subacute myocardial infarction*, in *J Am Coll Cardiol*. 2007. p. 2292-2300.

87. Piao, H., et al., *Effects of cardiac patches engineered with bone marrow-derived mononuclear cells and PGCL scaffolds in a rat myocardial infarction model*, in *Biomaterials*. 2007. p. 641-649.

88. Miyagi, Y., et al., *Surgical ventricular restoration with a cell- and cytokine-seeded biodegradable scaffold.* Biomaterials, 2010. **31**(30): p. 7684-94.

89. Kim, J.H., et al., *The enhancement of mature vessel formation and cardiac function in infarcted hearts using dual growth factor delivery with self-assembling peptides.* Biomaterials, 2011. **32**(26): p. 6080-8.

90. Dubois, G., et al., *Self-assembling peptide nanofibers and skeletal myoblast transplantation in infarcted myocardium.* J Biomed Mater Res Part B Appl Biomater, 2008. **87**(1): p. 222-8.

91. Davis, M.E., et al., *Injectable self-assembling peptide nanofibers create intramyocardial microenvironments for endothelial cells.* Circulation, 2005. **111**(4): p. 442-50.

92. Lin, Y.D., et al., *Instructive nanofiber scaffolds with VEGF create a microenvironment for arteriogenesis and cardiac repair.* Science Translational Medicine, 2012. **4**: p. 146ra109.

93. Christman, K.L., et al., *Injectable fibrin scaffold improves cell transplant survival, reduces infarct expansion, and induces neovasculature formation in ischemic myocardium.* Journal of the American College of Cardiology, 2004. **44**(3): p. 654-60.

94. Guo, H.D., et al., *Transplantation of marrow-derived cardiac stem cells carried in fibrin improves cardiac function after myocardial infarction.* Tissue Eng Pt A, 2011. **17**(1-2): p. 45-58.

95. Danoviz, M.E., et al., *Rat Adipose Tissue-Derived Stem Cells Transplantation Attenuates Cardiac Dysfunction Post Infarction and Biopolymers Enhance Cell Retention*, in *PLoS ONE*. 2010. p. e12077.

96. Zhang, X., et al., *Preservation of the cardiac function in infarcted rat hearts by the transplantation of adipose-derived stem cells with injectable fibrin scaffolds.* Exp Biol Med (Maywood), 2010. **235**(12): p. 1505-15.

97. Landa, N., et al., *Effect of injectable alginate implant on cardiac remodeling and function after recent and old infarcts in rat.* Circulation, 2008. **117**(11): p. 1388-96.

98. Yu, J., et al., *The use of human mesenchymal stem cells encapsulated in RGD modified alginate microspheres in the repair of myocardial infarction in the rat*, in *Biomaterials*. 2010. p. 7012-7020.

99. Hao, X., et al., *Angiogenic effects of sequential release of VEGF-A165 and PDGF-BB with alginate hydrogels after myocardial infarction.* Cardiovasc Res, 2007. **75**(1): p. 178-85.

100. Ruvinov, E., J. Leor, and S. Cohen, *The promotion of myocardial repair by the sequential delivery of IGF-1 and HGF from an injectable alginate biomaterial in a model of acute myocardial infarction*, in *Biomaterials*. 2011. p. 565-578.

101. Leor, J., et al., *Intracoronary injection of in situ forming alginate hydrogel reverses left ventricular remodeling after myocardial infarction in Swine.* J Am Coll Cardiol, 2009. **54**(11): p. 1014-23.

102. BioLineRx, L., *Safety and Feasibility of the Injectable BL-1040 Implant. Clinical Trials.gov NCT00557531*. 2007.

103. Okada, M., et al., *Differential efficacy of gels derived from small intestinal submucosa as an injectable biomaterial for myocardial infarct repair*, in *Biomaterials*. 2010. p. 7678-7683.

104. Lu, W.N., et al., *Functional improvement of infarcted heart by co-injection of embryonic stem cells with temperature-responsive chitosan hydrogel.* Tissue Eng Pt A, 2009. **15**(6): p. 1437-47.

105. Lue, S., et al., *Both the Transplantation of Somatic Cell Nuclear Transfer- and Fertilization-Derived Mouse Embryonic Stem Cells with Temperature-Responsive Chitosan Hydrogel Improve Myocardial Performance in Infarcted Rat Hearts*, in *Tissue Eng Pt A*. 2010. p. 1303-1315.

106. Wang, H., et al., *Improved myocardial performance in infarcted rat heart by co-injection of basic fibroblast growth factor with temperature-responsive Chitosan hydrogel*, in *J Heart Lung Transpl*. 2010. p. 881-887.

107. Shao, Z.Q., et al., *Effects of intramyocardial administration of slow-release basic fibroblast growth factor on angiogenesis and ventricular remodeling in a rat infarct model*, in *Circ J*. 2006. p. 471-477.

108. Liu, Y., et al., *Effects of basic fibroblast growth factor microspheres on angiogenesis in ischemic myocardium and cardiac function: analysis with dobutamine cardiovascular magnetic resonance tagging*, in *Eur J Cardio-Thorac*. 2006. p. 103-107.

109. Davis, M.E., et al., *Local myocardial insulin-like growth factor 1 (IGF-1) delivery with biotinylated peptide nanofibers improves cell therapy for myocardial infarction*, in *Proc Natl Acad Sci USA*. 2006. p. 8155-8160.

110. Lin, Y., et al., *Intramyocardial peptide nanofiber injection improves postinfarction ventricular remodeling and efficacy of bone marrow cell therapy in pigs.* Circulation, 2010. **122**(11 Suppl): p. S132-41.

111. Kraehenbuehl, T.P., et al., *Human embryonic stem cell-derived microvascular grafts for cardiac tissue preservation after myocardial infarction*, in *Biomaterials*. 2011. p. 1102-1109.

112. Wall, S.T., et al., *Biomimetic matrices for myocardial stabilization and stem cell transplantation.* Journal of Biomedical Materials Research Part A, 2010. **95A**(4): p. 1055-1066.

113. Yoon, S.J., et al., *Regeneration of Ischemic Heart Using Hyaluronic Acid-Based Injectable Hydrogel*, in *J Biomed Mater Res B*. 2009. p. 163-171.

114. Wall, S.T., et al., *Theoretical impact of the injection of material into the myocardium: a finite element model simulation.* Circulation, 2006. **114**(24): p. 2627-35.

115. Rane, A.A., et al., *Increased Infarct Wall Thickness by a Bio-Inert Material Is Insufficient to Prevent Negative Left Ventricular Remodeling after Myocardial Infarction.* PLoS One, 2011. **6**(6).

116. Dobner, S., et al., *A Synthetic Non-degradable Polyethylene Glycol Hydrogel Retards Adverse Post-infarct Left Ventricular Remodeling.* J Card Fail, 2009. **15**(7): p. 629-636.

117. Singelyn, J.M. and K.L. Christman, *Injectable Materials for the Treatment of Myocardial Infarction and Heart Failure: The Promise of Decellularized Matrices.* J Cardiovasc Transl Res, 2010. **3**(5): p. 478-486.

118. Writing Group, M., et al., *Heart Disease and Stroke Statistics--2009 Update: A Report From the American Heart Association Statistics Committee and Stroke Statistics Subcommittee.* Circulation, 2009. **119**(3): p. e21-181.

119. Bergmann, O., et al., *Evidence for cardiomyocyte renewal in humans.* Science, 2009. **324**(5923): p. 98-102.

120. Mann, D.L., *Mechanisms and models in heart failure: A combinatorial approach.* Circulation, 1999. **100**(9): p. 999-1008.

121. Laflamme, M.A. and C.E. Murry, *Regenerating the heart.* Nat Biotechnol, 2005. **23**(7): p. 845-56.

122. Reffelmann, T. and R.A. Kloner, *Cellular cardiomyoplasty--cardiomyocytes, skeletal myoblasts, or stem cells for regenerating myocardium and treatment of heart failure?* Cardiovasc Res, 2003. **58**(2): p. 358-68.

123. Christman, K.L. and R.J. Lee, *Biomaterials for the treatment of myocardial infarction.* J Am Coll Cardiol, 2006. **48**(5): p. 907-13.

124. Martinez, E.C. and T. Kofidis, *Myocardial tissue engineering: the quest for the ideal myocardial substitute.* Expert Rev Cardiovasc Ther, 2009. **7**(8): p. 921-8.

125. Christman, K.L., et al., *Injectable fibrin scaffold improves cell transplant survival, reduces infarct expansion, and induces neovasculature formation in ischemic myocardium.* J Am Coll Cardiol, 2004. **44**(3): p. 654-60.

126. Christman, K.L., et al., *Fibrin glue alone and skeletal myoblasts in a fibrin scaffold preserve cardiac function after myocardial infarction.* Tissue Eng, 2004. **10**: p. 403-9.

127. Huang, N.F., et al., *Injectable biopolymers enhance angiogenesis after myocardial infarction.* Tissue Eng, 2005. **11**(11-12): p. 1860-6.

128. Landa, N., et al., *Effect of Injectable Alginate Implant on Cardiac Remodeling and Function After Recent and Old Infarcts in Rat.* Circulation, 2008. **117**(11): p. 1388-1396.

129. Lu, W.N., et al., *Functional improvement of infarcted heart by co-injection of embryonic stem cells with temperature-responsive chitosan hydrogel.* Tissue Eng Part A, 2009. **15**(6): p. 1437-47.

130. Hsieh, P.C., et al., *Controlled delivery of PDGF-BB for myocardial protection using injectable self-assembling peptide nanofibers.* J Clin Invest, 2006. **116**(1): p. 237-48.

131. Padin-Iruegas, M.E.M.D., et al., *Cardiac Progenitor Cells and Biotinylated Insulin-Like Growth Factor-1 Nanofibers Improve Endogenous and Exogenous Myocardial Regeneration After Infarction.* Circulation, 2009. **120**(10): p. 876-887.

132. Dobner, S., et al., *A synthetic non-degradable polyethylene glycol hydrogel retards adverse post-infarct left ventricular remodeling.* J Card Fail, 2009. **15**(7): p. 629-36.

133. Kofidis, T., et al., *Novel injectable bioartificial tissue facilitates targeted, less invasive, large-scale tissue restoration on the beating heart after myocardial injury.* Circulation, 2005. **112**(9 Suppl): p. I173-7.

134. Freytes, D.O., et al., *Preparation and rheological characterization of a gel form of the porcine urinary bladder matrix.* Biomaterials, 2008. **29**(11): p. 1630-1637.

135. Colombo, A., et al., *The pericardium covered stent (PCS).* EuroIntervention, 2009. **5**(3): p. 394-9.

136. Baharuddin, A., et al., *Bovine pericardium for dural graft: clinical results in 22 patients.* Clin Neurol Neurosurg, 2002. **104**(4): p. 342-4.

137. Rahimtoola, S.H., *Choice of prosthetic heart valve for adult patients.* J Am Coll Cardiol, 2003. **41**(6): p. 893-904.

138. Hvass, U. and M.F. O'Brien, *The stentless Cryolife-O'Brien aortic porcine xenograft: a five-year follow-up.* Ann Thorac Surg, 1998. **66**(6 Suppl): p. S134-8.

139. Garlick, R.B. and M.F. O'Brien, *The CryoLife-O'Brien composite stentless porcine aortic xenograft valve in 118 patients.* Jpn Circ J, 1997. **61**(8): p. 682-6.

140. O'Brien, M.F., *The Cryolife-O'Brien composite aortic stentless xenograft: surgical technique of implantation.* Ann Thorac Surg, 1995. **60**(2 Suppl): p. S410-3.

141. Braga-Vilela, A.S., et al., *Extracellular matrix of porcine pericardium: biochemistry and collagen architecture.* J Membr Biol, 2008. **221**(1): p. 15-25.

142. Badylak, S.F., *The extracellular matrix as a biologic scaffold material.* Biomaterials, 2007. **28**(25): p. 3587-93.

143. Fuster, V., *Hurst's the heart*. 10th ed. 2001, New York: McGraw-Hill Medical Publishing Division. xxi, 2568 [92] p., [48] p. of plates.

144. Duran, C.M., et al., *Aortic valve replacement with freehand autologous pericardium.* J Thorac Cardiovasc Surg, 1995. **110**(2): p. 511-6.

145. Chauvaud, S., et al., *Valve extension with glutaraldehyde-preserved autologous pericardium. Results in mitral valve repair.* J Thorac Cardiovasc Surg, 1991. **102**(2): p. 171-177.

146. David, T.E., C.M. Feindel, and G.V. Ropchan, *Reconstruction of the left ventricle with autologous pericardium.* J Thorac Cardiovasc Surg, 1987. **94**(5): p. 710-4.

147. Badylak, S., et al., *Extracellular matrix for myocardial repair.* Heart Surg Forum, 2003. **6**(2): p. E20-6.

148. McDonald, P.C., et al., *The challenge of defining normality for human mitral and aortic valves: geometrical and compositional analysis.* Cardiovasc Pathol, 2002. **11**(4): p. 193-209.

149. Mirsadraee, S., et al., *Development and characterization of an acellular human pericardial matrix for tissue engineering.* Tissue Eng, 2006. **12**(4): p. 763-73.

150. San Antonio, J.D., et al., *Isolation of heparin-insensitive aortic smooth muscle cells. Growth and differentiation.* Arterioscler Thromb, 1993. **13**(5): p. 748-57.

151. Reing, J.E., et al., *Degradation products of extracellular matrix affect cell migration and proliferation.* Tissue Eng Part A, 2009. **15**(3): p. 605-14.

152. Akahane, T., et al., *TIMP-1 inhibits microvascular endothelial cell migration by MMP-dependent and MMP-independent mechanisms.* Exp Cell Res, 2004. **301**(2): p. 158-67.

153. Danilatos, G.D. and R. Postle, *The environmental scanning electron microscope and its applications.* Scan Electron Microsc, 1982(Pt 1): p. 1-16.

154. Stuart, K. and A. Panitch, *Influence of chondroitin sulfate on collagen gel structure and mechanical properties at physiologically relevant levels.* Biopolymers, 2008. **89**(10): p. 841-51.

155. Cornwell, K.G., et al., *Crosslinking of discrete self-assembled collagen threads: Effects on mechanical strength and cell-matrix interactions.* J Biomed Mater Res A, 2007. **80**(2): p. 362-71.

156. Partis, M.D., et al., *Cross-linking of protein by ω-maleimido alkanoyl<i>N</i>-hydroxysuccinimido esters.* Journal of Protein Chemistry, 1983. **2**(3): p. 263-277.

157. Di Luozzo, G., et al., *Nicotine induces mitogen-activated protein kinase dependent vascular smooth muscle cell migration.* Atherosclerosis, 2005. **178**(2): p. 271-7.

158. Lau, Y.T. and W.C. Ma, *Nitric oxide inhibits migration of cultured endothelial cells.* Biochem Biophys Res Commun, 1996. **221**(3): p. 670-4.

159. Limana, F., et al., *Identification of Myocardial and Vascular Precursor Cells in Human and Mouse Epicardium.* Circ Res, 2007. **101**(12): p. 1255-1265.

160. Young, D.A., et al., *Injectable hydrogel scaffold from decellularized human lipoaspirate.* Acta Biomater. **7**(3): p. 1040-9.

161. Seif-Naraghi, S.B., et al., *Design and characterization of an injectable pericardial matrix gel: a potentially autologous scaffold for cardiac tissue engineering.* Tissue Eng Part A. **16**(6): p. 2017-27.

162. Vogel, B.E. and E.M. Hedgecock, *Hemicentin, a conserved extracellular member of the immunoglobulin superfamily, organizes epithelial and other cell attachments into oriented line-shaped junctions.* Development, 2001. **128**(6): p. 883-94.

163. Bengtsson, E., et al., *The primary structure of a basic leucine-rich repeat protein, PRELP, found in connective tissues.* J Biol Chem, 1995. **270**(43): p. 25639-44.

164. Zhao, Z., et al., *The gene for a human microfibril-associated glycoprotein is commonly deleted in Smith-Magenis syndrome patients.* Hum Mol Genet, 1995. **4**(4): p. 589-97.

165. Pan, T.C., et al., *Structure and expression of fibulin-2, a novel extracellular matrix protein with multiple EGF-like repeats and consensus motifs for calcium binding.* J Cell Biol, 1993. **123**(5): p. 1269-77.

166. Zhang, R.Z., et al., *Fibulin-2 (FBLN2): human cDNA sequence, mRNA expression, and mapping of the gene on human and mouse chromosomes.* Genomics, 1994. **22**(2): p. 425-30.

167. Utani, A., M. Nomizu, and Y. Yamada, *Fibulin-2 binds to the short arms of laminin-5 and laminin-1 via conserved amino acid sequences.* J Biol Chem, 1997. **272**(5): p. 2814-20.

168. Superti-Furga, A., et al., *Complementary DNA sequence and chromosomal mapping of a human proteoglycan-binding cell-adhesion protein (dermatopontin).* Genomics, 1993. **17**(2): p. 463-7.

169. Colombatti, A., et al., *The EMILIN protein family.* Matrix Biol, 2000. **19**(4): p. 289-301.

170. Esch, F.S., et al., *Structural characterization of follistatin: a novel follicle-stimulating hormone release-inhibiting polypeptide from the gonad.* Mol Endocrinol, 1987. **1**(11): p. 849-55.

171. Ueno, N., et al., *Isolation and partial characterization of follistatin: a single-chain Mr 35,000 monomeric protein that inhibits the release of follicle-stimulating hormone.* Proc Natl Acad Sci U S A, 1987. **84**(23): p. 8282-6.

172. Kielty, C.M., et al., *Fibrillin: from microfibril assembly to biomechanical function.* Philos Trans R Soc Lond B Biol Sci, 2002. **357**(1418): p. 207-17.

173. Kielty, C.M., et al., *Fibrillin-rich microfibrils: elastic biopolymers of the extracellular matrix.* J Muscle Res Cell Motil, 2002. **23**(5-6): p. 581-96.

174. Sakai, L.Y., D.R. Keene, and E. Engvall, *Fibrillin, a new 350-kD glycoprotein, is a component of extracellular microfibrils.* J Cell Biol, 1986. **103**(6 Pt 1): p. 2499-509.

175. Kavoussi, S.K., et al., *Oocyte cryopreservation in a woman with mosaic Turner syndrome: a case report.* The Journal of reproductive medicine, 2008. **53**(3): p. 223-6.

176. Laremore, T.N., et al., *Domain structure elucidation of human decorin glycosaminoglycans.* Biochem J. **431**(2): p. 199-205.

177. Santra, M., C.C. Reed, and R.V. Iozzo, *Decorin binds to a narrow region of the epidermal growth factor (EGF) receptor, partially overlapping but distinct from the EGF-binding epitope.* J Biol Chem, 2002. **277**(38): p. 35671-81.

178. Iozzo, R.V., et al., *Decorin is a biological ligand for the epidermal growth factor receptor.* J Biol Chem, 1999. **274**(8): p. 4489-92.

179. Bratt, A., et al., *Angiomotin regulates endothelial cell-cell junctions and cell motility.* J Biol Chem, 2005. **280**(41): p. 34859-69.

180. Kubo, H., et al., *Increased cardiac myocyte progenitors in failing human hearts.* Circulation, 2008. **118**(6): p. 649-57.

181. Etzion, S., et al., *Cellular Cardiomyoplasty of Cardiac Fibroblasts by Adenoviral Delivery of MyoD Ex Vivo: An Unlimited Source of Cells for Myocardial Repair.* Circulation, 2002. **106**(90121): p. I-125-130.

182. Kao, R.L., W. Browder, and C. Li, *Cellular Cardiomyoplasty: What Have We Learned?* Asian Cardiovasc Thorac Ann, 2009. **17**(1): p. 89-101.

183. Brown, L., *Cardiac extracellular matrix: a dynamic entity.* Am J Physiol Heart Circ Physiol, 2005. **289**(3): p. H973-4.

184. Francesco, R., et al., *From Cell-ECM interactions to tissue engineering.* Journal of Cellular Physiology, 2004. **199**(2): p. 174-180.

185. Uriel, S., et al., *Extraction and assembly of tissue-derived gels for cell culture and tissue engineering.* Tissue Eng Part C Methods, 2009. **15**(3): p. 309-21.

186. Li, F., et al., *Low-molecular-weight peptides derived from extracellular matrix as chemoattractants for primary endothelial cells.* Endothelium, 2004. **11**(3-4): p. 199-206.

187. Bader, A., et al., *Tissue engineering of heart valves--human endothelial cell seeding of detergent acellularized porcine valves.* Eur J Cardiothorac Surg, 1998. **14**(3): p. 279-84.

188. Beattie, A.J., et al., *Chemoattraction of progenitor cells by remodeling extracellular matrix scaffolds.* Tissue Eng Part A, 2009. **15**(5): p. 1119-25.

189. Brennan, E.P., et al., *Chemoattractant activity of degradation products of fetal and adult skin extracellular matrix for keratinocyte progenitor cells.* J Tissue Eng Regen Med, 2008. **2**(8): p. 491-8.

190. Sarikaya, A., et al., *Antimicrobial activity associated with extracellular matrices.* Tissue Eng, 2002. **8**(1): p. 63-71.

191. Brennan, E.P., et al., *Antibacterial activity within degradation products of biological scaffolds composed of extracellular matrix.* Tissue Eng, 2006. **12**(10): p. 2949-55.

192. Isoda, M., *Eosinophil chemotactic activity of collagen-derived fragments--a preliminary report.* J Dermatol, 1988. **15**(1): p. 83-6.

193. Mundy, G.R., S. DeMartino, and D.W. Rowe, *Collagen and collagen-derived fragments are chemotactic for tumor cells.* J Clin Invest, 1981. **68**(4): p. 1102-5.

194. Moore, A.R., et al., *The chemotactic properties of cartilage glycosaminoglycans for polymorphonuclear neutrophils.* Int J Tissue React, 1989. **11**(6): p. 301-7.

195. Hodde, J., *Naturally occurring scaffolds for soft tissue repair and regeneration.* Tissue Eng, 2002. **8**(2): p. 295-308.

196. Landsman, A., D. Taft, and K. Riemer, *The role of collagen bioscaffolds, foamed collagen, and living skin equivalents in wound healing.* Clin Podiatr Med Surg, 2009. **26**(4): p. 525-33.

197. Roberts, N.B. and W.H. Taylor, *The preparation and purification of individual human pepsins by using diethylaminoethyl-cellulose.* Biochem J, 1978. **169**(3): p. 607-15.

198. Stephens, E.H., et al., *Age-related changes in material behavior of porcine mitral and aortic valves and correlation to matrix composition.* Tissue Eng Part A. **16**(3): p. 867-78.

199. Fujita, M., et al., *Pericardial fluid as a new material for clinical heart research.* Int J Cardiol, 2001. **77**(2-3): p. 113-8.

200. Zipes, D.P. and E. Braunwald, *Braunwald's heart disease : a textbook of cardiovascular medicine*. 7th ed. 2005, Philadelphia, Pa.: W.B. Saunders. xxi, 2183, 74 p.

201. Sisson, K., et al., *Fiber diameters control osteoblastic cell migration and differentiation in electrospun gelatin.* J Biomed Mater Res A. **94**(4): p. 1312-20.

202. Christopherson, G.T., H. Song, and H.Q. Mao, *The influence of fiber diameter of electrospun substrates on neural stem cell differentiation and proliferation.* Biomaterials, 2009. **30**(4): p. 556-64.

203. Yang, F., et al., *Electrospinning of nano/micro scale poly(L-lactic acid) aligned fibers and their potential in neural tissue engineering.* Biomaterials, 2005. **26**(15): p. 2603-10.

204. Jawad, H., et al., *Myocardial tissue engineering: a review.* J Tissue Eng Regen Med, 2007. **1**(5): p. 327-42.

205. Marshall, A.J. and B.D. Ratner, *Quantitative characterization of sphere-templated porous biomaterials.* AIChE Journal, 2005. **51**(4): p. 1221-1232.

206. Crane, G.M., S.L. Ishaug, and A.G. Mikos, *Bone tissue engineering.* Nat Med, 1995. **1**(12): p. 1322-4.

207. Hutmacher, D.W., *Scaffolds in tissue engineering bone and cartilage.* Biomaterials, 2000. **21**(24): p. 2529-43.

208. Ishaug, S.L., et al., *Bone formation by three-dimensional stromal osteoblast culture in biodegradable polymer scaffolds.* J Biomed Mater Res, 1997. **36**(1): p. 17-28.

209. Langer, R. and J.P. Vacanti, *Tissue engineering.* Science, 1993. **260**(5110): p. 920-6.

210. Martina, M., et al., *Developing macroporous bicontinuous materials as scaffolds for tissue engineering.* Biomaterials, 2005. **26**(28): p. 5609-16.

211. Stosich, M.S., et al., *Vascularized adipose tissue grafts from human mesenchymal stem cells with bioactive cues and microchannel conduits.* Tissue Eng, 2007. **13**(12): p. 2881-90.

212. Augst, A.D., H.J. Kong, and D.J. Mooney, *Alginate hydrogels as biomaterials.* Macromol Biosci, 2006. **6**(8): p. 623-33.

213. Alsberg, E., et al., *Regulating bone formation via controlled scaffold degradation.* J Dent Res, 2003. **82**(11): p. 903-8.

214. Peek, K., N.B. Roberts, and W.H. Taylor, *Improved separation of human pepsins from gastric juice by high-performance ion-exchange chromatography.* J Chromatogr, 1989. **476**: p. 291-7.

215. Patel, Z.S. and A.G. Mikos, *Angiogenesis with biomaterial-based drug- and cell-delivery systems.* Journal of biomaterials science. Polymer edition, 2004. **15**(6): p. 701-26.

216. Drury, J.L. and D.J. Mooney, *Hydrogels for tissue engineering: scaffold design variables and applications.* Biomaterials, 2003. **24**(24): p. 4337-51.

217. Dai, W., et al., *Thickening of the infarcted wall by collagen injection improves left ventricular function in rats: a novel approach to preserve cardiac function after myocardial infarction.* Journal of the American College of Cardiology, 2005. **46**(4): p. 714-9.

218. Fujimoto, K.L., et al., *Synthesis, characterization and therapeutic efficacy of a biodegradable, thermoresponsive hydrogel designed for application in chronic infarcted myocardium.* Biomaterials, 2009. **30**(26): p. 4357-68.

219. Crapo, P.M., T.W. Gilbert, and S.F. Badylak, *An overview of tissue and whole organ decellularization processes.* Biomaterials. **32**(12): p. 3233-43.

220. Singelyn, J.M. and K.L. Christman, *Injectable materials for the treatment of myocardial infarction and heart failure: the promise of decellularized matrices.* J Cardiovasc Transl Res. **3**(5): p. 478-86.

221. Gilbert, T.W., T.L. Sellaro, and S.F. Badylak, *Decellularization of tissues and organs.* Biomaterials, 2006. **27**(19): p. 3675-83.

222. Singelyn, J.M., et al., *Catheter-Deliverable Hydrogel Derived From Decellularized Ventricular Extracellular Matrix Increases Endogenous Cardiomyocytes and Preserves Cardiac Function Post-Myocardial Infarction.* Journal of the American College of Cardiology, 2012. **59**(8): p. 751-763.

223. Emanueli, C., et al., *Rescue of impaired angiogenesis in spontaneously hypertensive rats by intramuscular human tissue kallikrein gene transfer.* Hypertension, 2001. **38**(1): p. 136-41.

224. Isner, J.M. and T. Asahara, *Angiogenesis and vasculogenesis as therapeutic strategies for postnatal neovascularization.* The Journal of clinical investigation, 1999. **103**(9): p. 1231-6.

225. Laham, R.J., et al., *Local perivascular delivery of basic fibroblast growth factor in patients undergoing coronary bypass surgery: results of a phase I randomized, double-blind, placebo-controlled trial.* Circulation, 1999. **100**(18): p. 1865-71.

226. Kellar, R.S., et al., *Scaffold-based three-dimensional human fibroblast culture provides a structural matrix that supports angiogenesis in infarcted heart tissue.* Circulation, 2001. **104**(17): p. 2063-8.

227. Hung, W.S., et al., *Cytotoxicity and immunogenicity of SACCHACHITIN and its mechanism of action on skin wound healing.* Journal of biomedical materials research, 2001. **56**(1): p. 93-100.

228. Binzen, E., et al., *Angiogenesis around new AB-polymer networks after one week of implantation in mice.* Clinical hemorheology and microcirculation, 2003. **28**(3): p. 183-8.

229. Pandit, A.S., D.S. Feldman, and J. Caulfield, *In vivo wound healing response to a modified degradable fibrin scaffold.* Journal of biomaterials applications, 1998. **12**(3): p. 222-36.

230. Pandit, A.S., et al., *Stimulation of angiogenesis by FGF-1 delivered through a modified fibrin scaffold.* Growth factors, 1998. **15**(2): p. 113-23.

231. Mann, B.K., R.H. Schmedlen, and J.L. West, *Tethered-TGF-beta increases extracellular matrix production of vascular smooth muscle cells.* Biomaterials, 2001. **22**(5): p. 439-44.

232. Tayalia, P. and D.J. Mooney, *Controlled growth factor delivery for tissue engineering.* Adv Mater, 2009. **21**(32-33): p. 3269-85.

233. Lee, K.Y., et al., *Controlled growth factor release from synthetic extracellular matrices.* Nature, 2000. **408**(6815): p. 998-1000.

234. Chen, R.R. and D.J. Mooney, *Polymeric growth factor delivery strategies for tissue engineering.* Pharm Res, 2003. **20**(8): p. 1103-12.

235. Berger, J., et al., *Structure and interactions in covalently and ionically crosslinked chitosan hydrogels for biomedical applications.* Eur J Pharm Biopharm, 2004. **57**(1): p. 19-34.

236. Seif-Naraghi, S.B., et al., *Patient-to-Patient Variability in Autologous Pericardial Matrix Scaffolds for Cardiac Repair.* Journal of cardiovascular translational research, 2011.

237. Johnston, N., et al., *Activity/stability of human pepsin: implications for reflux attributed laryngeal disease.* Laryngoscope, 2007. **117**(6): p. 1036-9.

238. Christman, K.L., et al., *Enhanced neovasculature formation in ischemic myocardium following delivery of pleiotrophin plasmid in a biopolymer.* Biomaterials, 2005. **26**(10): p. 1139-44.

239. Hodde, J.P., et al., *Glycosaminoglycan content of small intestinal submucosa: a bioscaffold for tissue replacement.* Tissue Eng, 1996. **2**(3): p. 209-17.

240. Camacho, N.P., et al., *FTIR microscopic imaging of collagen and proteoglycan in bovine cartilage.* Biopolymers, 2001. **62**(1): p. 1-8.

241. Huc, A. and J. Sanejouand, *[Study of the infra-red spectrum of acid-soluble collagen].* Biochim Biophys Acta, 1968. **154**(2): p. 408-10.

242. Lazarev, Y.A., B.A. Grishkovsky, and T.B. Khromova, *Amide I band of IR spectrum and structure of collagen and related polypeptides.* Biopolymers, 1985. **24**(8): p. 1449-78.

243. Potter, K., et al., *Imaging of collagen and proteoglycan in cartilage sections using Fourier transform infrared spectral imaging.* Arthritis Rheum, 2001. **44**(4): p. 846-55.

244. Johnson, T.D., S.Y. Lin, and K.L. Christman, *Tailoring material properties of a nanofibrous extracellular matrix derived hydrogel.* Nanotechnology, 2011. **22**(49): p. 494015.

245. Capila, I. and R.J. Linhardt, *Heparin-protein interactions.* Angew Chem Int Ed Engl, 2002. **41**(3): p. 391-412.

246. Shen, Y.H., M.S. Shoichet, and M. Radisic, *Vascular endothelial growth factor immobilized in collagen scaffold promotes penetration and proliferation of endothelial cells.* Acta biomaterialia, 2008. **4**(3): p. 477-89.

247. Peters, M.C., et al., *Release from alginate enhances the biological activity of vascular endothelial growth factor.* J Biomater Sci Polym Ed, 1998. **9**(12): p. 1267-78.

248. Perets, A., et al., *Enhancing the vascularization of three-dimensional porous alginate scaffolds by incorporating controlled release basic fibroblast growth factor microspheres.* J Biomed Mater Res A, 2003. **65**(4): p. 489-97.

249. Fasol, R., et al., *Experimental use of a modified fibrin glue to induce site-directed angiogenesis from the aorta to the heart.* J Thorac Cardiovasc Surg, 1994. **107**(6): p. 1432-9.

250. Fujisato, T., et al., *Effect of basic fibroblast growth factor on cartilage regeneration in chondrocyte-seeded collagen sponge scaffold.* Biomaterials, 1996. **17**(2): p. 155-62.

251. Ikada, Y. and Y. Tabata, *Protein release from gelatin matrices.* Adv Drug Deliv Rev, 1998. **31**(3): p. 287-301.

252. Kim, S.E., et al., *Porous chitosan scaffold containing microspheres loaded with transforming growth factor-beta1: implications for cartilage tissue engineering.* J Control Release, 2003. **91**(3): p. 365-74.

253. des Rieux, A., et al., *3D systems delivering VEGF to promote angiogenesis for tissue engineering.* J Control Release, 2011. **150**(3): p. 272-8.

254. Chiu, L.L. and M. Radisic, *Controlled release of thymosin beta4 using collagen-chitosan composite hydrogels promotes epicardial cell migration and angiogenesis.* Journal of controlled release : official journal of the Controlled Release Society, 2011.

255. Pieper, J.S., et al., *Loading of collagen-heparan sulfate matrices with bFGF promotes angiogenesis and tissue generation in rats.* J Biomed Mater Res, 2002. **62**(2): p. 185-94.

256. Steffens, G.C., et al., *Modulation of angiogenic potential of collagen matrices by covalent incorporation of heparin and loading with vascular endothelial growth factor.* Tissue Eng, 2004. **10**(9-10): p. 1502-9.

257. Zittermann, S.I. and A.C. Issekutz, *Basic fibroblast growth factor (bFGF, FGF-2) potentiates leukocyte recruitment to inflammation by enhancing endothelial adhesion molecule expression.* Am J Pathol, 2006. **168**(3): p. 835-46.

258. Zittermann, S.I. and A.C. Issekutz, *Endothelial growth factors VEGF and bFGF differentially enhance monocyte and neutrophil recruitment to inflammation.* J Leukoc Biol, 2006. **80**(2): p. 247-57.

259. Taylor, K.R. and R.L. Gallo, *Glycosaminoglycans and their proteoglycans: host-associated molecular patterns for initiation and modulation of inflammation.* FASEB J, 2006. **20**(1): p. 9-22.

260. Costa, C., J. Incio, and R. Soares, *Angiogenesis and chronic inflammation: cause or consequence?* Angiogenesis, 2007. **10**(3): p. 149-66.

261. Hodde, J.P., et al., *Vascular endothelial growth factor in porcine-derived extracellular matrix.* Endothelium : journal of endothelial cell research, 2001. **8**(1): p. 11-24.

262. Schwarz, E.R., et al., *Evaluation of the effects of intramyocardial injection of DNA expressing vascular endothelial growth factor (VEGF) in a myocardial infarction model in the rat--angiogenesis and angioma formation.* Journal of the American College of Cardiology, 2000. **35**(5): p. 1323-30.

263. Ribatti, D., et al., *Alterations of blood vessel development by endothelial cells overexpressing fibroblast growth factor-2.* The Journal of pathology, 1999. **189**(4): p. 590-9.

264. Brown, L.F., et al., *Strong expression of kinase insert domain-containing receptor, a vascular permeability factor/vascular endothelial growth factor receptor in AIDS-associated Kaposi's sarcoma and cutaneous angiosarcoma.* The American journal of pathology, 1996. **148**(4): p. 1065-74.

265. Uchida, Y., et al., *Angiogenic therapy of acute myocardial infarction by intrapericardial injection of basic fibroblast growth factor and heparin sulfate: an experimental study.* American heart journal, 1995. **130**(6): p. 1182-8.

266. Yanagisawa-Miwa, A., et al., *Salvage of infarcted myocardium by angiogenic action of basic fibroblast growth factor.* Science, 1992. **257**(5075): p. 1401-3.

267. Ifkovits, J.L., et al., *The influence of fibrous elastomer structure and porosity on matrix organization.* PLoS One. **5**(12): p. e15717.

268. Davis, M.E., et al., *Custom design of the cardiac microenvironment with biomaterials.* Circ Res, 2005. **97**(1): p. 8-15.

269. Deuse, T., et al., *Hepatocyte growth factor or vascular endothelial growth factor gene transfer maximizes mesenchymal stem cell-based myocardial salvage after acute myocardial infarction.* Circulation, 2009. **120**(11 Suppl): p. S247-54.

270. Yasuda, S., et al., *Enhanced secretion of cardiac hepatocyte growth factor from an infarct region is associated with less severe ventricular enlargement and improved cardiac function.* J Am Coll Cardiol, 2000. **36**(1): p. 115-21.

271. Nakamura, T., et al., *Myocardial protection from ischemia/reperfusion injury by endogenous and exogenous HGF.* J Clin Invest, 2000. **106**(12): p. 1511-9.

272. Ueda, H., et al., *A potential cardioprotective role of hepatocyte growth factor in myocardial infarction in rats.* Cardiovasc Res, 2001. **51**(1): p. 41-50.

273. Kitta, K., et al., *Hepatocyte growth factor protects cardiac myocytes against oxidative stress-induced apoptosis.* Free Radic Biol Med, 2001. **31**(7): p. 902-10.

274. Nakamura, T., et al., *Hepatocyte growth factor prevents tissue fibrosis, remodeling, and dysfunction in cardiomyopathic hamster hearts.* Am J Physiol Heart Circ Physiol, 2005. **288**(5): p. H2131-9.

275. Li, Y., et al., *Postinfarction treatment with an adenoviral vector expressing hepatocyte growth factor relieves chronic left ventricular remodeling and dysfunction in mice.* Circulation, 2003. **107**(19): p. 2499-506.

276. Taniyama, Y., et al., *Angiogenesis and antifibrotic action by hepatocyte growth factor in cardiomyopathy.* Hypertension, 2002. **40**(1): p. 47-53.

277. Kondo, I., et al., *Treatment of acute myocardial infarction by hepatocyte growth factor gene transfer: the first demonstration of myocardial transfer of a "functional" gene using ultrasonic microbubble destruction.* J Am Coll Cardiol, 2004. **44**(3): p. 644-53.

278. Esaki, M., et al., *Treatment with an adenoviral vector encoding hepatocyte growth factor mitigates established cardiac dysfunction in doxorubicin-induced cardiomyopathy.* Am J Physiol Heart Circ Physiol, 2008. **294**(2): p. H1048-57.

279. Ellison, G.M., et al., *Endogenous cardiac stem cell activation by insulin-like growth factor-1/hepatocyte growth factor intracoronary injection fosters survival and regeneration of the infarcted pig heart.* J Am Coll Cardiol, 2011. **58**(9): p. 977-86.

280. Rane, A.A., et al., *Increased Infarct Wall Thickness by a Bio-Inert Material Is Insufficient to Prevent Negative Left Ventricular Remodeling after Myocardial Infarction*, in *PLoS ONE*. 2011. p. e21571.

281. Pfeffer, J.M., et al., *Progressive ventricular remodeling in rat with myocardial infarction.* Am J Physiol, 1991. **260**(5 Pt 2): p. H1406-14.

282. Yu, J., et al., *The effect of injected RGD modified alginate on angiogenesis and left ventricular function in a chronic rat infarct model.* Biomaterials, 2009. **30**(5): p. 751-6.

283. Brown, B.N., et al., *Macrophage phenotype and remodeling outcomes in response to biologic scaffolds with and without a cellular component.* Biomaterials, 2009. **30**(8): p. 1482-91.

284. Jin, H., et al., *The therapeutic potential of hepatocyte growth factor for myocardial infarction and heart failure.* Curr Pharm Des, 2004. **10**(20): p. 2525-33.

285. Ido, A., et al., *Safety and pharmacokinetics of recombinant human hepatocyte growth factor (rh-HGF) in patients with fulminant hepatitis: a phase I/II clinical trial, following preclinical studies to ensure safety.* J Transl Med, 2011. **9**: p. 55.

286. Powell, R.J., *Update on clinical trials evaluating the effect of biologic therapy in patients with critical limb ischemia.* J Vasc Surg, 2012. **56**(1): p. 264-6.

287. Ikaria Holdings, I., *IK-500 for the Prevention of Remodeling of the Ventricle and Congestive Heart Failure After Acute Myocardial Infarction (PRESERVATION I) ClinicalTrials.gov NCT01226563*.

288. Dib, N., et al., *Endoventricular transplantation of allogenic skeletal myoblasts in a porcine model of myocardial infarction.* J Endovasc Ther, 2002. **9**(3): p. 313-9.

289. Dib, N., et al., *Safety and feasibility of percutaneous autologous skeletal myoblast transplantation in the coil-infarcted swine myocardium.* J Pharmacol Toxicol Methods, 2006. **54**(1): p. 71-7.

290. Perin, E.C., et al., *Transendocardial, autologous bone marrow cell transplantation for severe, chronic ischemic heart failure.* Circulation, 2003. **107**(18): p. 2294-302.

291. Silva, G.V., et al., *Catheter-based transendocardial delivery of autologous bone-marrow-derived mononuclear cells in patients listed for heart transplantation.* Tex Heart Inst J, 2004. **31**(3): p. 214-9.

292. Lunde, K., et al., *Intracoronary injection of mononuclear bone marrow cells in acute myocardial infarction.* N Engl J Med, 2006. **355**(12): p. 1199-209.

293. Laham, R.J., et al., *Intracoronary and intravenous administration of basic fibroblast growth factor: myocardial and tissue distribution.* Drug Metab Dispos, 1999. **27**(7): p. 821-6.

294. Laham, R.J., et al., *Intracoronary basic fibroblast growth factor (FGF-2) in patients with severe ischemic heart disease: results of a phase I open-label dose escalation study.* J Am Coll Cardiol, 2000. **36**(7): p. 2132-9.

295. Krause, K., et al., *Percutaneous intramyocardial stem cell injection in patients with acute myocardial infarction: first-in-man study.* Heart, 2009. **95**(14): p. 1145-52.

296. Badylak, S.F., D.O. Freytes, and T.W. Gilbert, *Extracellular matrix as a biological scaffold material: Structure and function.* Acta biomaterialia, 2009. **5**(1): p. 1-13.

297. Lutolf, M.P. and J.A. Hubbell, *Synthetic biomaterials as instructive extracellular microenvironments for morphogenesis in tissue engineering.* Nature Biotechnology, 2005. **23**(1): p. 47-55.

298. DeQuach, J.A., et al., *Simple and high yielding method for preparing tissue specific extracellular matrix coatings for cell culture.* PloS one, 2010. **5**(9): p. e13039.

299. DeQuach, J.A., et al., *Decellularized porcine brain matrix for cell culture and tissue engineering scaffolds.* Tissue engineering. Part A, 2011. **17**(21-22): p. 2583-92.

300. French, K.M., et al., *A naturally-derived cardiac extracellular matrix enhances cardiac progenitor cell behavior in vitro.* Acta biomaterialia, 2012. **in press**.

301. Dequach, J.A., et al., *Injectable skeletal muscle matrix hydrogel promotes neovascularization and muscle cell infiltration in a hindlimb ischemia model.* Eur Cell Mater, 2012. **23**: p. 400-12.

302. Valentin, J.E., et al., *Extracellular matrix bioscaffolds for orthopaedic applications. A comparative histologic study.* The Journal of bone and joint surgery. American volume, 2006. **88**(12): p. 2673-86.

303. Reing, J.E., et al., *Degradation products of extracellular matrix affect cell migration and proliferation.* Tissue engineering. Part A, 2009. **15**(3): p. 605-14.

304. Daly, K.A., et al., *Effect of the alphaGal epitope on the response to small intestinal submucosa extracellular matrix in a nonhuman primate model.* Tissue engineering. Part A, 2009. **15**(12): p. 3877-88.

305. Dib, N., et al., *A percutaneous swine model of myocardial infarction.* J Pharmacol Toxicol Methods, 2006. **53**(3): p. 256-63.

306. Badylak, S.F. and T.W. Gilbert, *Immune response to biologic scaffold materials.* Semin Immunol, 2008. **20**(2): p. 109-16.

307. Rosso, F., et al., *From cell-ECM interactions to tissue engineering.* J Cell Physiol, 2004. **199**(2): p. 174-80.

308. Rane, A.A. and K.L. Christman, *Biomaterials for the treatment of myocardial infarction a 5-year update.* Journal of the American College of Cardiology, 2011. **58**(25): p. 2615-29.

309. Laham, R.J., et al., *Transendocardial and transepicardial intramyocardial fibroblast growth factor-2 administration: myocardial and tissue distribution.* Drug Metab Dispos, 2005. **33**(8): p. 1101-7.

310. Nian, M., et al., *Inflammatory cytokines and postmyocardial infarction remodeling.* Circ Res, 2004. **94**(12): p. 1543-53.

311. Allman, A.J., et al., *The Th2-restricted immune response to xenogeneic small intestinal submucosa does not influence systemic protective immunity to viral and bacterial pathogens.* Tissue Eng, 2002. **8**(1): p. 53-62.

312. Korte, W., S. Clarke, and J.B. Lefkowitz, *Short activated partial thromboplastin times are related to increased thrombin generation and an increased risk for thromboembolism.* Am J Clin Pathol, 2000. **113**(1): p. 123-7.

313. Roger, V.L., et al., *Heart disease and stroke statistics--2012 update: a report from the American Heart Association.* Circulation, 2012. **125**(1): p. e2-e220.

314. Sutton, M.G. and N. Sharpe, *Left ventricular remodeling after myocardial infarction: pathophysiology and therapy.* Circulation, 2000. **101**(25): p. 2981-8.

315. Mann, D.L., *Mechanisms and models in heart failure: A combinatorial approach.* Circulation, 1999. **100**(9): p. 999-1008.

316. Fuchs, S., et al., *Catheter-based autologous bone marrow myocardial injection in no-option patients with advanced coronary artery disease: a feasibility study.* J Am Coll Cardiol, 2003. **41**(10): p. 1721-4.

317. Fuchs, S., et al., *Safety and feasibility of transendocardial autologous bone marrow cell transplantation in patients with advanced heart disease.* Am J Cardiol, 2006. **97**(6): p. 823-9.

318. Smits, P.C., et al., *Catheter-based intramyocardial injection of autologous skeletal myoblasts as a primary treatment of ischemic heart failure: clinical experience with six-month follow-up.* J Am Coll Cardiol, 2003. **42**(12): p. 2063-9.

319. Dib, N., et al., *Safety and feasibility of autologous myoblast transplantation in patients with ischemic cardiomyopathy: four-year follow-up.* Circulation, 2005. **112**(12): p. 1748-55.

320. Perin, E.C., et al., *A randomized study of transendocardial injection of autologous bone marrow mononuclear cells and cell function analysis in ischemic heart failure (FOCUS-HF).* Am Heart J, 2011. **161**(6): p. 1078-87 e3.

321. Singelyn, J.M. and K.L. Christman, *Injectable materials for the treatment of myocardial infarction and heart failure: the promise of decellularized matrices.* Journal of cardiovascular translational research, 2010. **3**(5): p. 478-86.

322. White, H.D., et al., *Left ventricular end-systolic volume as the major determinant of survival after recovery from myocardial infarction.* Circulation, 1987. **76**(1): p. 44-51.